SOIL NAIL HEAD REVIEW

GEO REPORT No. 175

Y.K. Shiu & G.W.K. Chang

GEOTECHNICAL ENGINEERING OFFICE
CIVIL ENGINEERING AND DEVELOPMENT DEPARTMENT
THE GOVERNMENT OF THE HONG KONG
SPECIAL ADMINISTRATIVE REGION

SOIL NAIL HEAD REVIEW

GEO REPORT No. 175

Y.K. Shiu & G.W.K. Chang

This report was originally produced in September 2004
as GEO Special Project Report No. SPR 8/2004

First published, December 2005

Prepared by:

Geotechnical Engineering Office,
Civil Engineering and Development Department,
Civil Engineering and Development Building,
101 Princess Margaret Road,
Homantin, Kowloon,
Hong Kong.

PREFACE

In keeping with our policy of releasing information which may be of general interest to the geotechnical profession and the public, we make available selected internal reports in a series of publications termed the GEO Report series. The GEO Reports can be downloaded from the website of the Civil Engineering and Development Department (http://www.cedd.gov.hk) on the Internet. Printed copies are also available for some GEO Reports. For printed copies, a charge is made to cover the cost of printing.

The Geotechnical Engineering Office also produces documents specifically for publication. These include guidance documents and results of comprehensive reviews. These publications and the printed GEO Reports may be obtained from the Government's Information Services Department. Information on how to purchase these documents is given on the last page of this report.

R.K.S. Chan
Head, Geotechnical Engineering Office
December 2005

FOREWORD

This Report presents the results of a study of the design of soil nail head.

In this study, a review of the role and load transfer mechanism of soil nail heads, previous studies and international practice in nail head design has been carried out. Numerical simulations have also been performed to examine the functions of nail heads and local stability of soil between nail heads. From the study, guidance on determination of size of nail head is provided.

The study was carried out by Mr Y.K. Shiu and Dr G.W.K. Chang of the Standards and Testing Division. Dr H.W. Sun of the Landslip Preventive Measures Division 1 has provided useful advice on the numerical simulations. Miss Florence Ko of the Planning Division performed simulations of active zone failure on nailed slopes. Their contributions are gratefully acknowledged.

W.K. Pun
Chief Geotechnical Engineer/Standards and Testing

Table of Contents
Table of Contents
Table of Contents

ABSTRACT

Soil nails are extensively used for slope improvement works in Hong Kong. A study has been carried out to review the role and load transfer mechanism of soil nail heads.

This study comprises a review of the fundamental mechanism of soil nail heads, case histories of previous studies and technical guidance documents from France, Japan, UK and USA. In addition, numerical simulations have been carried out to examine analytically the functions of soil nail heads. Local stability of the soil between soil nail heads has also been examined.

From the results of the study, soil nail heads can enhance stability of slopes. This beneficial effect is attributed to the lateral confinement to the soil resulting from combined action of the nail heads and soil nails.

Three options of design methods including design charts derived from numerical analyses, lower-bound solution as proposed by HA 68/94, and prescriptive design approach are provided to assist engineers in determining the dimension of nail heads. Guidance on prevention of local instability of soil between nail heads is also given.

CONTENTS

Page No.

1. INTRODUCTION

The Geotechnical Engineering Office (GEO) of the Civil Engineering Department engaged Maunsell Geotechnical Services Ltd. (MGSL) to undertake a review of soil nail head design. The review report (MGSL, 2003) recommends that the role of soil nail head in mitigating slope failure should be further investigated.

This study examines the role and mechanism of soil nail heads and proposed guidelines for determining nail head sizes. It comprises a review of the fundamental mechanism of soil nail heads, case histories of previous studies and international practice in nail head designs. In addition, numerical simulations have been carried out to examine analytically the functions of soil nail heads. Local stability of the soil between soil nail heads has also been examined and suggestions to minimise such failures have been made.

In Hong Kong, soil nail heads are usually in the form of concrete pads. They are either isolated or integrated into a shotcrete facing or grillage beams. In this study, only isolated concrete pads for soil nails in soil cut slopes are addressed.

2. LOAD TRANSFER MECHANISM OF SOIL NAIL HEADS

2.1 General

As part of the earlier study by MGSL (2003), an opinion survey was carried out to collect views on the design approach of soil nails. In the survey, questionnaires were sent to a number of local and overseas consultants. Many of the respondents indicated that nail heads could enhance the internal stability or the external stability of a nailed structure whereas some considered that there was no need to provide soil nail heads. This difference in views points to the need for a review of the basic mechanism of load transfer of soil nail head.

2.2 Fundamental Mechanism

To understand the fundamental behaviour of soil nail heads of a nailed structure, it is necessary to look at the whole load transfer mechanism of the structure. The soil in a nailed structure consists of two distinct zones, namely the active zone and the resistant zone as shown in Figure 1.

The load transfer mechanism of a nailed structure is the development of tensile forces in the nails as a result of the restraint that the nails and the nail heads provide in response to deformations of the structure. In the case of stabilization of marginally stable slopes, the deformations are associated with movements of the slope as a result of inadequate support. In the case of a soil nailed retaining wall, the deformations are due to expansion of the reinforced zone as a result of removal of lateral support as excavation proceeds from the top downwards. In either case, movement of the soil relative to the nails generates shear stresses at the soil/nail interface. Loads are induced within the soil nails as a result of the interfacial shear stresses between the nails and the soil in the active zone, and by the soil-structure interaction between the nail head and the soil (see Figure 1). In the active zone, the nails and the nail heads interact with the soil to support the ground. The tension loads induced in the soil nails are redistributed into the soil in the resistant zone through the nail/soil friction.

Under working conditions, shearing and bending resistance of the soil nails have little contributions to the system of forces maintaining stability within the soil-nailed structure. At failure condition when large deformations of the soil have taken place, the contribution can be more significant but still small (Jewell & Pedley (1992), Kitamura et al (1988), Plumelle & Schlosser (1990), Hong et al (2003)). As such, the influence of the shearing and bending resistance is often ignored in soil nail designs and the nails are considered to act in tension only. To ensure that the predominant action of the nails is in tension, soil nails are usually placed at inclinations close to the horizontal. These inclinations correspond in general with those of maximum tensile strains developed in the soil in the active zone (Jewell & Wroth (1987), Hayashi et al (1988)).

Interaction between the nail head and the soil gives rise to tensile load at the head of the nail. The soil nails and the nail heads act together to tie the active zone to the resistant zone. The reaction on the nail head and the pull-out resistance of the nail in the active zone must be adequate to provide the required nail tension at the slip surface between the active and resistant zones in order to prevent the active zone from sliding off the soil nail. This is illustrated in Figure 2. Plates 1 and 2 show examples of failures with the active zone sliding off the soil nails. For stability to be achieved, the soil behind isolated nail heads must have sufficient strength against bearing failure in the soil. For soil nail heads attached to a continuous reinforced shotcrete facing, bearing failure of the soil is usually not a controlling factor. To provide the support force to stabilise the active block, the nails must give adequate tensile strength. In addition, the nails must also be embedded a sufficient length into the resistant zone to prevent pull-out failure.

3. CASE HISTORIES

3.1 General

Our understanding of the magnitude and distribution of the nail head loading developed in nailed structures is not as good as our knowledge of the tensile loads developed within the nails (FHWA, 1998). This is because of the lack of good quality field monitoring data. The available data from instrumented nails are difficult to interpret in the vicinity of nail head, where bending effects of nail tend to be more significant as a result of the weight of nail head or facing (Thompson & Miller (1990), Shiu et al (1997)). There has been little field monitoring data obtained from load cells installed at the heads of soil nails probably because of the difficulties of placing load cells between nail heads and the soil (Stocker & Reidinger, 1990).

Despite the lack of good quality field monitoring data, a number of studies including model tests, full-scale field tests and numerical simulations have been carried out at different parts of the world. The results of these studies provide useful insight into the role and behaviour of soil nail heads. Many of the studies are related to soil nailed retaining walls where soil nail heads are integrated into a concrete facing.

3.2 Experimental Full-scale Structures and Laboratory Model Tests

Full-scale experiments on instrumented, sub-vertical nailed walls were carried out by Gässler & Gudehus (1981). Soil nails and shotcrete facing were constructed during

excavation. The soil nails were installed by driving bars into the ground. The test walls were 20 feet high. Earth pressures behind the shotcrete facing of the walls were measured by hydraulic cells and forces along selected soil nails were monitored by strain gauges. Figure 3 shows the instrumentation of the test walls. The reinforced soil bodies were brought to failure either by surcharging the wall crest or by pulling out the lowest row of soil nails.

Typical earth pressure measured behind the facing is shown in Figure 4. The distribution of the facing pressure was closer to uniform than triangular in shape, with a marked reduction close to the toe. Under self-weight loading, the resultant lateral earth pressure acting on the facing was about 50% of the active earth pressure calculated using Coulomb's theory. When surcharge was added from the wall crest, the resultant earth pressure on the facing increased to about 70% of the Coulomb's active value. Indeed, loads of 60 to 70% of the Coulomb active earth pressure were repeatedly observed on the facing of different experimental walls and so it was recommended that the shotcrete facing and the nail heads should be designed for these reduced earth pressures.

Plumelle & Schlosser (1990) reported a test on an experimental wall of 6 m in height. Three rows strain-gauged soil nails were installed at the upper portion of the wall whereas the lower portion was unreinforced (see Figure 5a). The unreinforced portion of the wall was supported by 1 m high panels numbered 1, 2 and 3. The face of the nailed portion was retained by another panel numbered 4. The panels supporting the unreinforced portion were removed one by one in the sequence of panel 3, 2 and 1. When panels 3 and 2 had been removed, local instability occurred and the failed soil was in the shape of an arch. When panel 1 was removed, a local failure took place, leading to the overall failure of the wall. The forces at the nail heads were monitored during the test. Figure 5b shows that the forces at the nailed head increased in steps that corresponded to the removal of the panels. This illustrates the effect of soil arching.

Gutierrez & Tatsuoka (1988) reported loading tests performed on three model sand slopes: (i) unreinforced slope, (ii) slope reinforced with metal strips but without a facing, and (iii) slope reinforced with metal strips and with a facing (Figure 6). The slopes were loaded at the crest by a footing with a smooth base. Result of the tests is shown in Figure 7. It indicates that the reinforced slope with facing can sustain a higher load than the reinforced slope with no facing, and a much higher load than the unreinforced slope. Figure 8 shows the failure planes of the slopes when loaded at the crest. Deep and shallow failure planes were observed in the unreinforced slope. For the reinforced slope with no facing, failure took place close to the slope face. This was because the reinforcement alone was not effective at retaining the active zone. For the reinforced slope with facing, the failure was observed at a greater depth. The maximum tensile force generated in the reinforcement was larger than that in the reinforced slope with no facing. Furthermore, substantial tensile force was induced in the reinforcement at the connection to the facing. This shows that the facing can enhance the stability of reinforced slope and help prevent shallow failures.

A series of small-scale model tests and full-scale field tests were carried out and analysed by Muramatsu et al (1992) to investigate the effects of soil nail heads. For the small-scale model tests, the model retaining walls were 50 cm wide, 200 cm long and 120 cm high. Excavation and cutting were simulated in the tests. The set up of the model walls is shown in Figure 9. Two types of facing were used. They were continuous "grating crib"

type and independent “bearing plate” type, as shown in Figure 10. The surface areas of each of these two types of facing were varied in the tests. Figure 10 also shows the typical test results for the case of using a 3 cm square bearing plate, and another case of using a “grating crib” of a width of 1 cm for the facing. Figure 11 depicts the relationship between the limiting excavation heights of the slopes and the areas occupied by the facing. The Figure shows that the excavation heights of the reinforced slopes increase with increasing ratios of the facing area to the slope face area. This indicates that the stability of the reinforced slopes is influenced by the proportion of the slope face supported by the nail head or facing. A comparison of the typical distribution of tensile forces along the lengths of the soil nails between the case of bearing plate and that of grating crib facing is shown in Figure 12. For the case of the bearing plate, the distribution of the tensile force along the nail is more or less symmetric with the maximum tension force developed at approximately the mid-length of the nails. The pattern of the force distribution is different for the case of the “grating crib” facing, where the maximum tension is developed close to the nail head.

For the field test undertaken by Muramatsu et al (1992), a steep cut slope was formed to a height of 9.5 m at a gradient of roughly 80°. Reinforcing bars of 5 m long were driven into the slope at an angle of 10 degrees downwards. Both the vertical and horizontal spacings of the bars were 1.5 m. Two different types of facing were used on two sides of the slope face. One type was 100 mm thick continuous shotcrete facing and the other was sprayed concrete crib (beam width: 20 cm, grating spacing: 1.5 m), see Figure 13. Figure 14 shows the tensile forces that were developed in the reinforcing bars together with results of numerical analysis using a two-dimensional finite element method. The measured and the calculated values show a similar trend. For the case of shotcrete facing, the maximum tensile force was observed near the mid-length of the reinforcing bars. In contrast, the maximum tensile force was observed at or close to the connection between the facing and the bar for the case of concrete crib. The magnitudes of the maximum tensile forces were generally higher than those of the shotcrete facing. This suggests that the flexible shotcrete facing used in the test contributed less to the improvement of the overall stability of the slope when compared to the more rigid concrete crib.

A series of centrifuge model tests of vertical and near vertical nailed slopes was conducted by Tei et al (1998). The model slopes were 200 mm high and constructed of Leighton Buzzard sand. Four types of facing were used to cover the slope face in order to investigate the influence of the stiffness and roughness of the facing on the stability of the nailed slopes. The model slopes were initially tested at 30 g acceleration, which corresponded to a prototype structure of 6.0 m high. If failure was not obtained, the acceleration was increased gradually to a maximum of 80 g. Figure 15 shows that the magnitudes of horizontal displacements were related to the stiffness of the facing - lesser displacements were for facings of higher stiffness.

3.3 Field Prototype Studies

Stocker & Riedinger (1990) present the results of field monitoring of instrumented nearly vertical nailed retaining walls of heights up to 15 m. The facing consisted of shotcrete of 250 mm in thickness. The field monitoring lasted for over 10 years. The earth pressure on the facing, inferred from the strain gauges installed at about 0.2 m behind the facing, was uniform with depth as shown in Figure 16. The measured pressure was about

63% of the calculated earth pressure.

Similar behaviour was observed in other nailed walls during the investigations carried out as part of French National Research Project: Clouterre. Under service conditions, the ratio of nail head load to the maximum nail load was typically in the range of 0.4 to 0.5. This ratio tends to increase with a wide spacing of the nails and pronounced rigidity of the facing (French National Research Project, 1991).

FHWA (1998) present results of earth pressure monitoring carried out on a number of instrumented nailed retaining walls. A summary of the normalised measured nail head loads, as a function of the nail depth within the wall, is plotted on Figure 17. It can be noted that the nail head loads were fairly uniform in the upper two-thirds of the walls and decreasing in the lower part of the walls. The normalised measured nail head loads in the upper part of the wall varied in general from 0.3 to 0.7. According to FHWA (1998), the average normalised nail head load was in the range of 0.4 to 0.45, or less than 60% of the maximum nail loads observed under the service condition.

3.4 Numerical Simulations

Parametric numerical studies were performed by Ehrlich et al (1996) using finite element modelling. Results of the analyses indicate that the facing stiffness influenced the bending moments of the soil nails and, to a lesser extent, the nail tension forces. It was concluded that the facing stiffness would help to control yielding of the soil close to the facing.

Babu et al (2002) investigated the behaviour of nailed retaining walls with structural facing by carrying out numerical simulations. One of the aspects examined in the simulations was the effect of connections of the facing and the nails on the behaviour of nailed walls. The results of the simulations are shown in Figure 18, which show that the connection significantly improves the critical excavation height and contributes to additional stability for the same height. Figure 19 shows the typical results of the distribution of tensile forces along the length of the nails for case (a) with, and case (b) without connection to the facing. The trends are markedly different between the two cases. The maximum tension is mobilised at locations close to the facing when connection is provided whereas the mobilised maximum tensile force is located at approximately the mid-length of the nails when connection is not provided. The maximum axial forces are shown as a function of z/H in Figure 20 for the two cases. It can be seen that the higher maximum tensile forces were developed when nails were connected to the facing. The higher tensile forces increased the stability and reduced lateral deformation of the walls.

A parametric study was carried out by MGSL (2003) using the finite difference program “FLAC”. The objective of the study was to understand more about the general behaviour of the soil nail head relating to the soil nail force for different slope geometry, ground conditions, soil nail patterns and loading conditions. From the study, the ratio of the soil nail head force to the maximum nail tension force was reported to vary between 0.1 and 0.46 for different groundwater conditions considered.

3.5 Other Studies

Mitchell & Villet (1987) reviewed various design methods for soil nailing in excavations. They indicate that facing elements could be designed to support local soil pressure on the facing.

Tatsuoka (1992) provided a comprehensive overview of the role of the rigidity of facing on the stability of nailed slopes and retaining walls. He concluded that local and overall facing rigidities could help reduce the deformations and increase the stability of nailed structures. He also remarked that a nailed retaining wall could be much lighter than a conventional reinforced concrete retaining wall because most of the earth pressure acting on the back face of the facing would be supported by the nails if they were at close spacing.

3.6 Discussion

Results of the above model tests, field measurements and numerical simulations highlight the importance of soil nail heads in the soil nailing applications. They show that soil nail heads, whether in the form of individual concrete pads or as part of concrete facing, play a beneficial role in enhancing the shearing resistance of the soil in the active zone.

The above studies also indicate that the nail head loads mobilised under service loading for typical nail spacing are less than the maximum tensile loads developed in the nails.

4. SOIL NAIL HEAD DESIGN METHODS

4.1 General

The design methods as used in Hong Kong, UK, France, USA, Japan and Germany are summarised below, drawing attention to common similarities and relevant differences. It should be noted that many of the design methods are based on the results of some of the studies described in Section 3 above. For example, some full-scale experiments on actual nailed structures illustrate that the loads induced at the soil nail heads are typically some fractions of the maximum tensile load developed in the soil nails. This observation is included in many of the design methods.

Some of the design methods are related mainly to nailed retaining walls where the nail heads are integrated into a continuous reinforced shotcrete facing. As such, they mostly deal with the determination of the structural strength of the nail heads (e.g. flexural strength and punching shear strength) and the nail-facing connections. In some countries (e.g. UK and Japan), guidance is also given for the design of isolated nail heads whose capacities are also controlled by bearing failure in soil.

4.2 Hong Kong Approach

There is no standard for the design of soil nail head in Hong Kong. Watkins & Powell (1992) proposed that the soil beneath the nail head should have a minimum factor of

safety of 3 against bearing failure resulting from the load induced by the nail head. No details are given as how the bearing capacity should be determined.

Standard nail head size of 400 x 400 mm x 250 mm thick is normally used in the LPM design. Construction details typically follow those shown in Figure 21. The standard nail head size is used empirically and bearing capacity check or structural designs are in general not carried out in design.

From the survey on soil nail head design practice undertaken by MGSL (2003), for private projects, most practicing engineers base their designs on the presumed allowable bearing capacity of soils for foundation on horizontal ground given in the PNAP 141: Foundation Design. Some engineers use the approach stipulated in HA68/94 (Department of Transport, 1994); and some other use bearing capacity equations but assuming that the nail heads are founded on horizontal ground.

4.3 United Kingdoms Approach

The code of practice for strengthened/reinforced soil and other fills (BS8006: 1995) gives little guidance on design of soil nail head/facing. It advises that the facing should be designed to accommodate soil pressures corresponding to the reactions in the connections, which themselves are forces corresponding to between 75% and 100% of the maximum tensile force resisted by the reinforcement.

Methods for design of nailed structures and reinforced fill structures can be found in HA68/94. The design is based on limit state principles incorporating partial factors. According to HA68/94, if the soil nails are not connected to a continuous facing but to a 'waling plate', the bearing capacity of the front face 'waling plate' should be checked.

The bearing force acting on the slope surface by the nail head is taken as the difference between the designed tension in the nail and the soil/nail frictional force developed along the nail length at the active zone. Lower- and upper-bound solutions for checking the bearing capacity of the 'waling plate' in soil are provided and they are shown in Figure 22 (a) and Figure 22 (b) respectively. The bearing capacity of a nail head is estimated based on the angle of shearing resistance (ϕ) of the soil whereas the cohesion is not considered. The dimensions of nail head can be determined using these solutions. Derivations of the lower-bound solution are provided in Appendix A, which are based on Love (2003).

4.4 US Approach

The recommended soil nail design method is given in FHWA (1998). The design recommendations are primarily related to nailed retaining walls and as such mainly nail heads attached to a facing are considered. This method considers directly the influence of the facing and the magnitude and distribution of nail forces. In this approach, a trial pattern of soil nails is first selected. An allowable nail load support diagram is then developed based on factored nail head resistance, factored pull-out resistance and the allowable tensile strength of the nail (see Figure 23). The nail forces contributing to the overall stability of the nailed soil mass are determined at the location where the failure plane intersects the nail loading

diagram.

It can be noted from Figure 23 that the strength of nail head (T_F) is an important parameter for developing the nail load diagram that gives the magnitude and distribution of tensile forces along the soil nail. It is one of the elements required to define the overall reinforcing capacity of the nail. It is emphasized in FHWA (1998) that the distribution of pressure on the facing between the nails is non-uniform and arching effects tend to develop horizontally and vertically between the nails, and as a result, stresses are concentrated at the nail head. The non-uniformity of the facing pressure distribution is illustrated in Figure 24. The higher pressure at the nail head needs to be considered in design. A nail head load corresponding to 50% of the maximum nail load is recommended to be adopted for design purposes. Details of typical permanent and temporary nail heads used in the U.S. are shown in Figure 25.

FHWA (1998) also provides comprehensive guidelines for the structural design of the facing, with particular emphasis on the nail heads. The structural design requires provision of adequate concrete thickness, reinforcement, and moment capacity to resist the earth pressure applied to the facing spanning between adjacent nail heads, and provision of adequately sized bearing plates at the nail heads to provide enough punching shear capacity. Joshi (2003) has examined the behaviour of soil nail head strength for different nail spacing, and developed a number of design charts for determining nail head strength against various failure modes.

4.5 French Approach

The approach of soil nail design is given in French National Research Project (1991). As the design approach is mainly for nailed retaining walls, method for designing facing rather than isolated nail heads is provided in the document. The facing is designed on the basis of a uniform earth pressure corresponding to a fraction of the maximum tension that can be developed in the soil nail. It requires the determination of the tension, T_o, at the soil nail heads, and the soil pressure P on the facing resulting from the tension. P can be calculated from the following equation:

$$P = T_o / (S_h S_v) \quad \text{.....(1)}$$

where S_h and S_v are the horizontal spacing and vertical spacing of the soil nails respectively.

The maximum value of the ratio T_o / T_{max} obtained from the following empirical equations is to be used in the design:

$$\begin{aligned} T_o / T_{max} &= 0.5 + (S - 0.5) / 5 \quad && \text{when } 1 \le S \le 3 \text{ m} \quad \text{.....(2)} \\ T_o / T_{max} &= 0.6 && \text{when } S \le 1 \text{ m} \\ T_o / T_{max} &= 1 && \text{when } S \ge 3 \text{ m} \end{aligned}$$

where S = maximum of S_v and S_h, expressed in meter.

Same as the US approach, the French National Research Project (1991) points out that the distribution of pressure on the facing between soil nails is non-uniform because arching

effects tend to develop between the nails and this results in stress concentrations in the vicinity of the nails.

Guidance for the structural design of the facing is also provided in the French National Research Project (1991). Structural failures due to bending, shearing and punching of the facing around the nail head need to be considered in the design.

Typical details of the nail head and facing connection are shown in Figure 26.

4.6 Japanese Approach

Similar to the US approach, the design used in Japan also considers the earth pressure acting on the nail head (T_o) when calculating the distribution of tension force in the soil nails. According to Miki et al (1997), the design axial load of a soil nail, T_{pa}, should be the lowest among: (i) pull-out resistance that can be developed at the active zone, T_{1pa}; (ii) pull-out resistance that can be developed at the resistant zone, T_{2pa}; and (iii) allowable tensile strength of the soil nail, T_{sa}. Figure 27 depicts the principles. It also shows that the pull-out resistance in the active zone will be very small if the force at soil nail head (T_o) is not considered.

For the soil nail head design load, Japan Highway Public Corporation (1998) suggests that a force reduction coefficient, $\mu = T_o / T_{max}$, is to be applied to the soil nail head. The coefficient is based on measurements of actual nailed structures and model tests. It lies between 0.2 and 1.0, depending on the nail spacing, nail length and the type of surface where the nail heads rest on. Figure 28 shows a plot of the distribution of the coefficient. The tension at the nail head is determined by:

$$T_o = \mu \ T_d \quad \text{.....(3)}$$

where T_d is the designed tension in the soil nail.

Details of different types of soil nail heads used in Japan are shown in Figure 29.

4.7 German Approach

During the course of this study, no English literature on the soil nail head/facing standard has been located. However, according to Stocker & Riedinger (1990), the standard German practice is that shotcrete linings are designed for 85% of the active Coulomb's earth pressure at the back face of the wall.

4.8 Discussion

Most of the overseas design approaches recognize the soil nail head or facing as a significant component of the overall soil nail system, and they provide specific recommendations for design pressures. These approaches also recognize that the magnitudes of pressures induced in the soil nail heads are controlled by many factors such as

the density and length of the nails and the stiffness of the nail head. Both the UK and the Japanese approaches require that the pull-out failure at the active zone is to be checked. The UK approach also requires the checking of the bearing capacity failure in soil.

The French, Japanese and German methods use empirical earth pressures which are related either to the maximum tension developed in the soil nail (T_{max}) or Coulomb earth pressure.

The U.S. and Japanese approaches consider directly the strength of nail head when determining the magnitude and distribution of nail forces along the length of the soil nails. If the beneficial effect of the nail head is not considered, the pull-out resistance of the soil nail at the active zone would be significantly reduced. This may lead to more number of soil nails being required.

In all the overseas design methods, the size, thickness and reinforcement details of soil nail heads are determined on the basis of the earth pressure acting on the nail heads. Two main design aspects are considered; they are the bearing capacity of the soil beneath the nail head and the structural strength of the nail head itself. Many of the design methods (such as those used in France and U.S.) are developed mainly for nailed walls where the nail heads form part of the concrete facing. In those cases, bearing failure of the nail head or facing is unlikely to occur and as such little guidance has been provided in respect of bearing capacity failure. A method on design against bearing failure of the soil behind isolated nail heads is given in the UK guidance document HA68/94.

Unlike all the overseas approaches considered, a single sized (400 x 400 mm) nail head is used in the LPM designs in Hong Kong irrespective of the magnitude of the nail head load or the ground condition.

The overseas design methods described above recognize the beneficial effect of confinement provided by soil nail heads.

5. NUMERICAL ANALYSES

5.1 General

Numerical simulations were carried out using the two-dimensional finite difference code, Fast Lagrangian Analysis of Continua (FLAC), which was developed by Itasca (1996). A Mohr Coulomb model was used for the soil. The soil nail was modeled as cable elements. Soil-nail interaction was represented by a spring-slider system having shear springs located at the nodal points along the cable elements.

The numerical simulations were divided into two principal parts:

(a) investigation of the effect of nail heads on stability of nailed slopes; and

(b) determination of the sizes of individual nail heads based on bearing capacity consideration.

5.2 Effect of Nail Heads on Stability of Nailed Slopes

5.2.1 Slope Model and Material Parameters

Two cases were considered in the analysis: (i) unreinforced slope, and (ii) slope reinforced with soil nails. For both cases, the model slopes were 20 m high, standing at an angle of 55°, and with an up-slope of 10° in gradient at the crest. For the case of reinforced slope, seven rows of soil nails were provided. This corresponds to a vertical nail spacing (S_v) of 2 m. The horizontal spacing of the nails (S_h) was taken to be 1.5 m. Each nail was 20 m long with 40 mm diameter steel bar in a 100 mm grouted hole. The initial shear strength parameters of the soil were assumed to be $c_i' = 10$ kPa, and $\phi_i' = 43°$, so that the unreinforced slope had a factor of safety greater than 1. Figures 30 shows the geometry of the slope and the material parameters used in the numerical analysis for the reinforced slope. The model for the unreinforced slope was the same as that shown in the Figure except without soil nails and nail heads.

A Mohr Coulomb model was used for the soil. The nail heads and facing were modelled as linear elastic materials. A cable element was used to represent the soil nail as the bending stiffness of the soil nail was not considered. Developments of the tensile forces in the nails were governed either by the tensile strength of the nail or the peak shear strength at the soil-grout interface.

Since the FLAC adopts 2-dimensional plain strain analysis, the nail heads were modelled as infinitely long beams of specific widths. In order to investigate the influence of the size of the nail heads on the stability of slopes, two nail head sizes were considered. They were 400 mm wide and 800 mm wide. All of them were 250 mm thick. In addition, continuous concrete facing of 250 mm in thickness was also studied.

5.2.2 Analytical Approach

Slope stability analysis was first carried out on the unreinforced slope. From the results of the analysis, the unreinforced slope has a minimum factor of safety (FoS) close to 1.0 for the initial soil strength parameters of $c_i' = 10$ kPa, and $\phi_i' = 43°$.

In slope engineering, the FoS is conventionally defined as the ratio of the actual soil shear strength to the minimum shear strength required for equilibrium. As pointed out by Duncan (1996), FoS can also be defined as "the factor by which the shear strength of the soil would have to be divided to bring the slope into a state of barely equilibrium". FoS can therefore be determined simply by reducing the soil shear strength until failure occurs. This strength reduction approach is often used to compute FoS using finite element or finite difference programs (Dawson et al (1999), Krahn (2003)). In this study, the approach was adopted to determine the FoS of slopes for the following cases:

(a) nailed slope with no nail heads,

(b) nailed slope with nail head size of 400 mm wide,

(c) nailed slope with nail head size of 800 mm wide, and

(d) nailed slope with nail heads integrated in a full surface facing of 250 mm thick.

For each case, the factor of safety (FoS) was determined by progressively reducing the shear strength of the soil in the model until numerical non-convergence of unbalanced forces and displacements at chosen monitoring points occurred. This analysis was done by trial and error using parameters c_m' and ϕ_m', where

$$c_m' = c_i' / FoS = 10 / FoS \quad (kPa) \quad .....(4)$$

$$\phi_m' = \tan^{-1} (\tan \phi_i' / FoS) = \tan^{-1} (\tan 43° / FoS) \quad .....(5)$$

This strength reduction approach is similar to that described by Dawson et al (1999) and Krahn (2003).

5.2.3 Results of Numerical Simulations

Typical outputs obtained from the FLAC analyses are given in Appendix B.

The relationship between the calculated FoS and the nail head sizes for the model slopes is plotted in Figure 31. The FoS increases from 1.0 for the unreinforced slope to 1.2 for the nailed slope with no nail heads. Substantial increases in the FoS are obtained with nail head sizes from 400 mm wide to about 800 mm wide. The trend of increase levels off for nail head sizes larger than 800 mm wide. It shows that nail head has significant effect on the stability of a soil nailed slope.

The total of the maximum tensile forces mobilised in all the soil nails (ΣT_{max}) at limit equilibrium condition of the model are given below:

Nail Head Sizes	Total of Maximum Nail Tensile Forces, ΣT_{max}
Nil	247 kN
400 mm wide	957 kN
800 mm wide	1211 kN
Full surface facing	1220 kN

The above values are also plotted in Figure 32 which shows that ΣT_{max} increases with the increasing size of the nail heads. Close similarity between Figure 31 and Figure 32 indicates that the FoS of the nailed slopes is directly related to ΣT_{max}.

Figure 33 compares the distribution and magnitude of the axial forces developed in the soil nails for the reinforced slope with no nail head and the reinforced slope with nail head of 800 mm wide. For the slope with no nail head, no tension forces are induced at the front end of the nails and the maximum tension (T_{max}) occurs close to the slope face. For the slope with 800 mm wide nail head, the force distribution pattern is markedly different from that of no nail head. Substantial tension force is generated at the nail head (T_o), and the maximum tension (T_{max}) occurs at a distance behind from the slope face. Similar results are also

obtained in the nailed slopes with other nail head sizes.

Results of the FLAC analyses show that substantial tension forces are induced in the soil nails at the nail heads (T_o). Figure 34 shows the distribution of the ratio of T_o / T_{max} for nailed slopes with different nail head sizes. The values for T_o / T_{max} range mainly between 0.55 and 0.75.

Figure 35 shows the locations of the maximum nail forces developed in the soil nails for the reinforced slopes with different nail head sizes at the limit equilibrium condition. The locations of T_{max} in general lie further away from the slope face for larger nail heads. As the locus of the T_{max} in a nailed slope at limit equilibrium corresponds with the failure plane, larger nail heads tend to force the failure planes further away from the slope face. This is consistent with the observations made by Gutierrez & Taksuoka (1988).

5.3 Simulation of Active Zone Failure on Slope

Analyses were also performed to simulate the situation that the interfacial shear stress between the nails and the soil in the active zone were all lost, such as that when the active zone had disintegrated. The profile and geometry of the model considered are shown in Figure 36. It was assumed in the analyses that the soil nails were not bonded to the surrounding soil, i.e. zero soil/nail friction. Simulations were run for a series of thicknesses of the failed active zone.

The strength reduction approach as described in Section 5.2.2 was applied in the simulations. For a given thickness, the shear strength of the soil within that layer was adjusted using equations (4) and (5) above until numerical instability occurred.

No changes were made to the shear strength parameters (c_i' and ϕ_i') of the soil outside the failed active zone. Typical results of the simulations are shown in Figure 37. Shear zones of the soil developed behind the nail heads resemble the shape of failure zone considered in HA68/94. The calculated FoS decreases with increasing thickness of the failed active zone.

5.4 Determination of Nail Head Sizes Based on Bearing Capacity Considerations

5.4.1 Material Parameters and Analytical Approach

FLAC analysis was performed to examine the bearing capacity failure of square soil nail heads. Three slope angles were considered: 45°, 55° and 65°. Since it was a plain strain analysis, the nail head force was adjusted based on the length of one side of the nail head. Take a 400 mm x 400 mm nail head as an example, if the actual nail head force is F (kN), the adjusted force would be: F x 1000 / 400 (kN/m). In the following discussions, the nail head forces or nail forces presented are unadjusted values.

A small slope model of 5 m in height was used in the analysis. Typical details of the model used are shown in Figure 38. In the analysis, the nail head was pushed into the soil face by a nail force (T_o) to simulate the situation of soil moving out from a slope and pressing against a soil nail head. The nail head was placed at the lower part of the small model slope.

This is based on the result of a sensitivity check carried out to determine the effect of the locations of nail force on the results of simulations. The result showed that bearing failures were sensitive to the vertical extent of the slope above the nail head but insensitive to the extent of the slope below the nail head.

The nail forces used were determined from the allowable tensile strength of steel bars (f_m), using the following equations:

$$T_o = f_m A_s \text{ (kN)} \quad \text{.....(6)}$$

$$f_m = 0.55\, f_y \leq 0.23 \text{ (kN / mm}^2\text{)} \quad \text{.....(7)}$$

where f_y is the characteristic strength of high yield bar, and A_s is the cross-sectional area of the steel bar.

The values of T_o vary directly with the cross-sectional area of the steel bar. The nail load T_o calculated in this way is based on a simplifying assumption that $T_o = T_{max}$. The assumption ignores the contribution from the pull-out resistance at the active zone. This does not have any significant effect on the result because the pull-out resistance that can be developed at the active zone is low owing to small overburden pressure at the front part of slope. Besides, the soil mass near to the slope face can easily be disturbed by environmental changes (such as erosion, cyclic pore water pressure changes etc.) and other activities (such as construction and planting works). As such the amount of pull-out resistance that can be mobilised is uncertain.

The nail force was applied at the center of the nail head at an inclination of 20° from the horizontal. Bar sizes commonly used in soil nailing were considered. As the current corrosion measures require the provision of a 2 mm sacrificial thickness on the bar radius, the reduced bar sizes resulting from this corrosion were also considered. This means a smaller value of T_o. Table 1 shows the values of T_o and the corresponding bar diameters used in the analysis.

Simulations were performed for three nail head sizes: 400 mm x 400 mm, 600 mm x 600 mm and 800 mm x 800 mm. The thickness of the nail heads was taken to be 250 mm. For a given nail head size and a given T_o, the strength parameters of the model slopes were varied until the failure state or excessive displacement occurred. The failure state was reached when the prescribed out-of-balance forces at some monitoring points could not be reached, and the displacement/strain varying with the time steps at the same time did not show trend of convergence. A common range of shear strength parameters for saprolithic soils was considered in the simulations.

5.4.2 Results of Analyses

Figures 39 and 40 show respectively the displacement vectors and shear strains at the point of bearing failure for a 600 mm x 600 mm nail head on a 45° slope. Nail heads of other sizes also have the same failure mode which is similar to that considered in HA68/94 (see Figure 22).

Results of the analyses in terms of c' – ϕ' envelope for limiting equilibrium (i.e. bearing failure occurs) for different sizes of soil nail heads are plotted in Figures C1 to C9 in Appendix C. In these plots, the nail head loads are expressed as diameters of steel bars. Figures C1, C2 and C3 show the variation of nail head loads for slope angle of 45° for nail head sizes of 400 mm x 400 mm, 600 mm x 600 mm, and 800 mm x 800 mm respectively. Similarly, Figures C4 to C6 show the variation of nail loads for slope angle 55° and Figures C7 to C9 for slope angle 65°. In each plot, the limit stability line sets a boundary below which the slope models become numerically unstable even without the application of nail head force. Soils below this limit stability line generally have low c' values.

For ease of reference, the plots in Appendix C are simplified and summarised in Table 2 for a common range of c'- ϕ' values of Hong Kong soils and steel bars with allowance for sacrificial thickness. For soils with c'- ϕ' values below the limit stability lines, the nail head sizes in Table 2 are determined from the method proposed by HA68/94. This approach is conservative as HA68/94 ignores soil cohesion. Based on the results of FLAC analyses, nail heads larger than 800 mm x 800 mm would be required for a few cases in which bar of 40 mm diameter was used. Since conservative assumptions have been adopted in the analyses, the maximum nail head size in Table 2 is set to be 800 mm x 800 mm. For the same reason, in few cases where a slightly larger nail head size is obtained from the analysis, the smaller size is still adopted. Conservatism of the assumptions used is discussed in Section 7.1 below.

It should be noted that the bearing capacity of a soil head is related to slope angles, with lower bearing capacity for smaller angles. This is because the overburden pressure at the front section of the soil nails is lower for less steep slope face. This does not mean that a steep slope is more stable than a gentle slope because when the angle of a slope face increases, other failure modes will govern although bearing failure is less critical.

The FLAC analysis was performed with the orientation of T_o at 20° downwards from horizontal. A sensitive analysis has been carried out by varying the orientation of T_o from 10° to 30°. The results do not show any significant differences.

5.4.3 Comparison of FLAC Results with HA68/94

For comparison purpose, nail head sizes were calculated for different nail head loads using the lower bound method adopted in HA68/94 (see Figure 22(a)). In the calculations, the contribution from the pull-out resistance at the active zone was not considered. The slope angle was taken to be 55° and the soil strength parameters were assumed to be c' = 5 kPa, and ϕ' = 38°. Figure 41 compares the results based on HA68/94 with those based on the FLAC analyses given in Appendix C. It shows that the head sizes obtained from the FLAC analyses are mostly smaller than those from HA68/94, probably because the latter assumes c' = 0.

6. LOCAL INSTABILITY OF SOIL BETWEEN NAIL HEADS

Soil between the nail heads is unsupported. It is susceptible to local failure on steep slopes, especially when the nail head spacing is large and the soil is saturated with water.

Plates 3 and 4 show examples of such failures. An analysis has been performed to investigate local instability of the soil between the nail heads. Both dry and wet conditions of the soil were considered in the analysis.

A sliding failure mechanism as shown in Figure 42 was considered in the analysis. The shape of the sliding soil wedge is similar to that observed by Plumelle & Schlosser (1990), see Figure 5. It was assumed that owing to the soil arching effect above and below the soil wedge, the overburden pressure above the horizontal plane AB was transferred to the surrounding soil and nail heads and would not act on the soil wedge.

For the wet condition, groundwater level was assumed to be at the slope surface and the water was flowing in the soil in a direction parallel to the slope face. This mainly accounts for the situation that a transient water table is perched near the slope surface during heavy rain. Soil movements are required for mobilizing resistance in the soil nails. They may increase the permeability of the soil mass near the slope surface (due to opening up of relict joints or formation of new cracks), leading to the formation of the transient water table. Besides, perched water table may be developed due to heterogeneity in soil permeability. The forces considered on the soil wedge are illustrated in Figure 42.

Figure 43 shows the typical critical vertical distances between nail heads derived from the analysis. Sliding of the soil wedge will occur if the critical vertical distance is exceeded. It can be noted from the Figure that the critical vertical distances decrease significantly when the soil changes from dry to wet. They are more sensitive to c' than ϕ' of the soil.

From the result of the analysis, the thickness of the soil wedge (plane AB in Figure 42) at limit equilibrium decreases with increasing slope angles. It also reduces from dry condition to wet condition.

7. DISCUSSION

7.1 Soil Nail Head

Soil nail heads serve the following functions:

(a) working as a reaction pad for the mobilization of tensile force in the soil nail and confining the soil in the active zone, and

(b) preventing local failure between nails.

The confinement effect provided by nail heads is particularly important for nailed excavations, which usually involve relief of stress. Failures with the active zone sliding off from front of soil nails have been observed in temporary nailed excavation in Hong Kong (see Plates 1 and 2). This emphases the need for timely installation of adequately sized soil nail heads. Soil movement is necessary to mobilise the nail resistance even if rigid nail heads are provided. In cases where unfavourably oriented relict discontinuities are present in the soil mass (e.g. sub-vertical relict joints striking in the same direction of the slope), small soil movement can open up the discontinuities and thereby weaken the mass strength of the soil (Shiu et al, 1998). For such cases, other stabilization measures that cause less soil

movements should also be considered.

The bearing capacity of soil behind nail head has been reviewed and analysed. The results derived from the FLAC simulations provide a rational basis for dimensioning soil nail heads. Adoption of these nail head sizes given in Table 2 will make bearing failure in soil not a critical failure mechanism and improve the stability of soil between nail heads. Under the same nail head load, the lower bound method given in HA68/94 (U.K. Department of Transport, 1994) generally gives more conservative results than Table 2.

Table 2 as well as the plots contained in Appendix C have been devised based on the ultimate bearing capacity of the nail head in soil. No additional safety factor is considered necessary for the following reasons:

(a) a factor of safety against overall stability has been applied when calculating the stabilization force required from the soil nails;

(b) the maximum tension force to be developed in the soil nail has been assumed to be totally transferred to the nail head (i.e. $T_o = T_{max}$) and the soil/nail friction at the active zone is ignored; and

(c) in soil nail design, the design nail force is usually less than $0.55f_y$.

7.2 Local Stability of Soil between Nail Heads

The result of analysis shows that local instability of the soil between nail heads could occur on steep slopes, particularly when the soil is saturated. HA68/94 suggests that netting and pin could be used to prevent superficial "sloughing" of the soil from happening. The details are shown in Figure 44.

Rüegger et al (2001) describe the use of high-tensile wire mesh in combination with soil nails for preventing local instabilities. This method makes use of the high tensile capacity of the wire mesh to retain the soil between soil nails. The mesh is fixed and often pretensioned to soil nails. The force required to support the soil will be transmitted to the soil nails through the connections of the mesh and the nail heads. Figure 45 shows the mechanism.

For LPM works in Hong Kong, a steel mesh is used in conjunction with a non-degradable erosion protection mat as part of the prescriptive measures for erosion protection works. The steel mesh is laid on top of the mat. Both the mesh and mat are fixed onto the slope surface by galvanised steel pins and connected to the nail heads by anchor bolts. Details of this prescriptive approach can be found in Appendix C to Wong et al (1999). Typical fixing details are given in CEDD Standard Drawing No. C2511 (see Figure 46).

The prescriptive method used in the LPM works is similar to that recommended in

HA68/94 and Rüegger et al (2001). In a recent exercise on assessing the effectiveness of erosion control mats, a number of slopes on which the prescriptive method has been applied have been inspected. No local instability has been found on the slopes inspected but soil erosions are still observed on some steep and high slopes. The reason of the erosion is that the vegetation fails to establish and grow because of the steep gradients of the slopes. The inspections also reveal that on such slopes, the wire mesh can help control the surface erosion. Should erosion occur, the debris is trapped between the wire mesh and the slope surface. This acts like a protective layer to prevent further erosion from happening.

8. RECOMMENDED DESIGN METHODS

8.1 Nail Head Size and Layout

It is recommended that the following three methods may be used for sizing nail heads,

(a) the design chart presented in Table 2,

(b) the lower-bound method proposed by HA68/94 (modified to ignore pull-out resistance at the active zone), and

(c) the prescriptive design approach as shown in Table 3.

For design method (a), details for the derivation of the design guidance given in Table 2 are presented in Section 5.4. The required nail head size (either 400 mm square, 600 mm square or 800 mm square) can be determined from the Table based on the slope face angle and the shear strength of the material behind the nail head.

For design method (b), the lower bound solution proposed in HA68/94 provides a rational basis for sizing soil nail heads. As discussed in Section 5.4.1 above, it would be more appropriate to disregard the pull-out resistance mobilised at the active zone when determining the nail head load. The HA68/94 method has been modified by ignoring the pull-out resistance at the active zone. The modified method is shown in Figure 47.

Steel bars used in prescriptive soil nail designs are either 25mm or 32 mm in diameter. From Table 2, the nail head sizes required for the two bar diameters are mostly 400 mm x 400 mm or 600 mm x 600 mm. A larger size of 800mm x 800mm is required only for slopes of smaller angles and lower soil shear strength. For prescriptive soil nail designs, the upper bound nail head sizes derived from the FLAC analyses could be used. Although there is not much experience in using the nail head sizes, they are considered to be adequately conservative. Details of the prescriptive design approach are given in Table 3.

For situations where large nail head sizes with close spacing are required, alternative forms of soil nail heads such as concrete grillage beams may be considered.

Local instability may occur on soil between nail heads. The current prescriptive approach of using steel mesh together with non-degradable erosion protection mat is considered to be an effective means of controlling local failures and surface erosion. This method is similar to the approaches used in other countries. Despite this, the method would not be able to completely prevent local instability on very steep slopes. In those cases, a

hard surface cover may have to be used.

8.2 Structural Design

The structural design of the nail heads shall follow the recommendations stipulated in relevant structural design codes. Nail force acting uniformly on the nail head may be assumed in the structural design.

8.3 Aesthetics

Exposed nail heads may have substantial influence on the appearance of a slope. Guidance on visual treatment of soil nail heads as given in GEO (2000) should be followed. In addition, recessed soil nail head with details similar to those shown in Figure 48 may be used.

9. CONCLUSIONS

The effect of soil nail head on stability of slopes has been examined analytically in this study. The results of the analysis together with previous research results and experiences attest to the benefits of soil nail heads to slope stability. Tensile force in the nails at the connections to nail heads effectively confines the soil immediately behind the head. This confinement effect can significantly increase the stability of the soil in the active zone.

Nail head design methods being used by overseas countries take into account the confinement effect. Also, loads induced in the nail heads are considered in the design. Bearing capacity failure of nail head in soil is a failure mode that needs to be considered in the design of nail head. Numerical simulations have been performed to study this aspect. Plots of nail head sizes derived from the simulations have also been prepared.

Three different design methods are proposed for determining the sizes of soil nail heads.

10. REFERENCES

Babu, G.L.S., Murthy, B.R.S. & Srinivas, A. (2002). Analysis of Construction Factors Influencing the Behaviour of Soil-Nailed Earth Retaining Walls. Ground Improvement, 6, No. 3, pp 137-143.

BSI (1995). Code of Practice for Strengthened/Reinforced Soils and Other Fills (BS 8006). British Standards Institution, London, U.K., 176p.

Dawson, E.M., Roth, W.H. and Drescher, A. (1999). Slope stability analysis by strength reduction. Géotechnique, Vol. 49, No. 6, pp 835-840.

Department of Transport (1994). Design Manual for Roads and Bridges: Design Methods for the Reinforcement of Highway Slopes by Reinforced Soil and Soil Nailing Techniques, HA68/94, Department of Transport, UK.

Duncan, J.M. (1996). State of the art: limit equilibrium and finite element analysis of slopes. Journal of Geotechnical Engineering. ASCE 122, No. 7, pp 577-596.

Ehrlich, M., Almeida, M.S.S. & Lima, A.M. (1996). Parametric Numerical Analyses of Soil Nailing Systems. Earth Reinforcement. (edited by H. Ochiai, N. Yasufuku & K. Omine), Balkema, Rotterdam, pp 747-752.

Elias, V. & Juran, I. (1991). Soil Nailing for Stabilization of Highway Slopes and Excavations. U.S. Department of Transportation, Federal Highway Administration, Washington, D.C.

FHWA (1998). Manual for Design & Construction monitoring of Soil Nail Walls. Federal Highway Publication No. SA-96-069R, U.S. Department of Transportation, Federal Highway Administration, Washington, D.C.

French National Research Project (1991). Recommendations Clouterre: Soil Nailing Recommendations for Designing, Calculating, Constructing and Inspecting Earth Support Systems Using Soil Nailing (English Translation), Presses de lecole Nationale des Ponts et Chaussees.

Gässler, G., and Gudehus, G., 1981. Soil Nailing - Some Aspects of a New Technique, Proceedings of Tenth International Conference on Soil Mechanics and Foundation Engineering, Vol. 3, Session 12, Stockholm, pp 665-670.

GEO (2000). Technical Guidelines on Landscape Treatment and Bio-engineering for Man-made Slopes and Retaining Walls (GEO Publication No. 1/2000). Geotechnical Engineering Office, Hong Kong, 146p.

GEO (2004). Detailed Study of the May 2003 and 13 June 2003 Landslides on Slopes No. 6NE-B/C8 Fan Kam Road, Pat Heung. Landslide Study Report LSR 1/2004. Geotechnical Engineering Office, Hong Kong, 51p.

Gutierrez V. & Tatsuoka, F. (1988). Roles of Facing in Reinforcing Cohesionless Soil Slopes by Means of Metal Strips. Proceedings of the International Geotechnical Symposium on Theory and Practice of Earth Reinforcement, IS Kyushu '88, Fukuoka, Balkema, Rotterdam, pp 289-294.

Hayashi, S., Ochiai, H., Yoshimoto, A., Sato, K. & Kitamura, T. (1988). Functions and effects of reinforcing materials in earth reinforcement. Proceedings of International Geotechnical Symposium on Theory and Practice of Earth Reinforcement, IS Kyushu '88, Fukuoka, Balkema, Rotterdam, pp 99-104.

Hong, Y.S., Wu, C.S. & Chen, R.H. (2003). Mechanical Behaviour of Vertical Excavated Nailed Walls. Journal of the Southeast Asian Geotechnical Society, August, pp 87-99.

Table of Contents
Table of Contents
Table of Contents
Table of Contents

Itasca (1996). Fast Lagrangian Analysis of Continua (FLAC) Manual, Version 4.0. Itasca Consulting Group, Inc., Minnesota.

Japan Highway Public Corporation (JH) (1998). Design & Works Outlines on the Soil-Cutting Reinforcement Soilworks (English Translation), Japan Highway Public Corporation.

Jewell, R.A. & Pedley, M.J. (1992). Analysis for Soil Reinforcement with Bending Stiffness. Journal of Geotechnical Engineering, ASCE. 118(10): pp 1505-1528.

Jewell, R.A. & Wroth, C.P. (1987). Direct Shear Tests on Reinforced Soil. Géotechnique, Vol.37, No.1, pp 53-68.

Joshi, B. (2003). Behaviour of Calculated Nail Head Strength in Soil Nailed Structures. Journal of Geotechnical and Geoenvironmental Engineering, ASCE, September, pp 819-828.

Kitamura, T., Nagao, A. & Uehara, S. (1988). Model Loading Tests of Reinforced Slope with Steel Bars. Proceedings of the International Geotechnical Symposium on Theory and Practice of Earth Reinforcement, IS Kyushu '88, Fukuoka, Balkema, Rotterdam, pp 311-316.

Krahn, J. (2003). The 2001 R.M. Hardy Lecture: The limits of limit equilibrium analyses. Canadian Geotechnical Journal, Vol. 40, pp 643-660.

Love, J. (2003). Private communication.

MGSL (2003). Soil Nail Head Review Report (Final). Report prepared under Consultancy Agreement No. CE76/2001(GE) - 10 Year Extended LPM Project, Phase 3, Package D for the Civil Engineering Department of HKSAR Government, April. Maunsell Geotechnical Services Ltd.

Miki, H., Fukuda, N., Murata, O., Tayama, S., Yamamoto, A., Otani, Y. & Yokota, Y. (1997). Present State and Perspective of Design Methods of Reinforced Soil Structures. Earth Reinforcement, (edited by H. Ochiai, N. Yasufuku & K. Omine), Balkema, Rotterdam, pp 1147-1158.

Mitchell, J.K., & Villet, W.C.B. (1987). Reinforcement of earth slopes and embankments. National Cooperative Highway Research Program Report No. 290, Transport Research Board, Washington, D.C., 323 p.

Muramatsu, M., Nagura, K., Sueoka, T., Suami, K. & Kitamura, T. (1992). Stability analysis for reinforced cut slopes with facing. Proceedings of the International Symposium on Earth Reinforcement Practice, (edited by H. Ochiai, S. Hayashi & J. Otani) Fukuoka, Kyushu, Japan, 11-12 November, pp 503-508.

Murray, R.T. (1993). The Development of Specifications for Soil Nailing. Research Report 280, Transport Research Laboratory, Department of Transport, UK.

Plumelle, C., & Schlosser, F. (1990). A French National Research Project on Soil Nailing: Clouterre. Performance of Reinforced Soil Structures, British Geotechnical Society, (edited by A. McGown, K.C. Yeo & K.Z. Andrawes), pp 219-223.

Rüegger, R., Flum, D. & Haller, B. (2001). Slope Stabilisation with High-Performance Steel Wire Mesh in Combinations with Nails and Anchors. Proceedings of International Conference on Landslides - Causes, Impacts and Countermeasures, 17-21 June, Davos, Switzerland (edited by H.H. Einstein, E. Krauter, H. Klapperich & R. Pöttler), pp 597-606.

Shiu, Y.K., Yung, P.C.Y., & Wong, C.K. (1997). Design, Construction and Performance of Soil Nailed Excavation in Hong Kong. Proceedings of the XIVth International Conference on Soil Mechanics and Foundation Engineering, 6-12 September, Hamburg, Germany, pp 1339-1342.

Shiu, Y.K., Lai, A.C.S. & Lee, J.W. (1998). Investigation and Design of Remedial Works for Two Cut Slopes in Hong Kong. Proceedings of the Thirteenth Southeast Asian Geotechnical Conference, 16-20 November, Taipei, pp 643-648.

Stocker, M.F. & Riedinger, G. (1990). The Bearing Behaviour of Nailed Retaining Wall. Proceedings of Design and Performance of Earth Structure, Geotechnical Special Publication No. 25, ASCE. (edited by Lambe and Hansen), pp 613-628.

Tatsuoka, F. (1992). Keynote Lecture: Roles of Facing Rigidity in Soil Reinforcing. Proceedings of the International Symposium on Earth Reinforcement Practice, (edited by H. Ochiai, S. Hayashi & J. Otani) Fukuoka, Kyushu, Japan, 11-12 November, pp 831-870.

Tayama, S., Kawai, Y. & Maeno, H. (1996). An investigation of the durability of the soil nailing method. Proceedings of the International Symposium on Earth Reinforcement, Kysuhu, A.A. Balkema Publishers, Rotterdam, pp 161-166.

Tei, K., Tayor, R.N. & Milligan, G.W.E. (1998). Centrifuge Model Tests of Nailed Soil Slopes. Soils and Foundations, Vol. 38, No. 2, June, Japanese Geotechnical Society, pp 165-177.

Thompson, S.R. & Miller, R. (1990). Design, construction and performance of a soil nailed wall in Seattle, Washington. Proceedings of a Conference on Design and Performance of Earth Retaining Structures, Geotechnical Special Publication No. 25, June 18-21, 1990, New York, pp 629-643.

Watkins, A.T. & Powell, G.E. (1992). Soil nailing to existing slopes as landslip preventive works. Hong Kong Engineer, March, pp 20-27.

Wong, H.N., Pang, L.S., A.C.W., Pun, & Yu, Y.F. (1999). Application of Prescriptive Measures to Slopes and Retaining Walls. Geotechnical Engineering Office, Hong Kong, 73 p. (GEO Report No. 56, Second Edition)

Table of Contents
Table of Contents
Table of Contents
Table of Contents

LIST OF TABLES

Table 1 - Sizes of Steel Bars and Corresponding Nail Head Loads

Diameter of Steel Bar (mm)	Nail Head Load, T_o (kN) ($T_o = 0.23 \times A_s$)
25	113
(21)	79.7
32	185
(28)	141.6
40	289
(36)	234

Notes: (1) The bracketed values are bar diameters with allowance made for sacrificial thickness provided for corrosion protection.
(2) A_s is the cross-sectional area of steel bar.

Table 2 - Sizes of Square Concrete Soil Nail Heads (For Soil Nail Bars with Allowance for 2 mm Sacrificial Thickness on Radius)

ϕ'	c'(kPa)	45° ≤ Slope Angle < 55°			55° ≤ Slope Angle < 65°			Slope Angle ≥ 65°		
		Steel Bar Diameter (mm)			Steel Bar Diameter (mm)			Steel Bar Diameter (mm)		
		25	32	40	25	32	40	25	32	40
34°	2	800	800	800	600	600	800	600	600	800
	4	600	800	800	600	600	800	600	600	800
	6	600	800	800	400	600	800	400	600	600
	8	600	600	800	400	600	800	400	600	600
	10	400	600	800	400	600	600	400	600	600
36°	2	600	800	800	600	600	800	600	600	800
	4	600	800	800	400	600	800	400	600	800
	6	600	600	800	400	600	800	400	600	600
	8	400	600	800	400	600	600	400	600	600
	10	400	600	800	400	600	600	400	400	600
38°	2	600	800	800	400	600	800	600	600	600
	4	600	600	800	400	600	800	400	600	600
	6	400	600	800	400	600	600	400	600	600
	8	400	600	800	400	600	600	400	400	600
	10	400	600	800	400	400	600	400	400	600
40°	2	600	600	800	400	600	800	600	600	600
	4	400	600	800	400	600	600	400	400	600
	6	400	600	800	400	600	600	400	400	600
	8	400	600	600	400	400	600	400	400	600
	10	400	600	600	400	400	600	400	400	600

Notes:
(1) Dimensions in mm unless stated otherwise.
(2) Only the length of one side of square nail head is shown in the Table.
(3) The minimum thickness of soil nail head should be 250 mm.
(4) The shear strength parameters (c' and ϕ') of the soil near the slope surface should be used.

Table 3 - Prescriptive Soil Nail Head Design for Soil Cut Slopes or the Soil Portion of CR Features

Soil Nail Steel Bar Diameter [1] (mm)	Geology	Square Nail Head Size (mm x mm)	
		Slope Angle < 55°	55° ≤ Slope Angle ≤ 65°
25 or 32	Highly decomposed granitic or volcanic rock.	600 x 600	600 x 600
25 or 32	Soils including colluvial, residual or completely decomposed materials of granitic and volcanic origin, and weathered sedimentary rocks.	800 x 800	600 x 600

Notes:
(1) Refer to GEO Report No. 56 for prescriptive design of soil nails for cut slopes and Special Project Report No. SPR 2/2004 for prescriptive soil nail design for concrete and masonry retaining walls.
(2) The minimum thickness of the nail head should be 250 mm.
(3) For slope angles larger than 65°, reinforced concrete grillage beams instead of isolated soil nail heads should be used.

LIST OF FIGURES

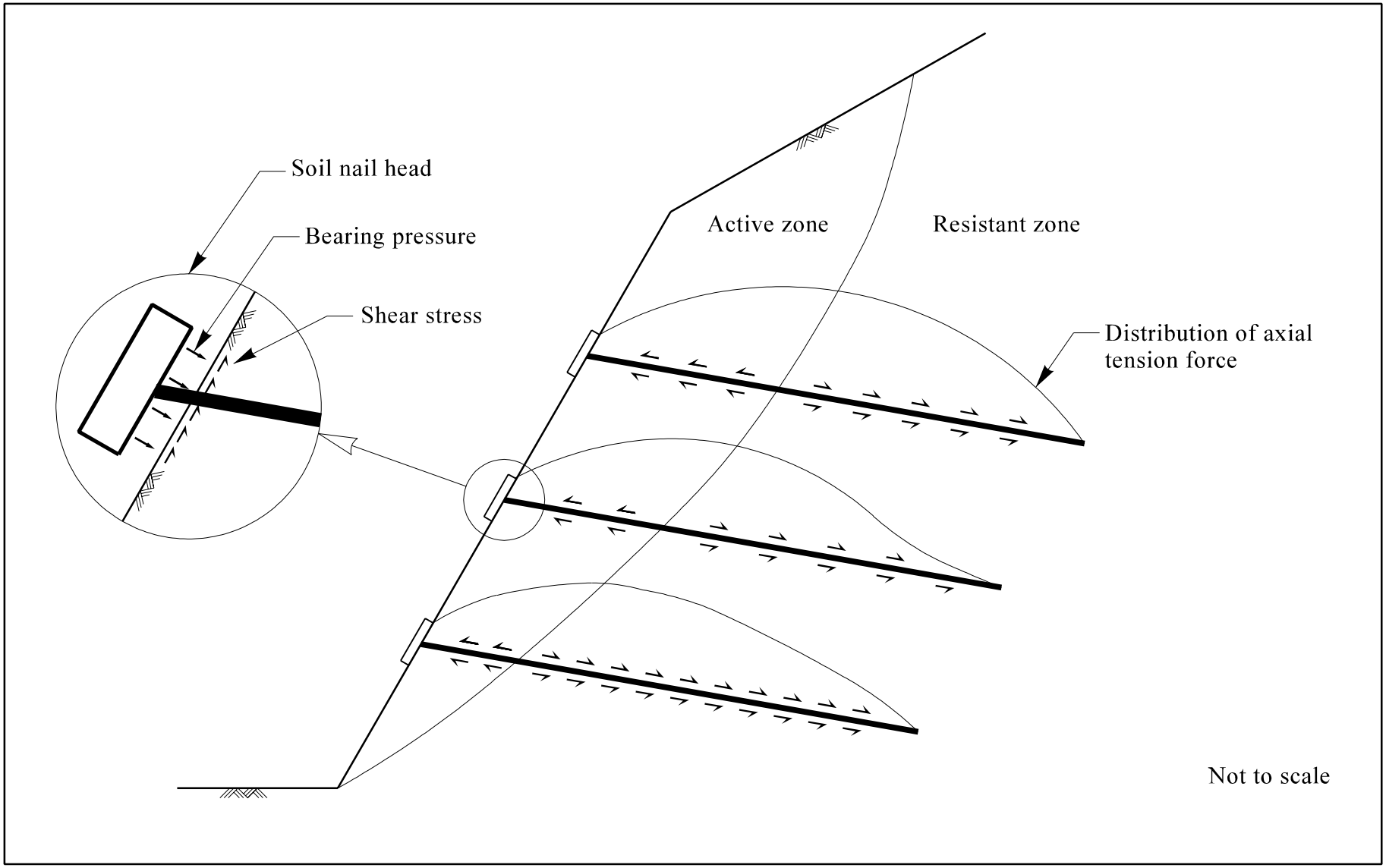

Figure 1 - Load Transfer Mechanism of Soil Nailed Structure

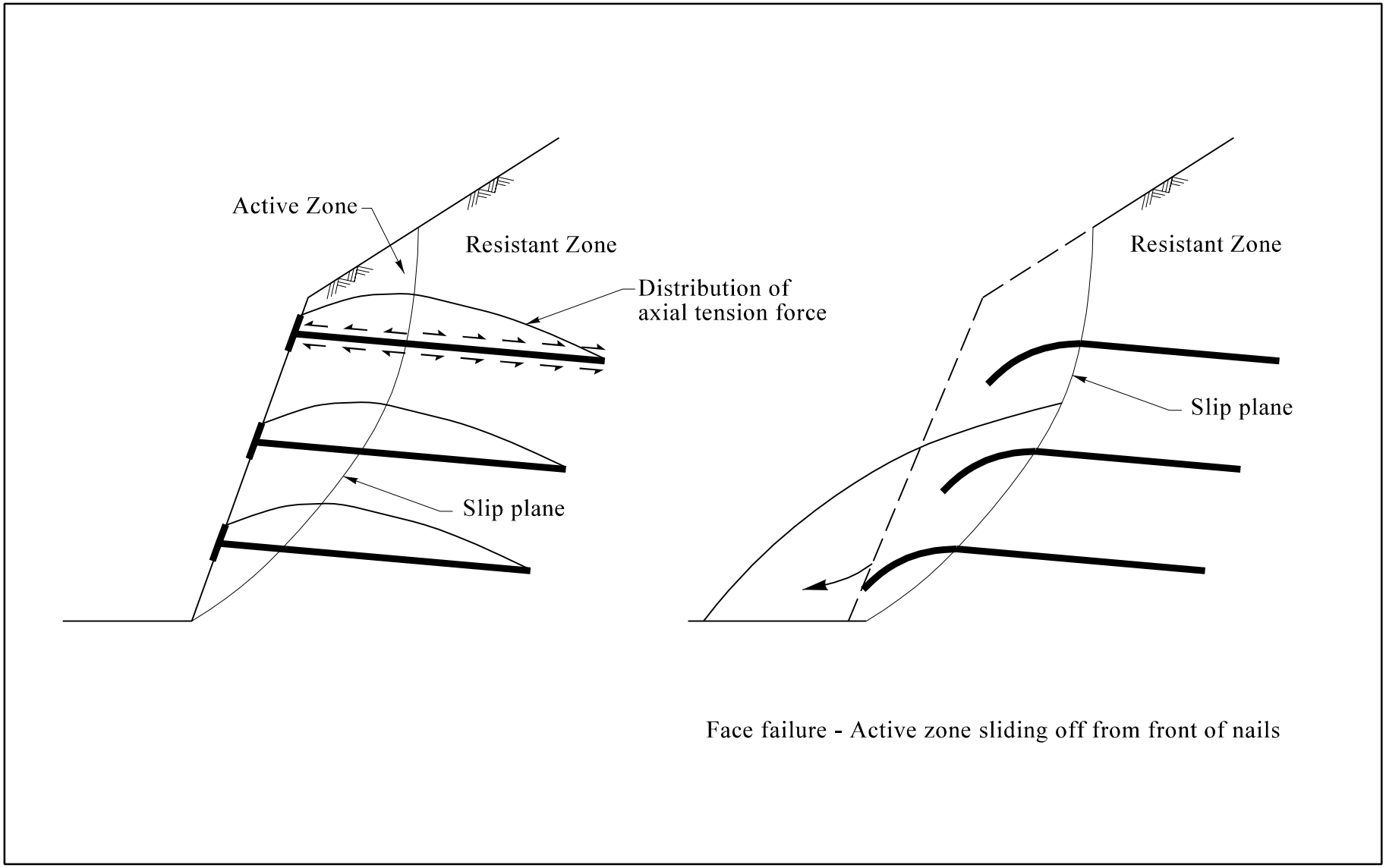

Figure 2 - Failure by Sliding of Active Zone

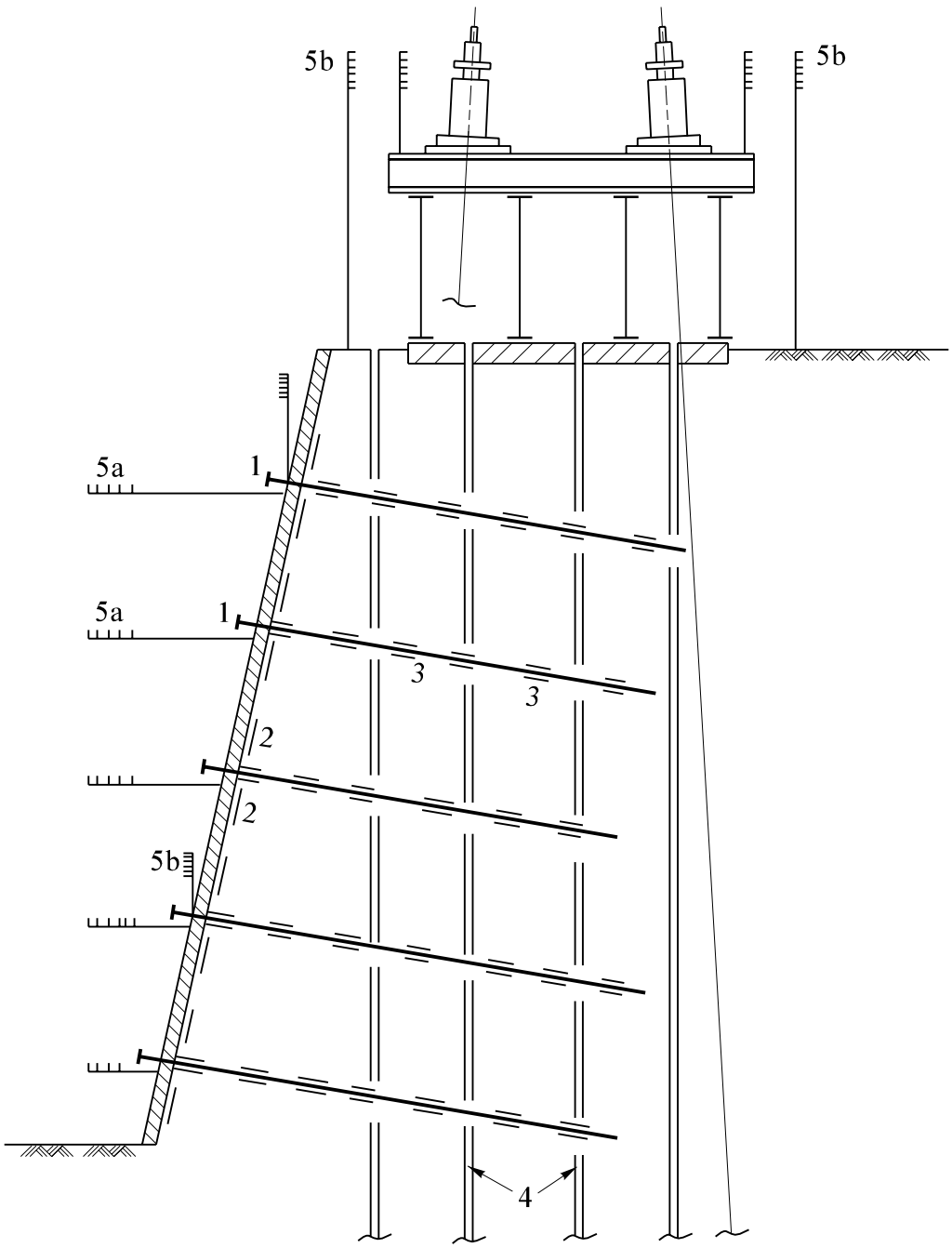

Legend:

1	Gauges for nail forces	2	Earth pressure cells
3	Strain gauges	4	Boreholes for inclinometer
5	Displacement gauges		
	(a) Horizontal		
	(b) Vertical		

Figure 3 - Measuring Facilities of the Test Walls (after Gässler & Gudehus, 1981)

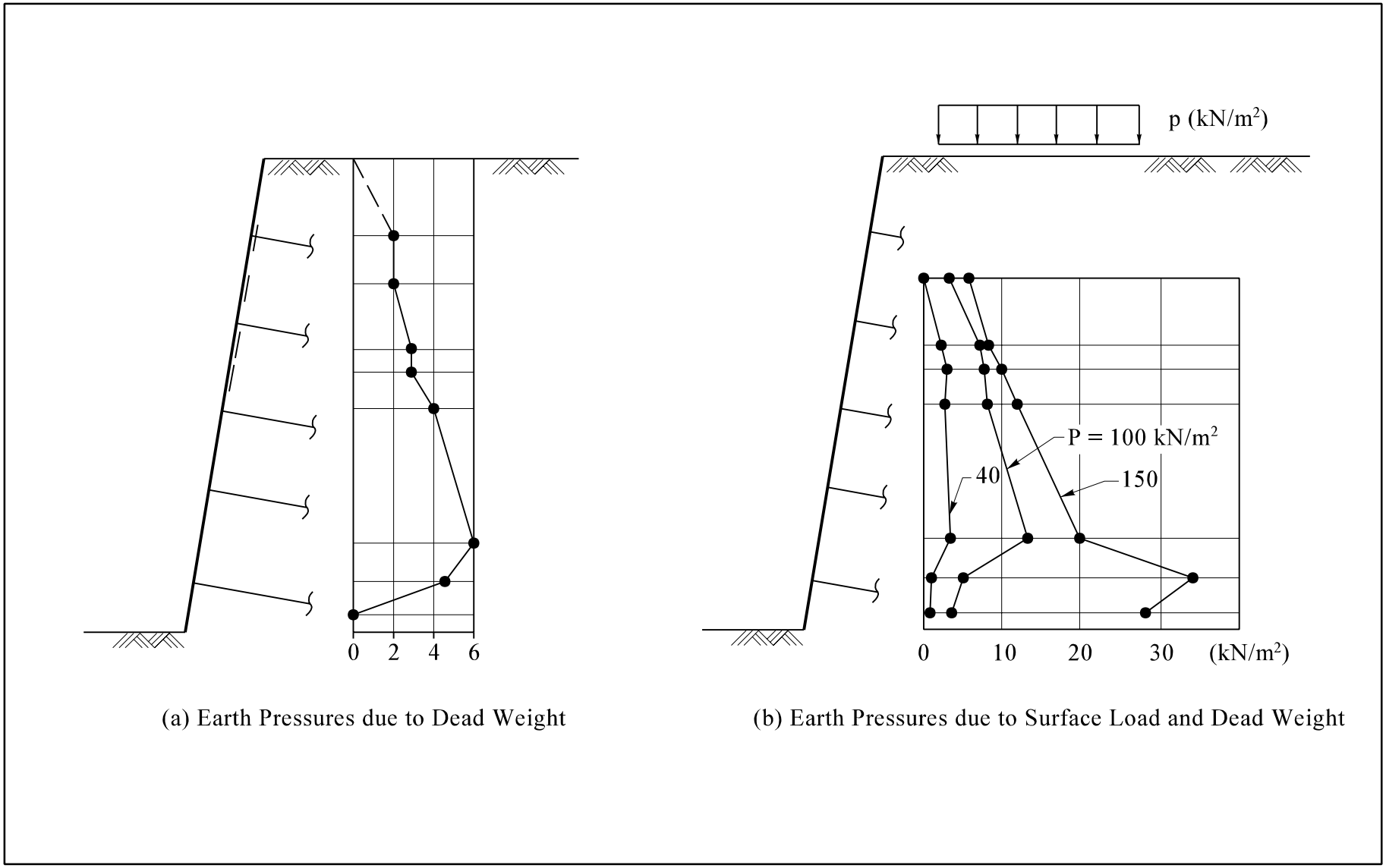

(a) Earth Pressures due to Dead Weight

(b) Earth Pressures due to Surface Load and Dead Weight

Figure 4 - Earth Pressures behind Facing (after Gässler and Gudehus, 1981)

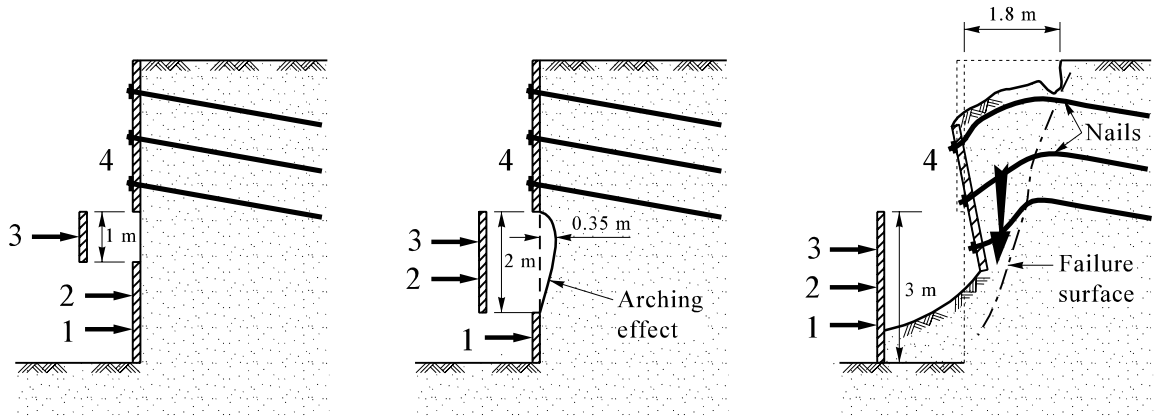

(i) Stable (ii) At Stability Limit (iii) Failure

(a) Stability of Excavation Phases

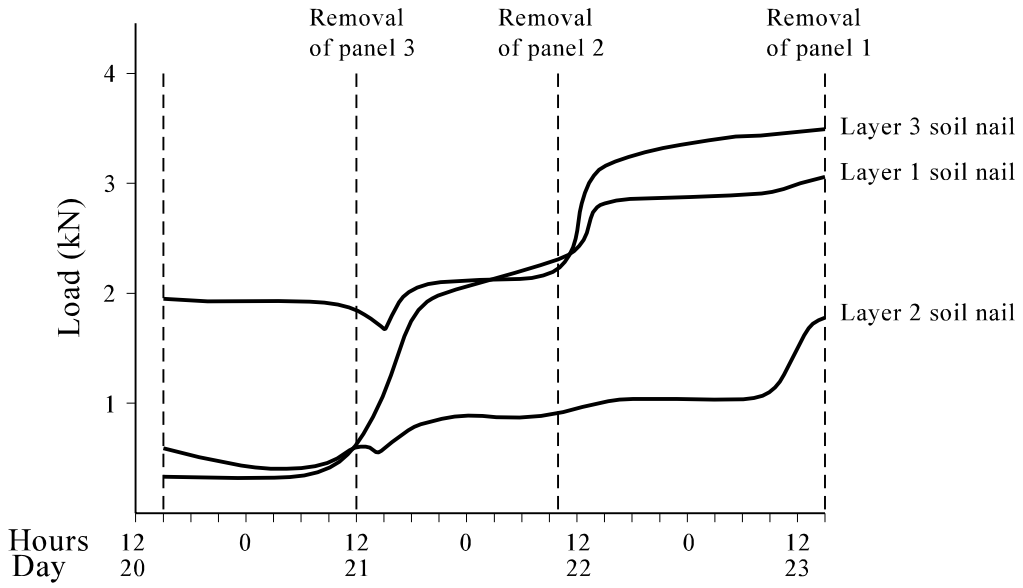

(b) Changes of Load at Nail Heads

Figure 5 - Stability of Excavation and Changes of Load at Nail Heads (after Plumelle and Schlosser, 1990)

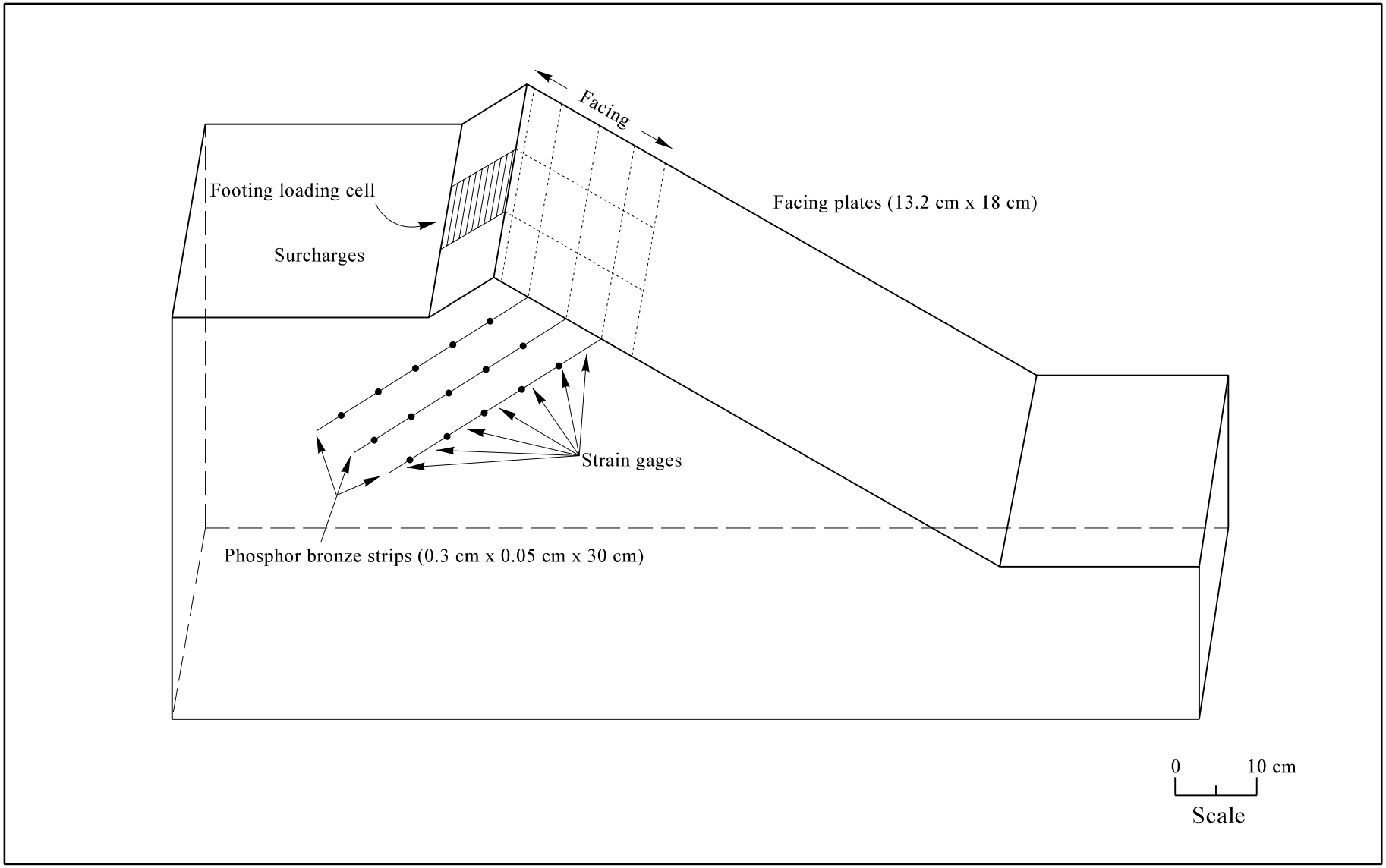

Figure 6 - Instrumentation of Model Slope Reinforced with Metal Strips and Facing (after Gutierrez and Tatsuoka, 1988)

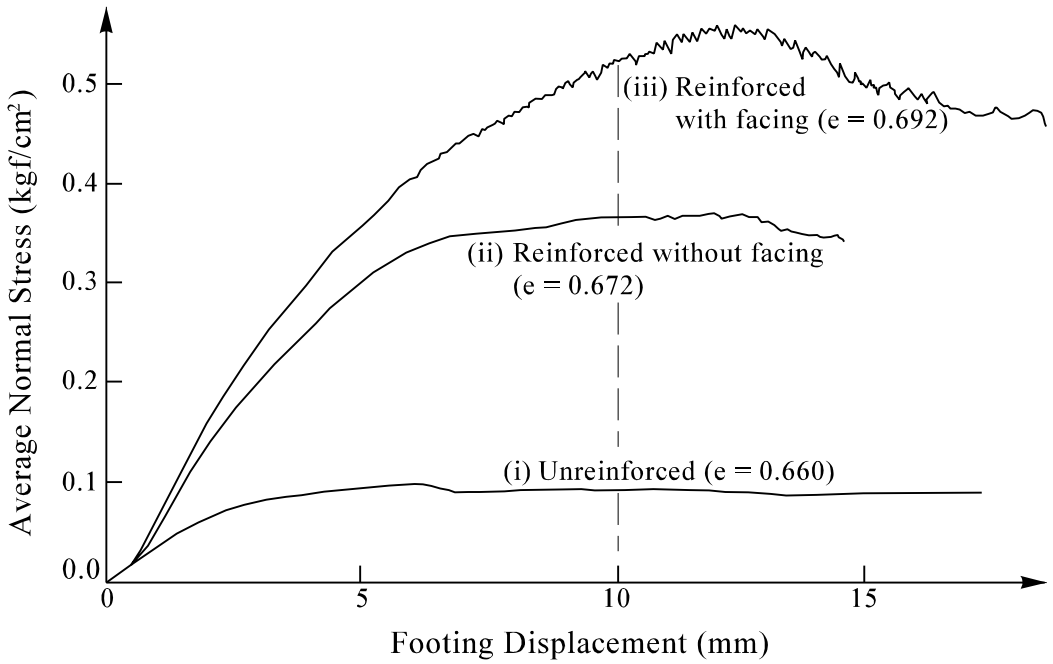

e = Void ratio

Figure 7 - Comparative Normal Stress-Displacement Relationships (after Gutierrez and Tatsuoka, 1988)

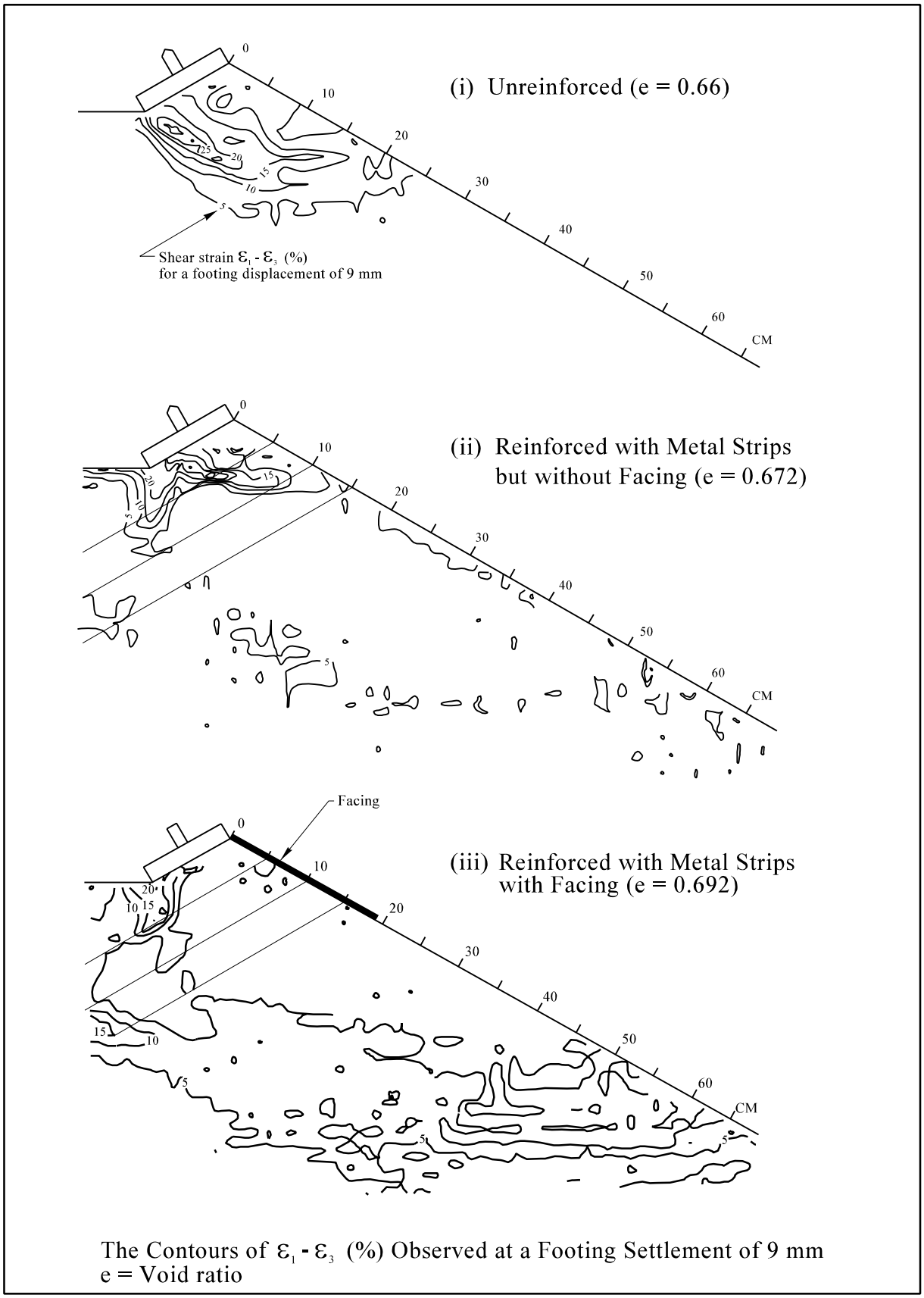

Figure 8 - Loading Tests on the Crest of Model Sand Slopes (after Gutierrez and Tatsuoka, 1988)

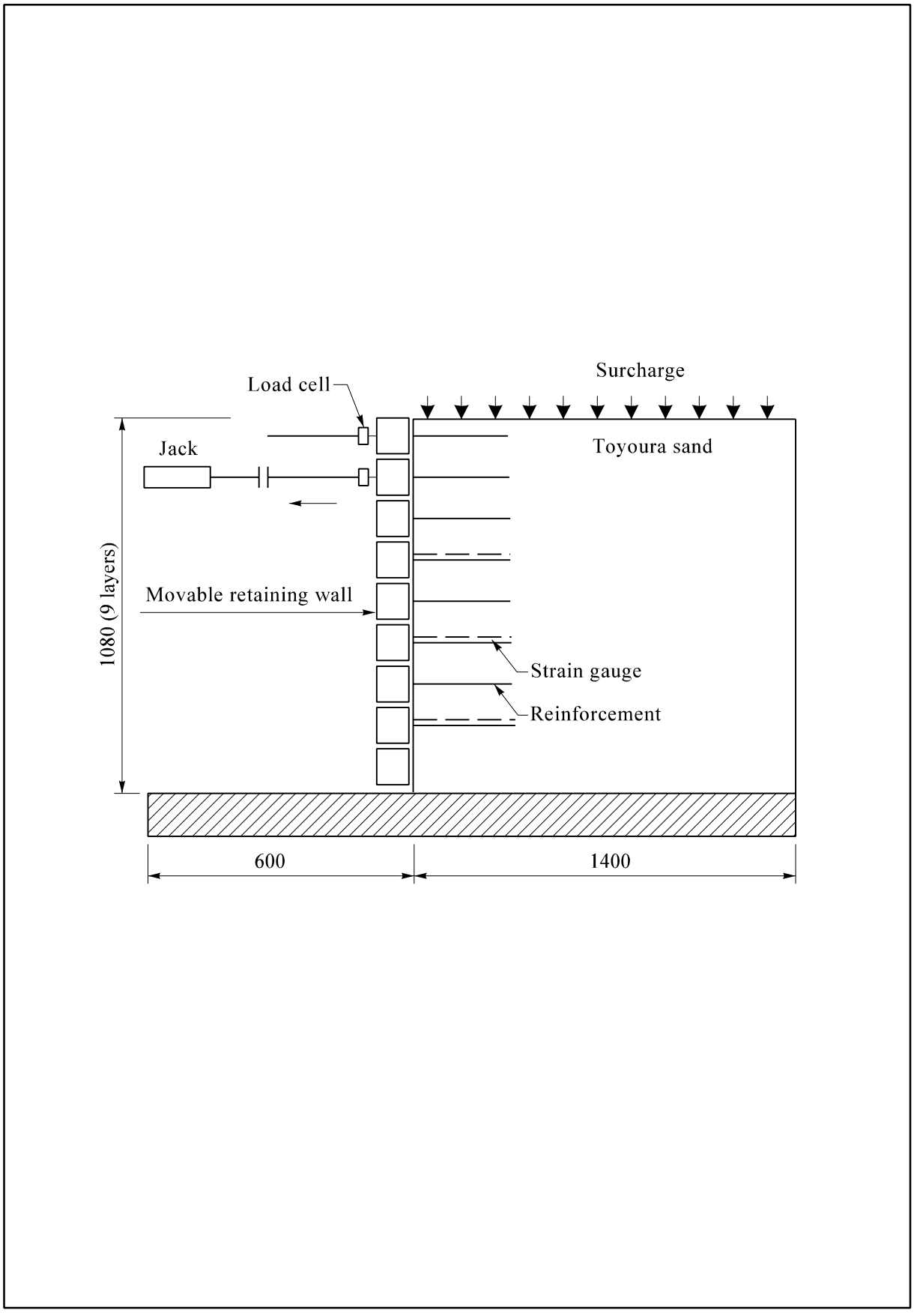

Figure 9 - Set Up of Experimental Model Wall (after Muramatsu et al, 1992)

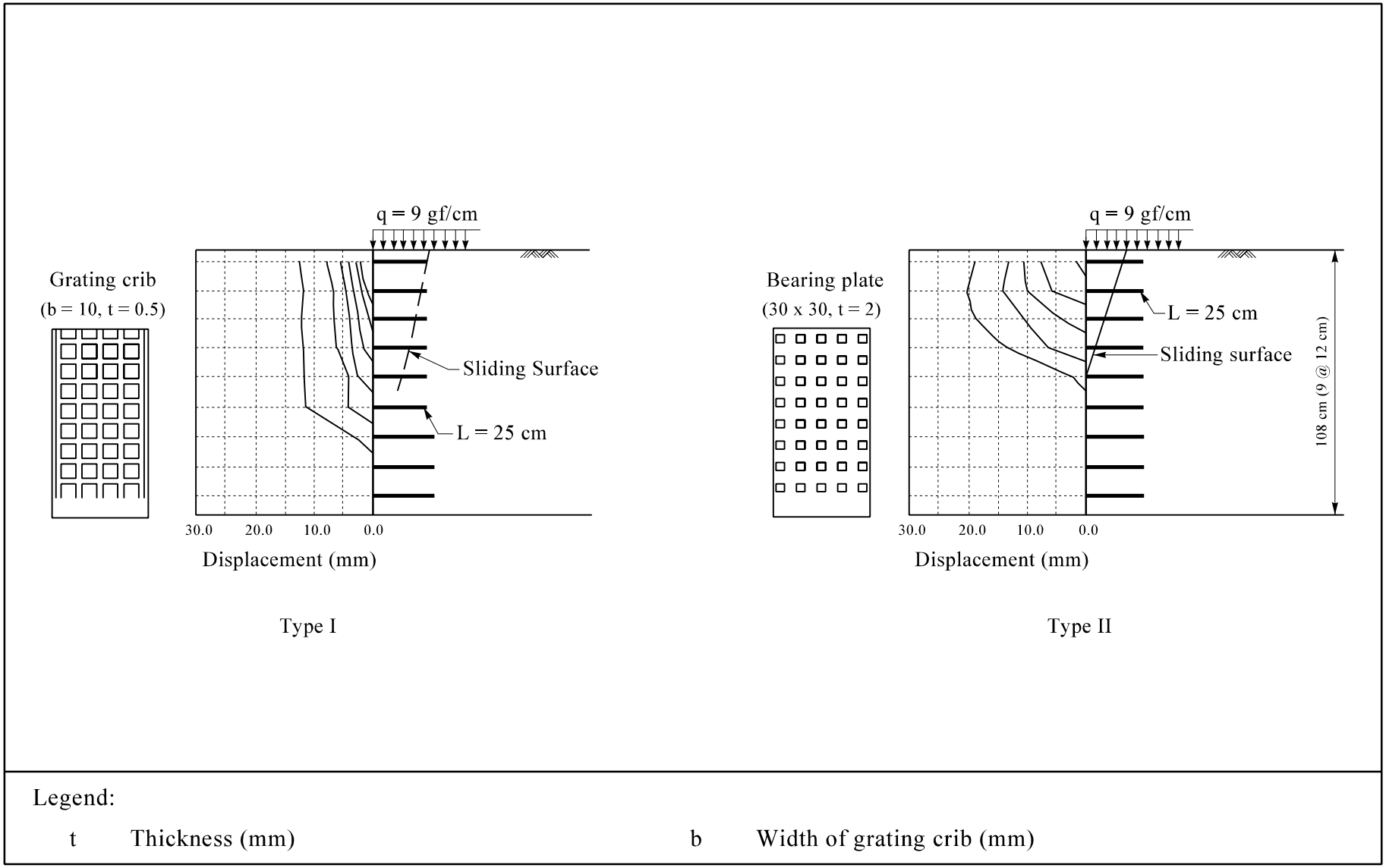

Figure 10 - Slope Facing Types and Reinforced Slope Deformation Modes (after Muramatsu et al, 1992)

Table of Contents
Table of Contents
Table of Contents
Table of Contents
Table of Contents

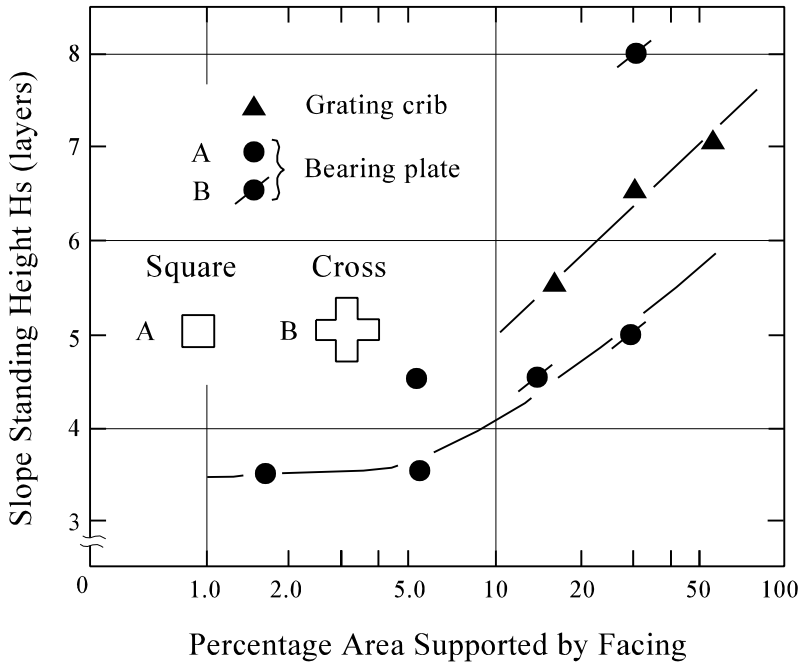

Figure 11 - Slope Standing Height vs Percentage Area Supported by Facing
(after Muramatsu et al, 1992)

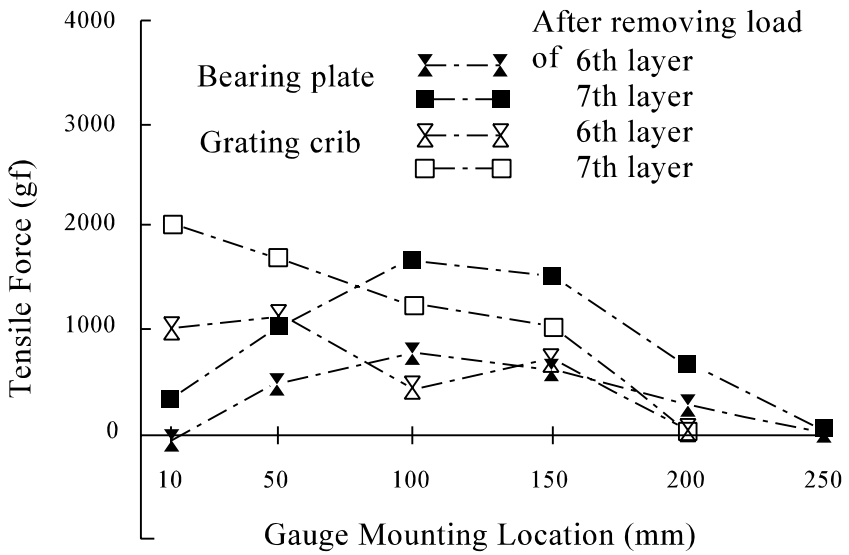

Figure 12 - Effect of Slope Facing on Distribution of Reinforcement Tensile Force (after Muramatsu et al, 1992)

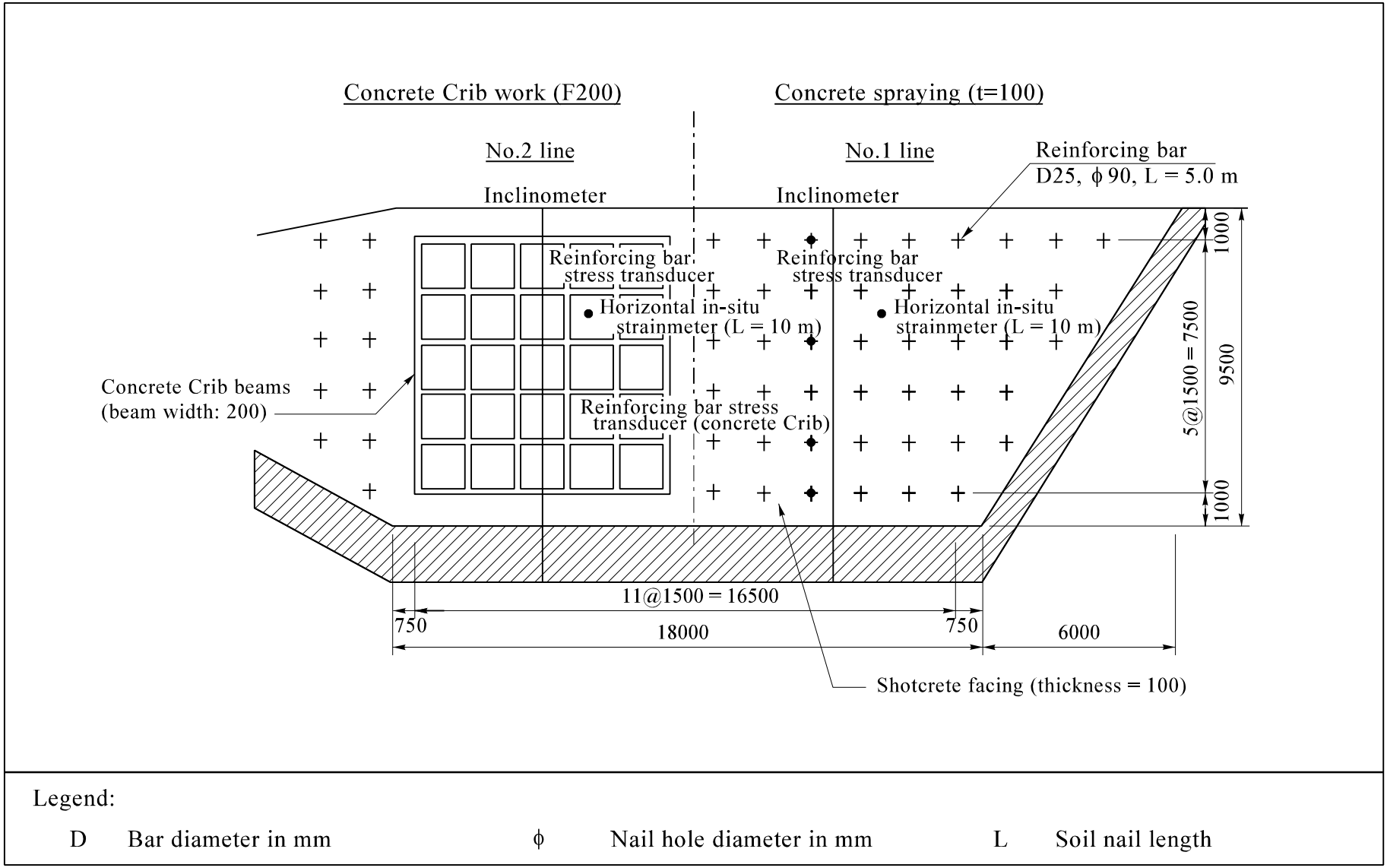

Legend:

D Bar diameter in mm ϕ Nail hole diameter in mm L Soil nail length

Figure 13 - Slope Frontal View and Monitoring Instruments (after Muramatsu et al, 1992)

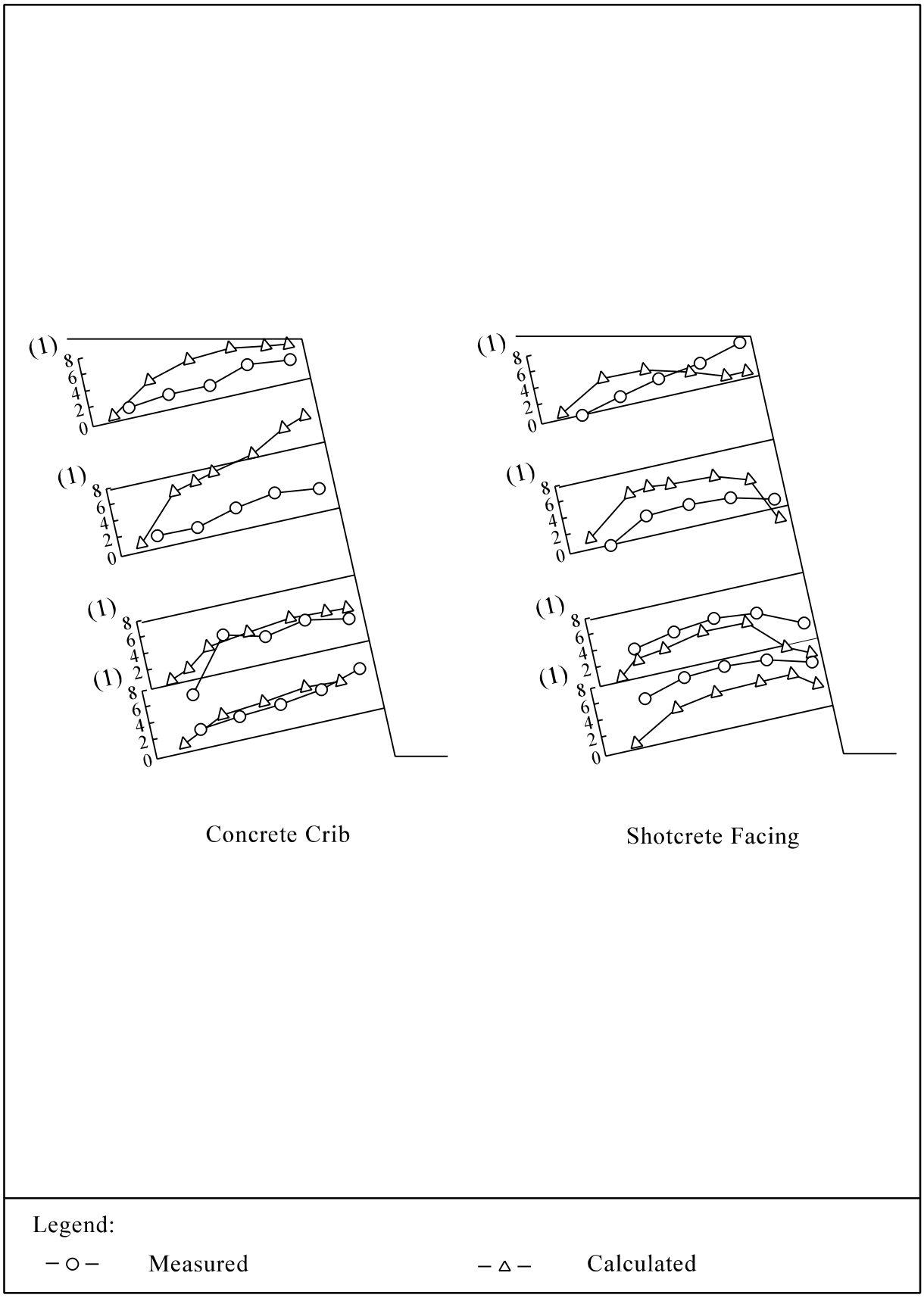

Figure 14 - Distribution of Tensile Force in Reinforcing Bars (after Muramatsu et al, 1992)

Table of Contents
Table of Contents
Table of Contents
Table of Contents

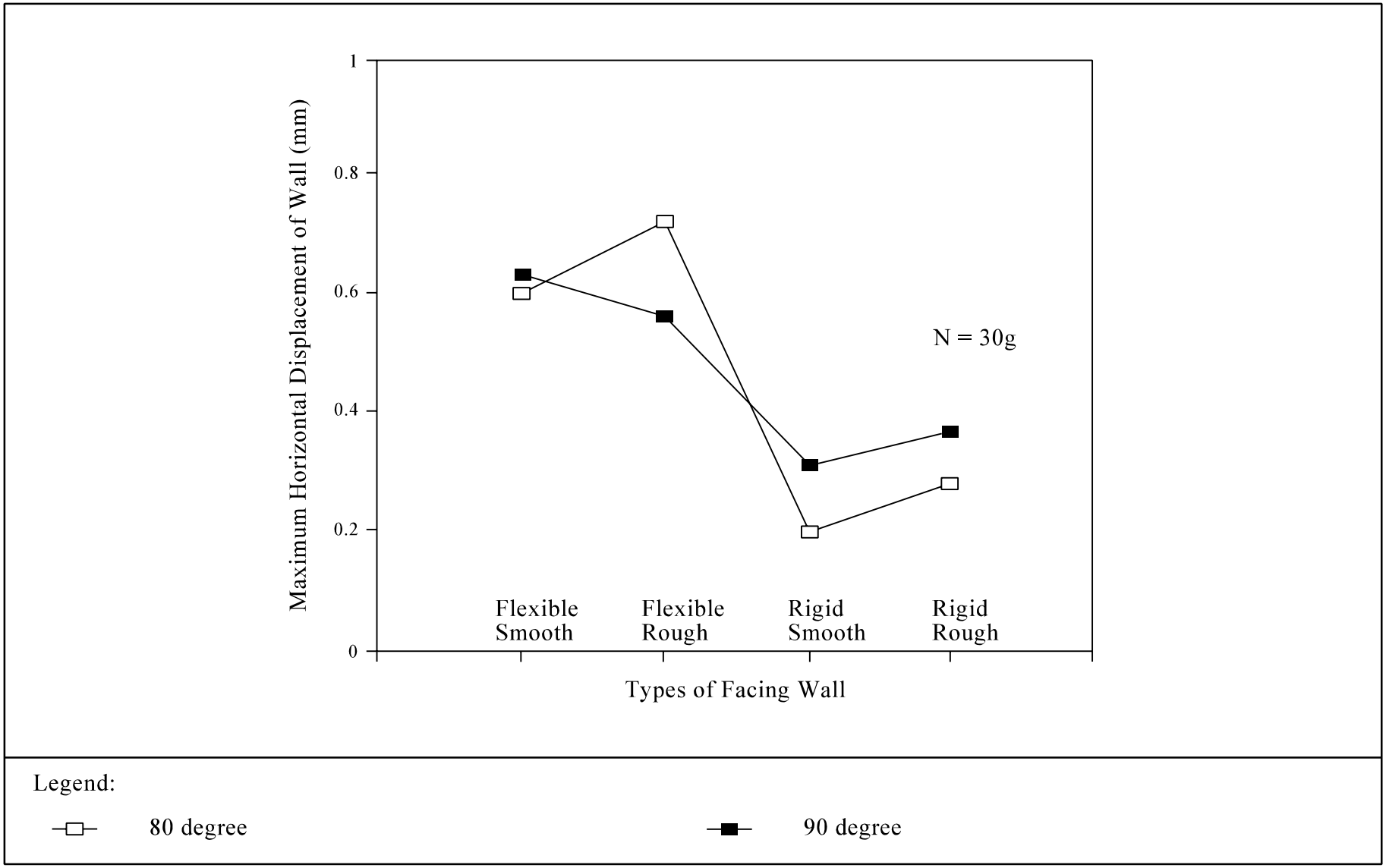

Figure 15 - Horizontal Displacements Related to Facing Roughness and Flexibility (after Tei et al, 1998)

Table of Contents
Table of Contents
Table of Contents
Table of Contents

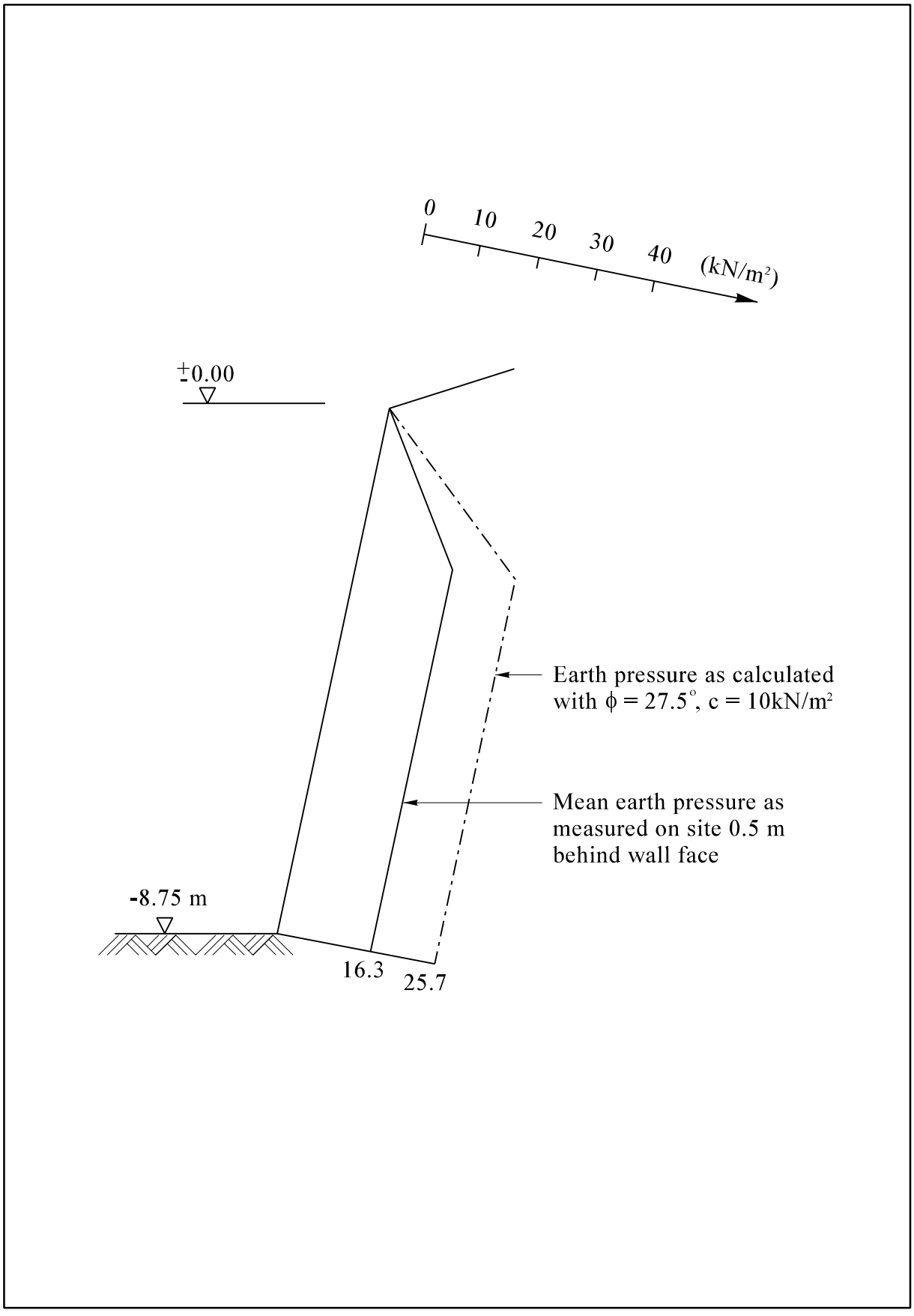

Figure 16 - Earth Pressure Acting on Wall Face at Control Section M 3
(after Stocker & Riedinger, 1990)

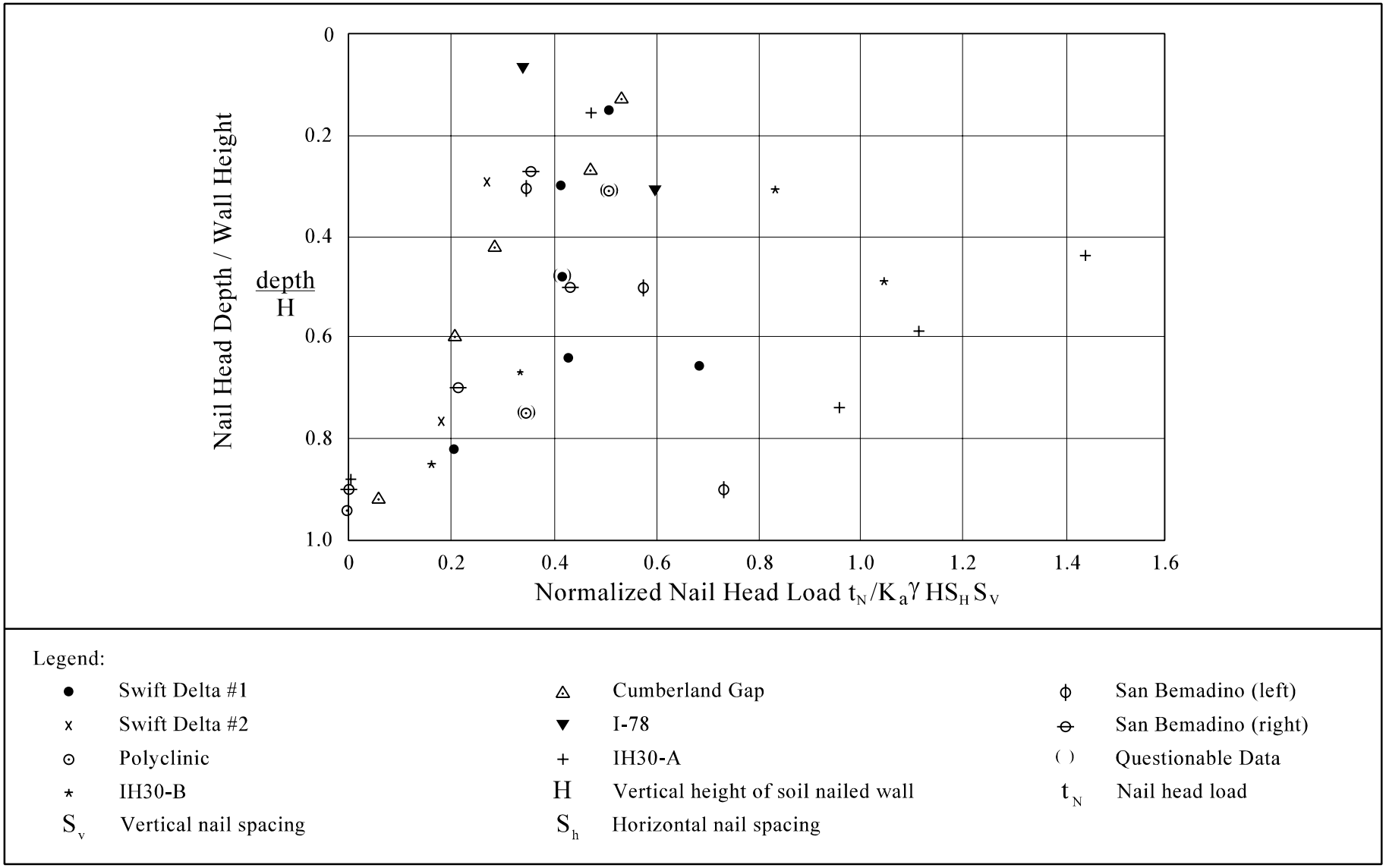

Figure 17 - Normalized Measured Nail Head Loads (after FHWA, 1998)

Table of Contents
Table of Contents
Table of Contents
Table of Contents
Table of Contents

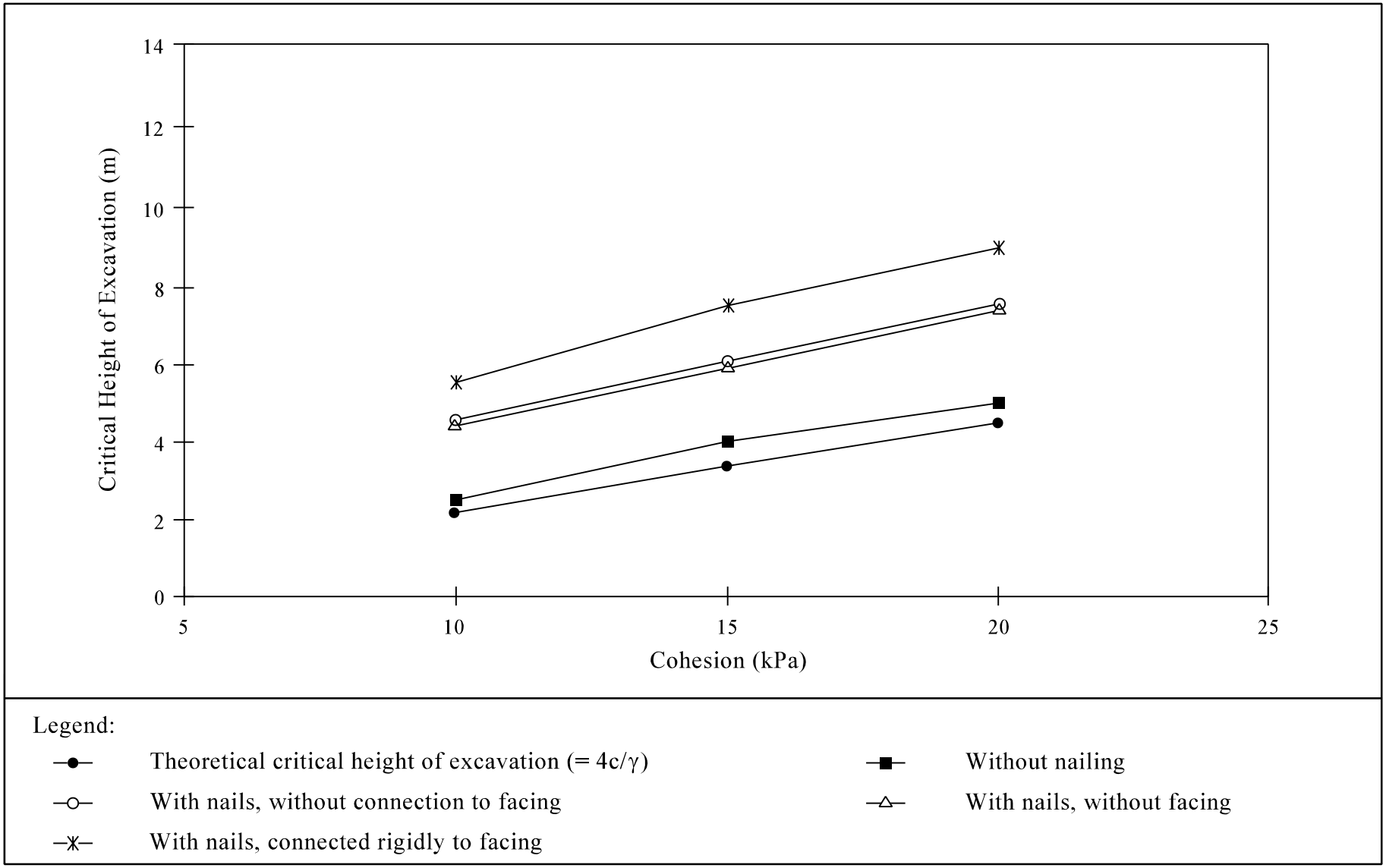

Figure 18 - Variation of Critical Height of Excavation with Connection between Nails and Facing (after Babu et al, 2002)

Table of Contents
Table of Contents
Table of Contents
Table of Contents
Table of Contents

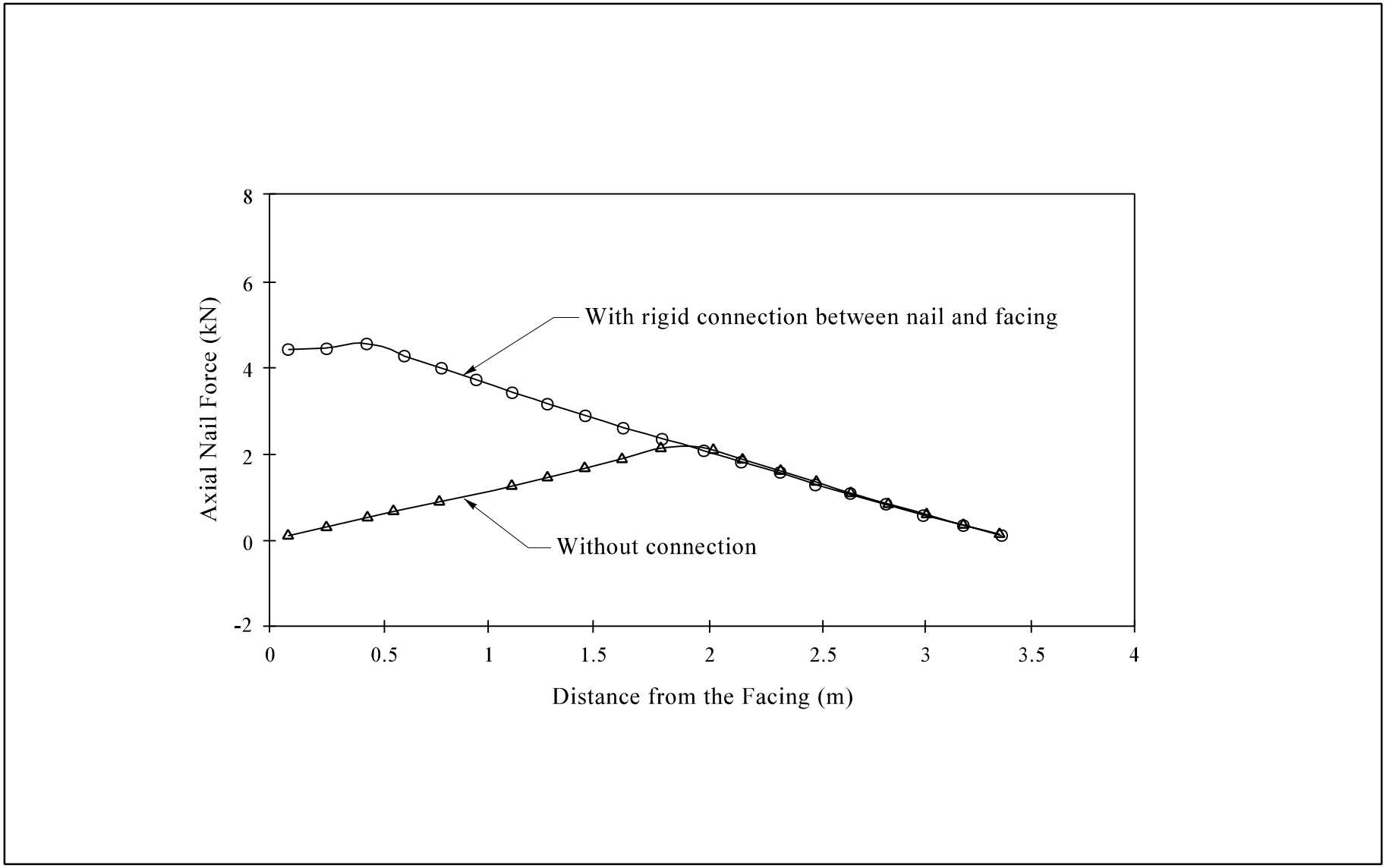

Figure 19 - Typical Distribution of Axial Force in Nail 5 along the Length (after Babu et al, 2002)

Table of Contents
Table of Contents
Table of Contents
Table of Contents

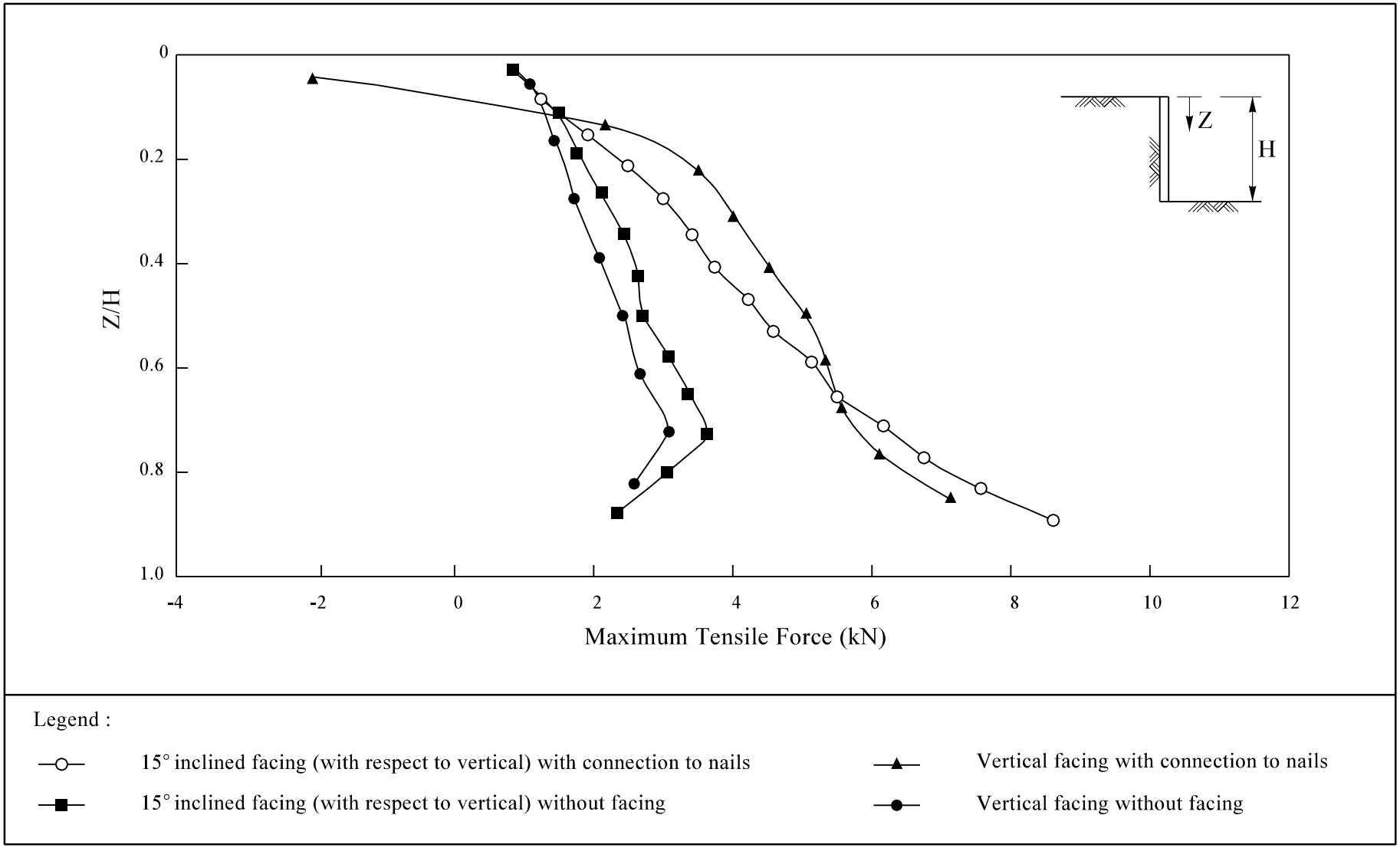

Figure 20 - Variation of Maximum Tensile Force in Nails with Depth for Vertical and Inclined Facings. c = 10 kPa, sequence I (after Babu et al, 2002)

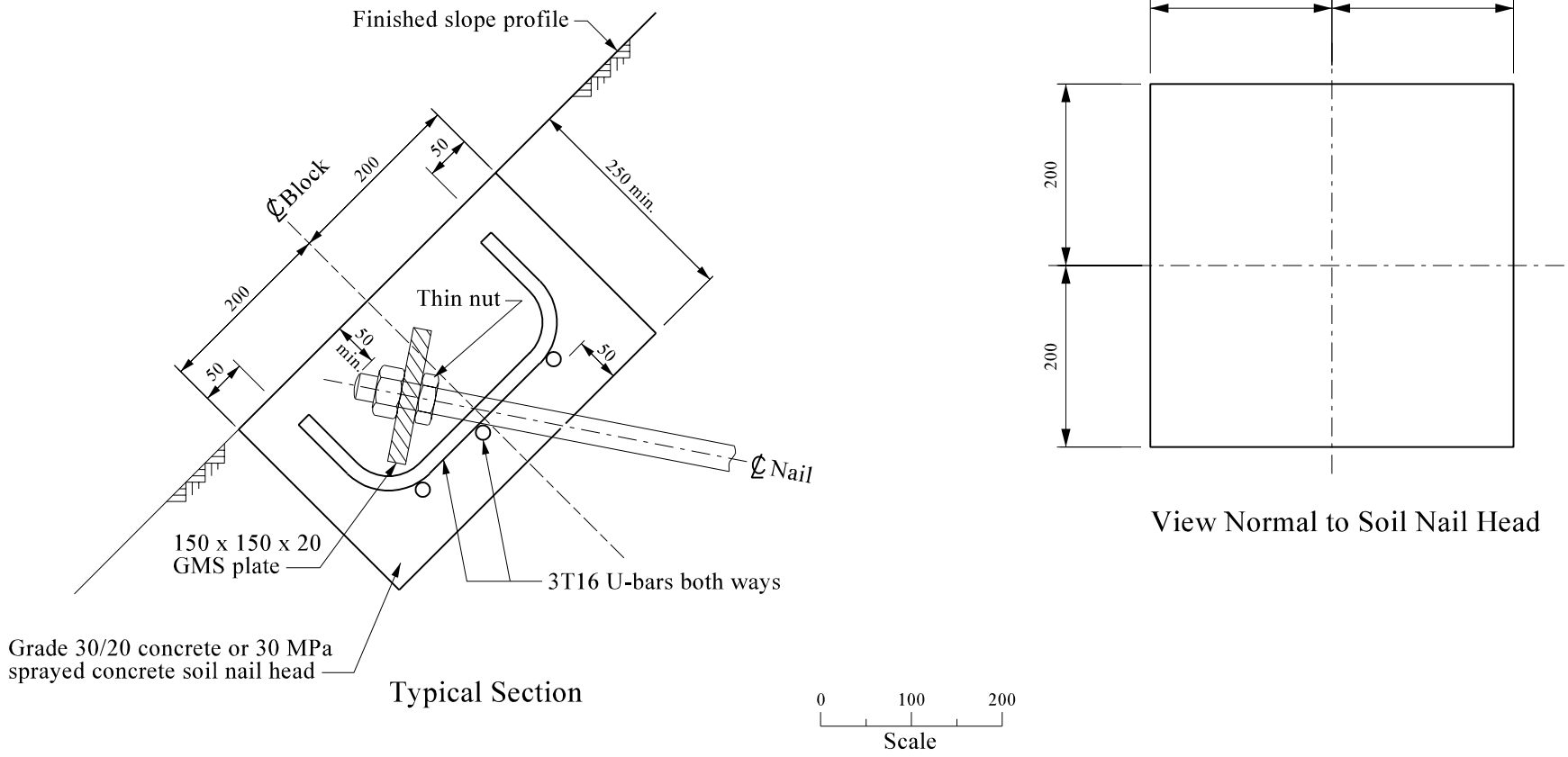

Notes:
(1) All dimensions are in millimetres.
(2) The clearance between the steel bar and the hole of the steel plate shall not be more than 2.
(3) Construction of nail head shall be referred to particular specifications.

Figure 21 - Typical Soil Nail Head Details (after CEDD Drawing No. C2106/2D)

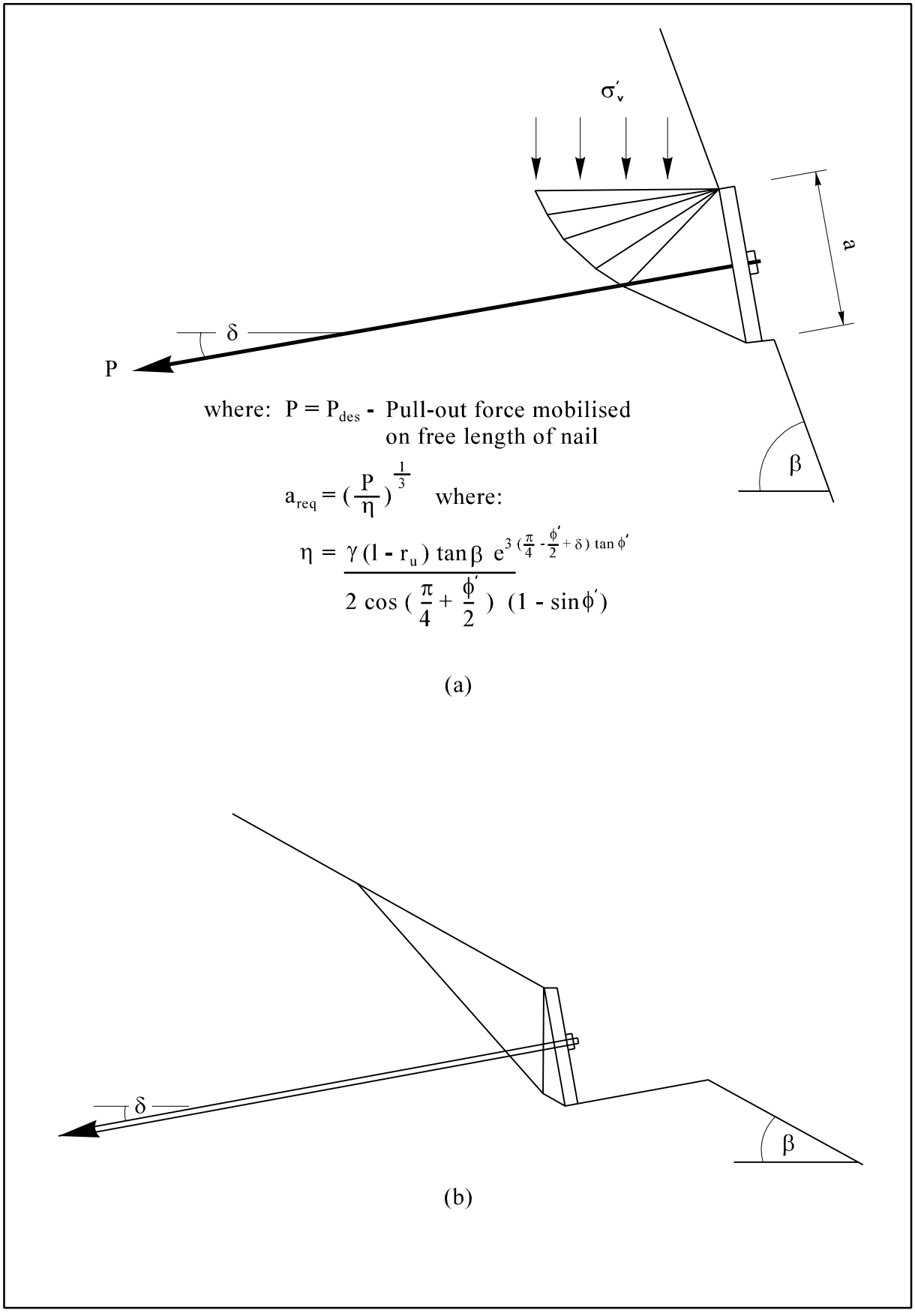

Figure 22 - Nail Plate Bearing Capacity (after HA 68/94)

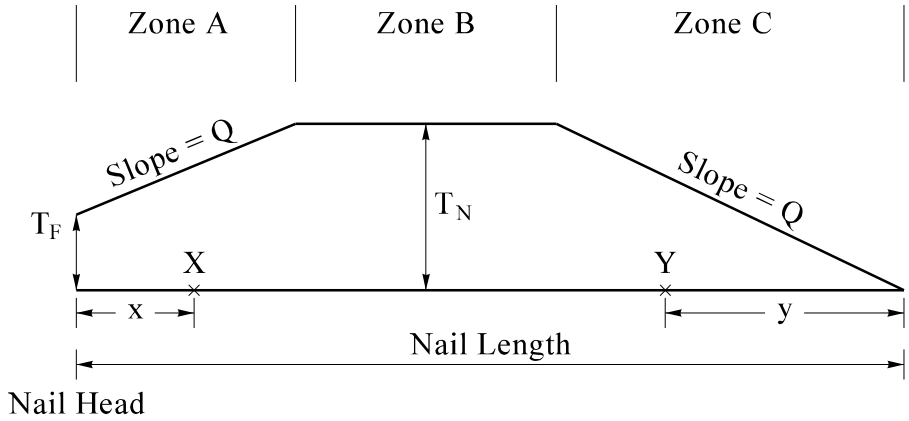

Nail support force to slip surfaces intersecting the nail in zone A at point X = T_F + Qx

Nail support force to slip surfaces intersecting the nail in zone B = T_N

Nail support force to slip surfaces intersecting the nail in zone C at point Y = Qy

T_F = nail head strength

T_N = nail bar tensile strength

Q = nail-soil pullout resistance

Figure 23 - Allowable Nail Load Support Diagram (after Joshi, 2003)

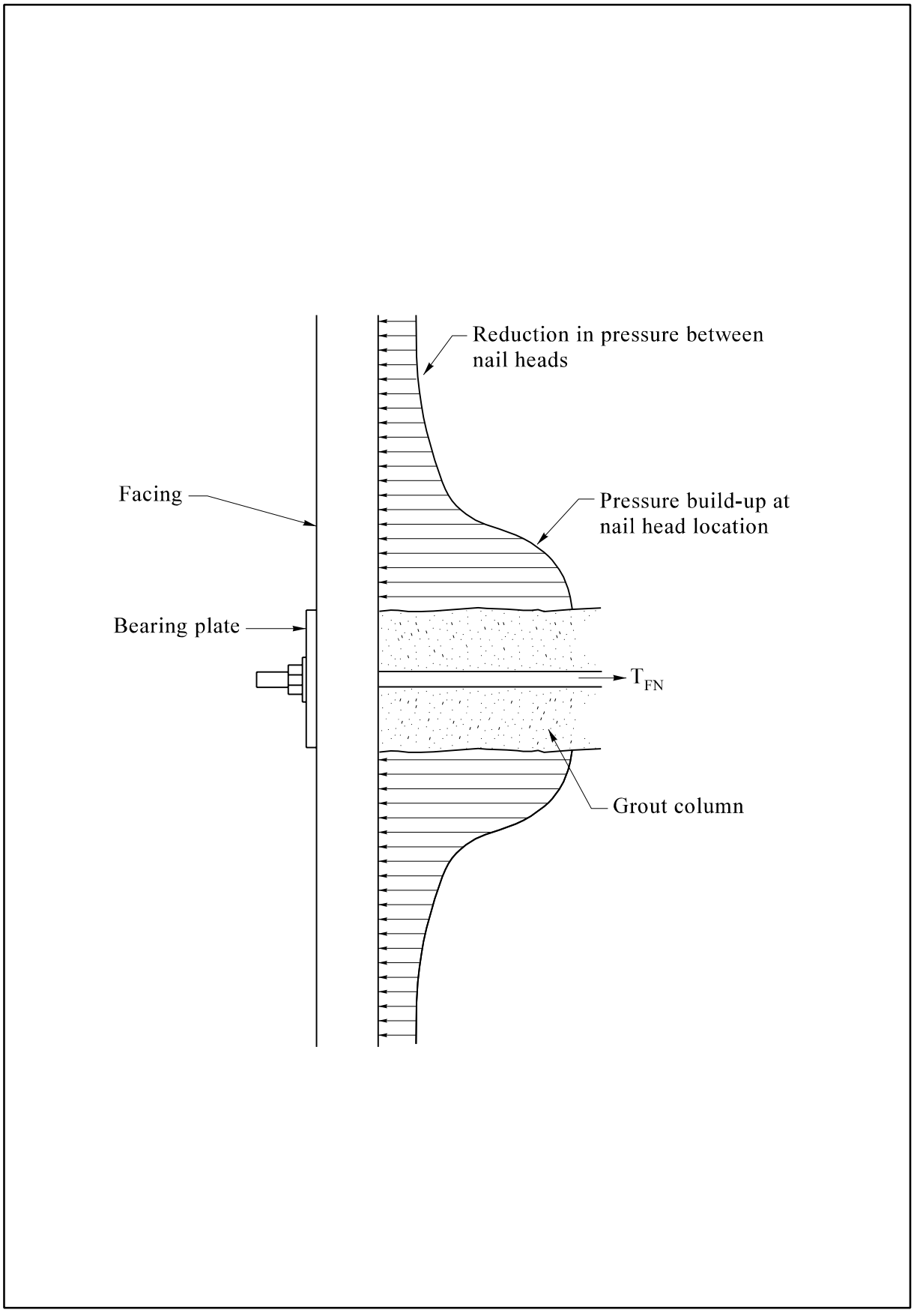

Figure 24 - Facing Pressure Distribution (after FHWA, 1998)

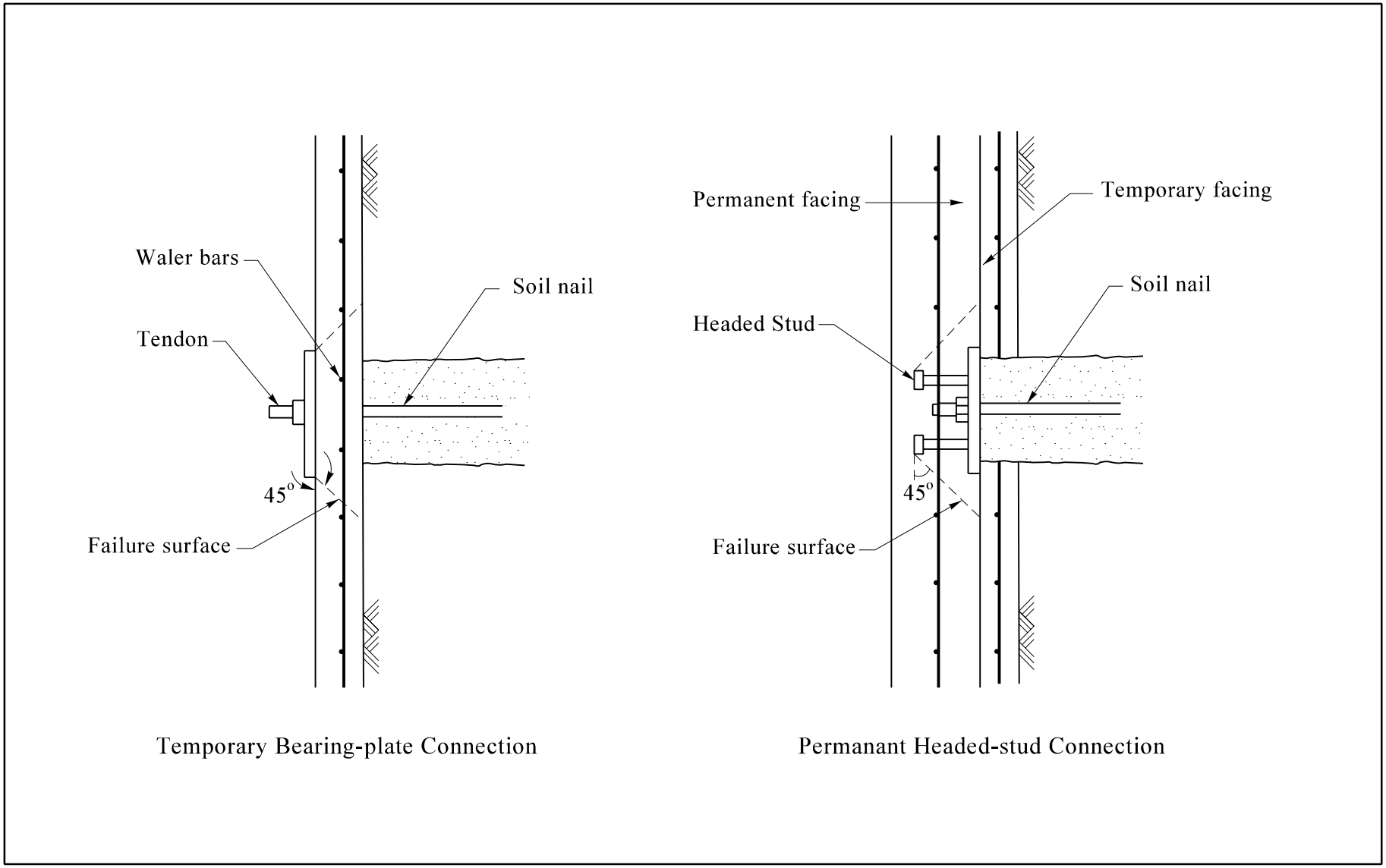

Figure 25 - Typical Nail Head Connections Used in USA (after FHWA, 1998)

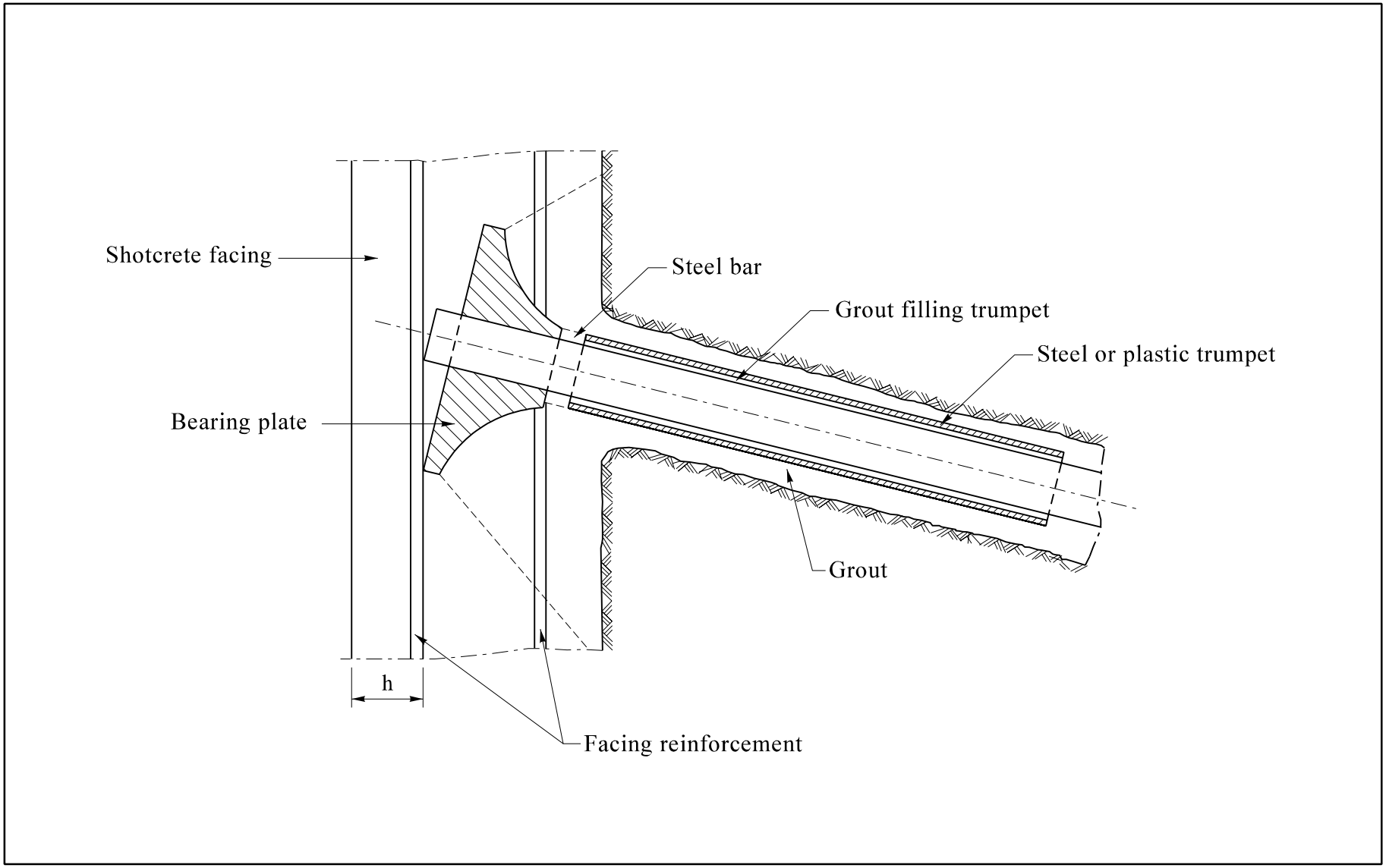

Figure 26 - Typical Details of "Head-nail-facing" Layout (after Clouterre, 1991)

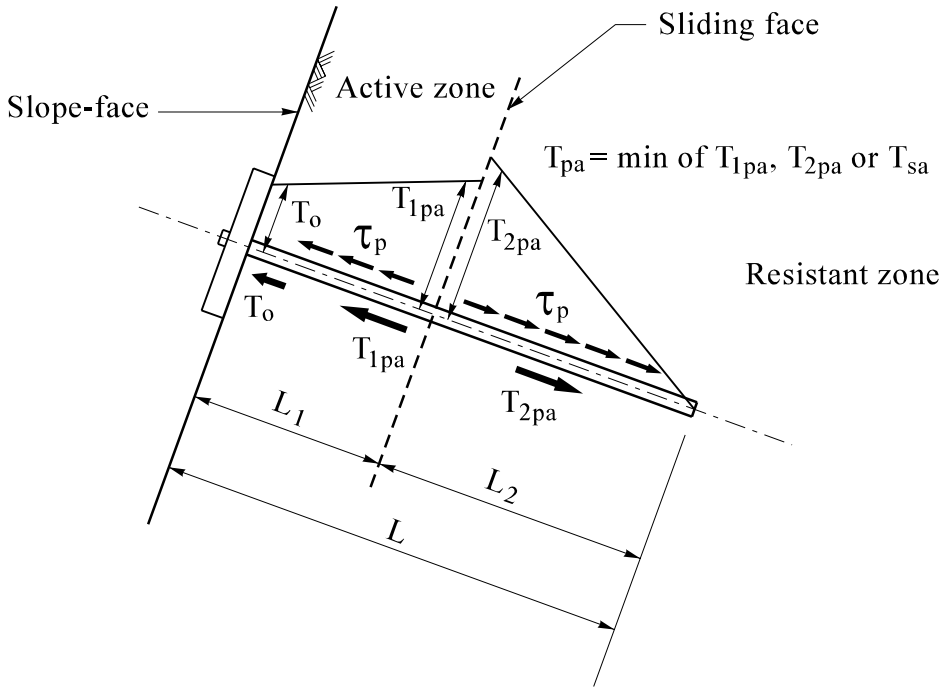

Legend:

T_{pa}	Design axial load of soil nail	T_{1pa}	Pull-out resistance that can be developed at active zone
T_{2pa}	Pull-out resistance that can be developed at resistant zone	T_{sa}	Allowable tensile strength of soil nail
T_o	Nail head load		

Figure 27 - Nail Force Distribution (after Miki et al, 1997)

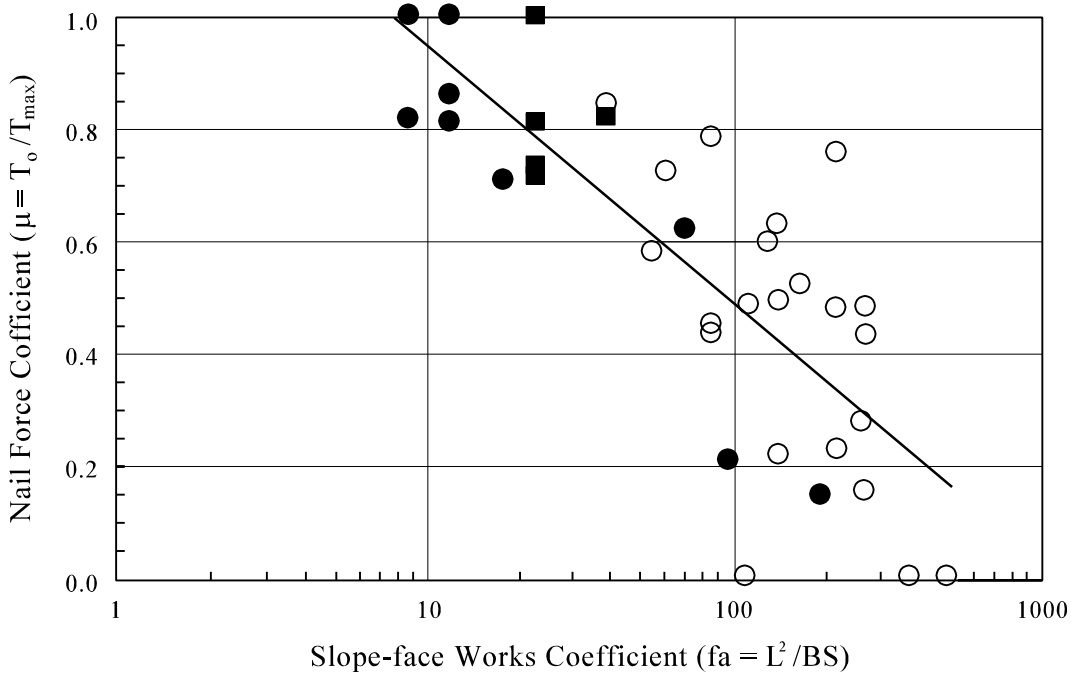

Legend:

L	Length of reinforcing material	B	Width of nail head
S	Spacing of reinforcing material	T_o	Tensile force of reinforcing material acting on nail head
T_{MAX}	Maximum tensile force of reinforcing material	●	Model experiment
■	Frame	○	Concrete spray + head plate

Figure 28 - Nail Force Cofficient μ (after Japan Highway Public Corporation, 1998)

Table of Contents
Table of Contents
Table of Contents
Table of Contents
Table of Contents

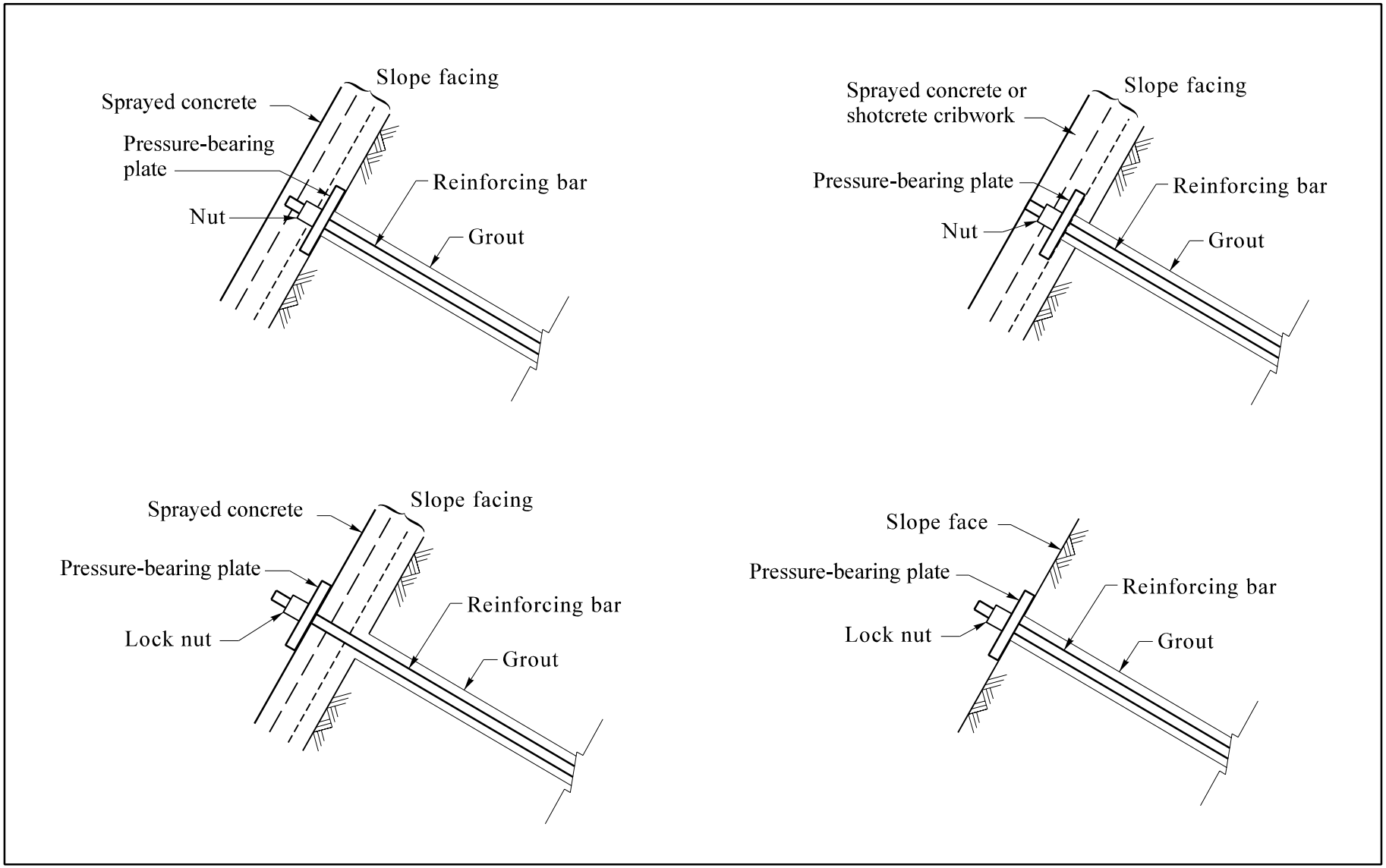

Figure 29 - Types of Soil Nail Heads Used in Japan (after Tayama et al, 1996)

Table of Contents
Table of Contents
Table of Contents
Table of Contents
Table of Contents

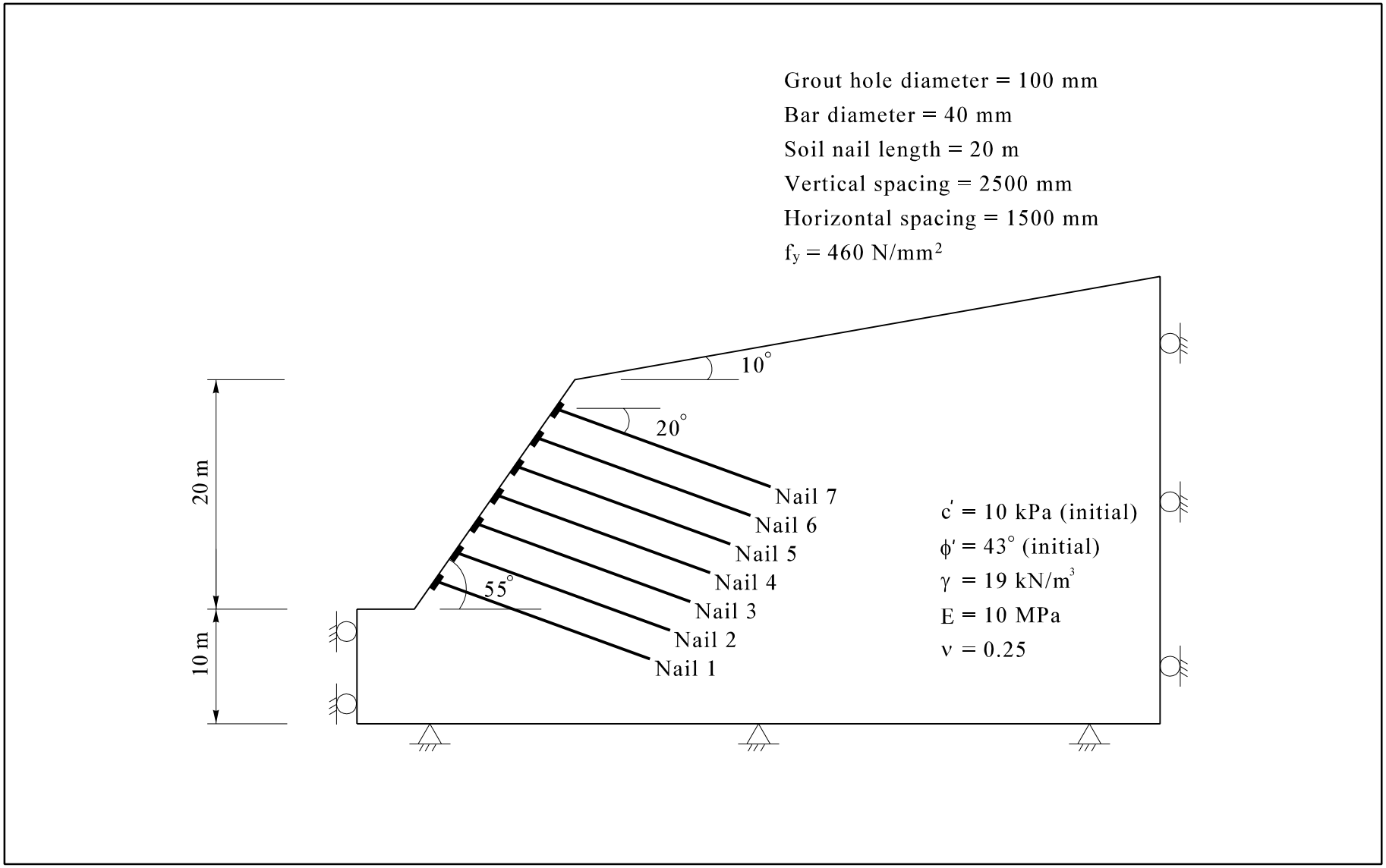

Figure 30 - Geometry and Material Parameters of Model Slope

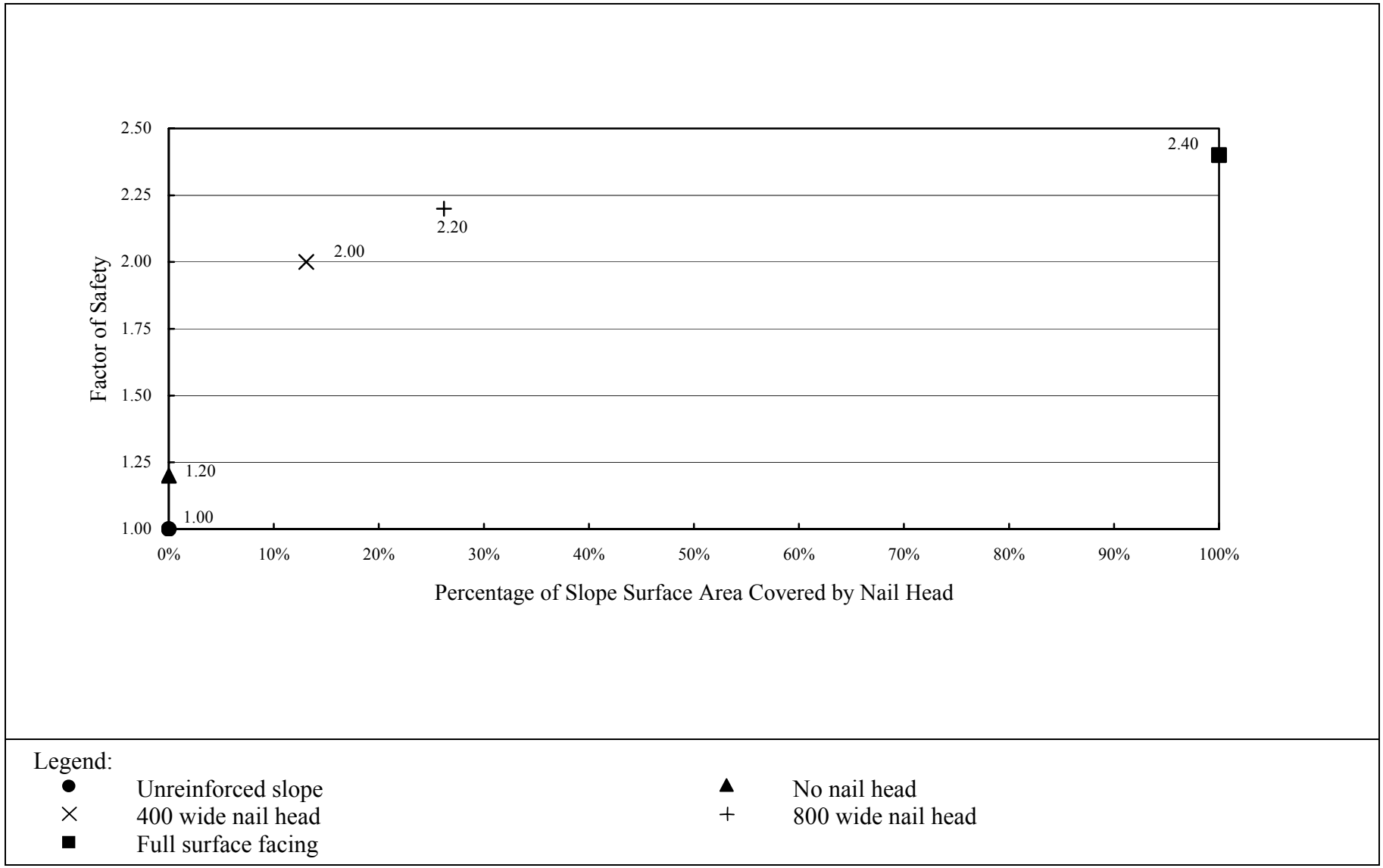

Figure 31 - Relationship between Factor of Safety and Nail Head Size

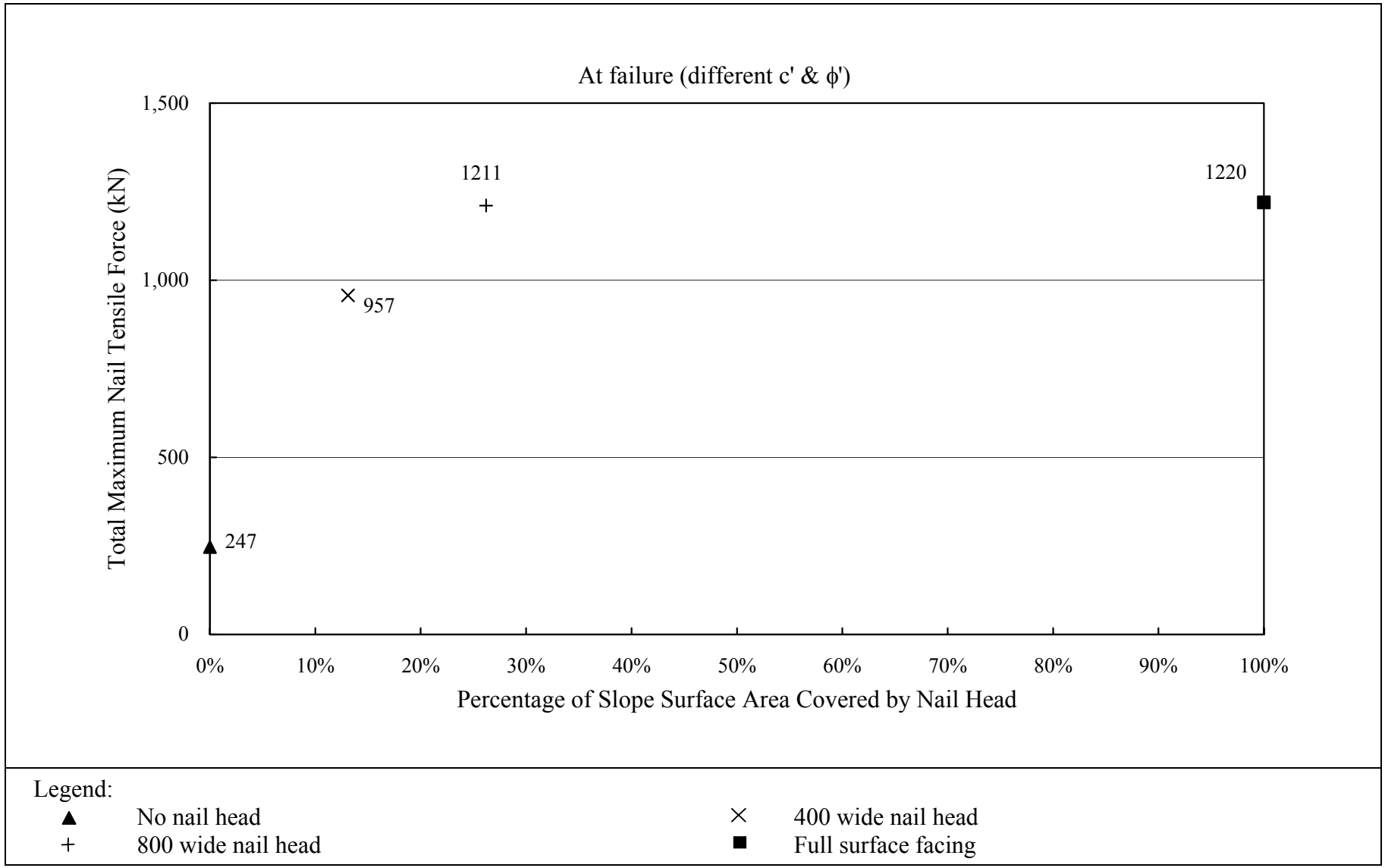

Figure 32 - Relationship between Total Maximum Nail Tensile Forces and Nail Head Size

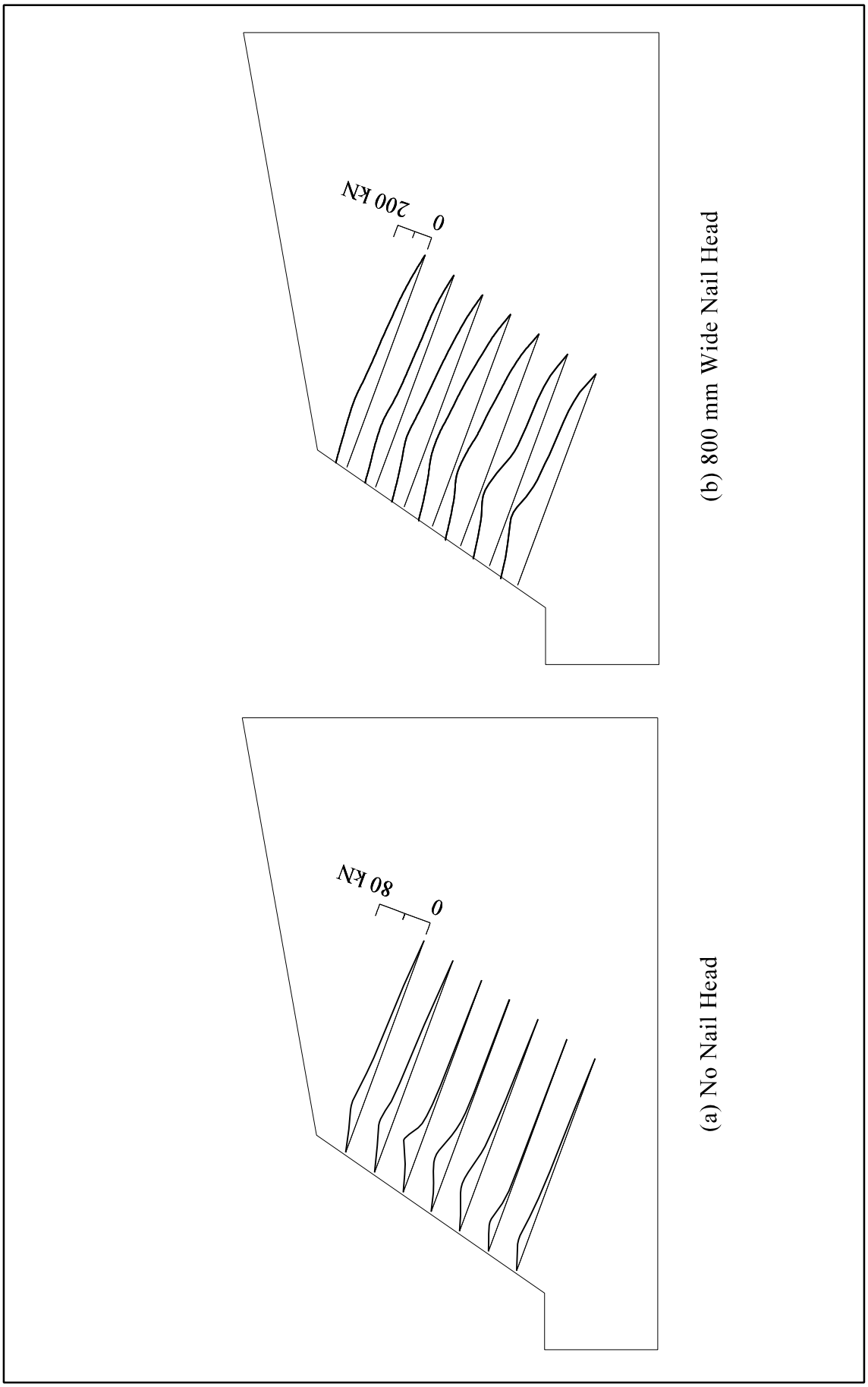

Figure 33 - Variation of Axial Nail Forces for (a) No Nail Head and (b) 800 mm Wide Nail Head

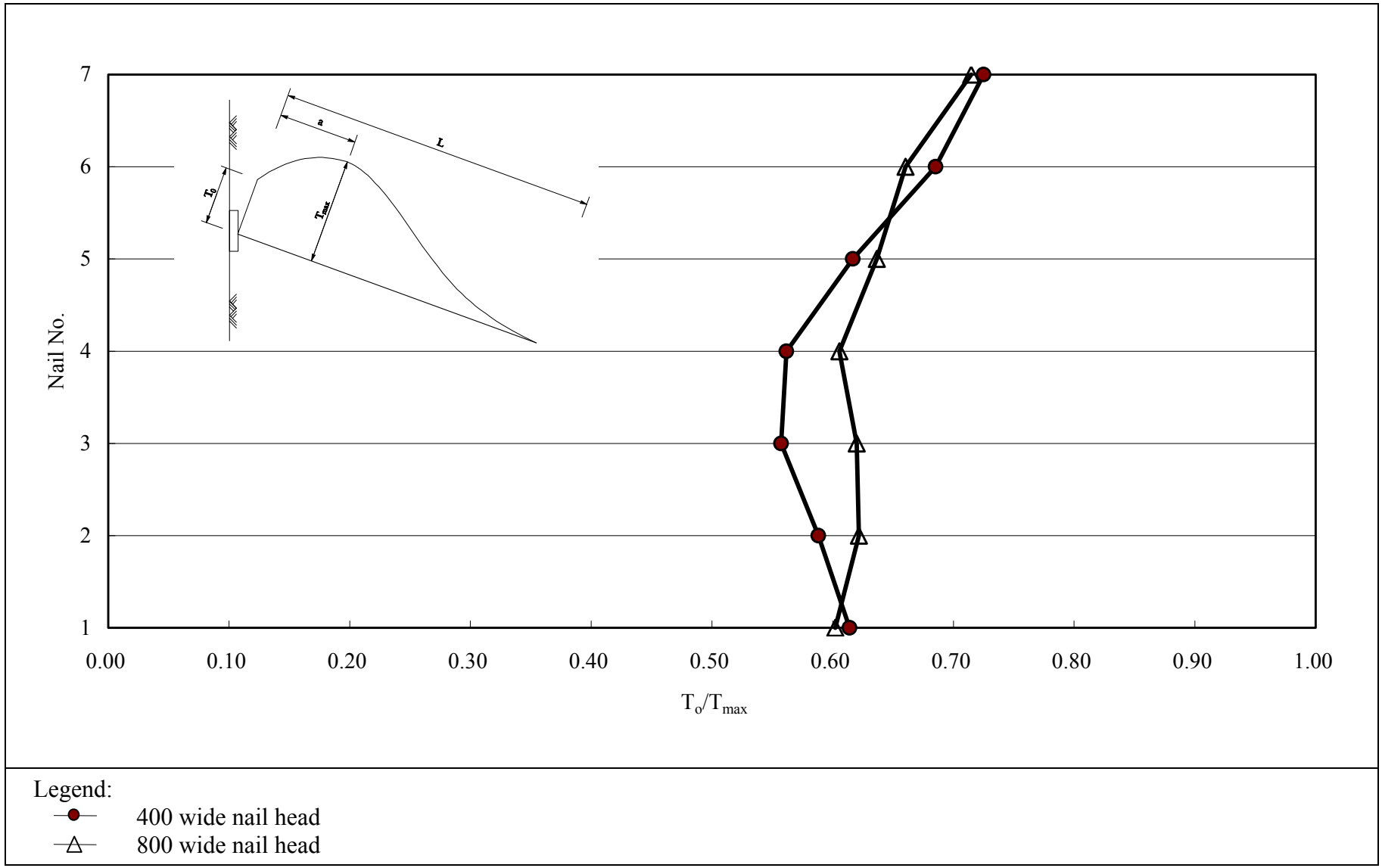

Figure 34 - Distribution of T_o/T_{max} in Soil Nails

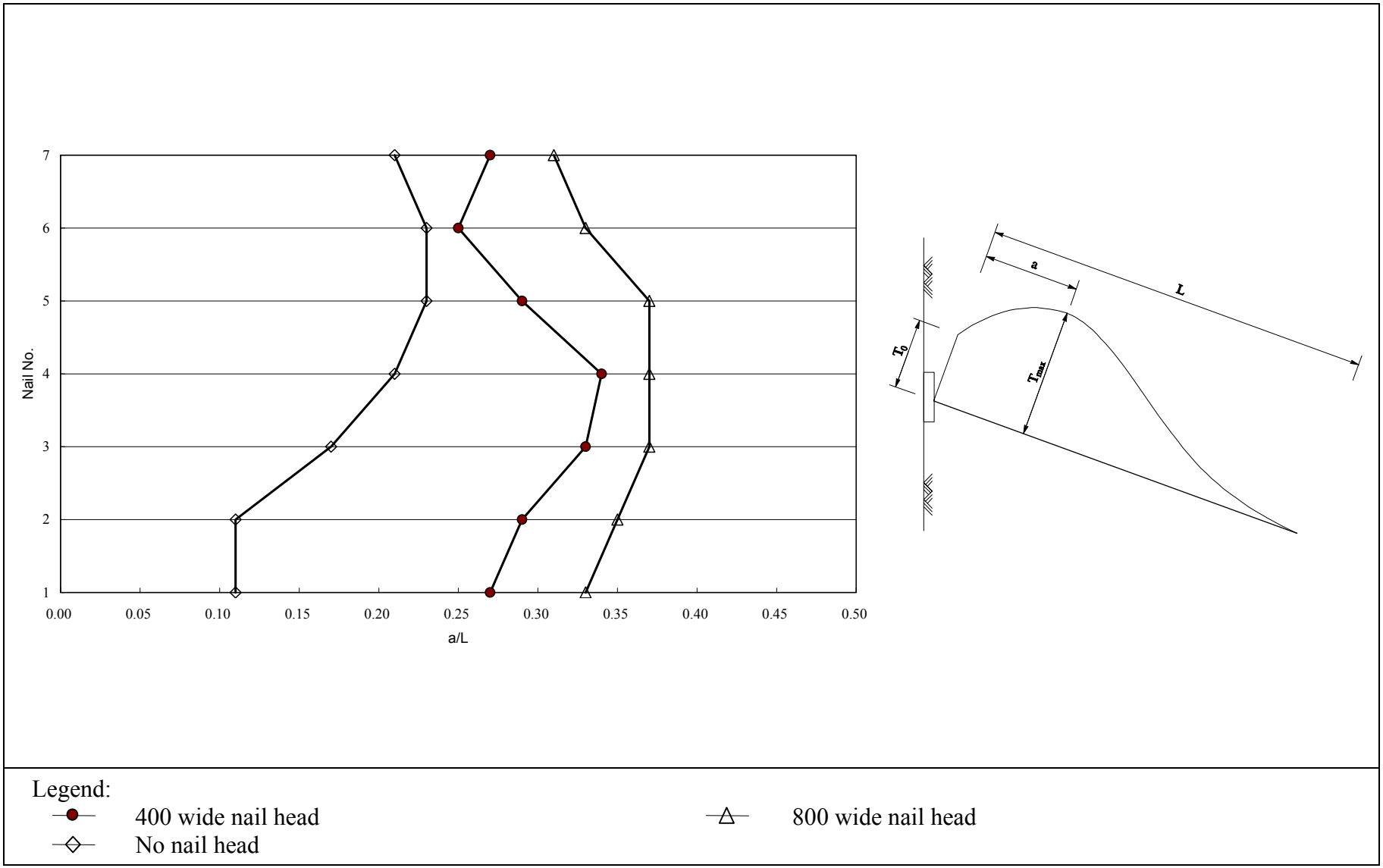

Figure 35 - Locations of Maximum Tensile Force in Soil Nails

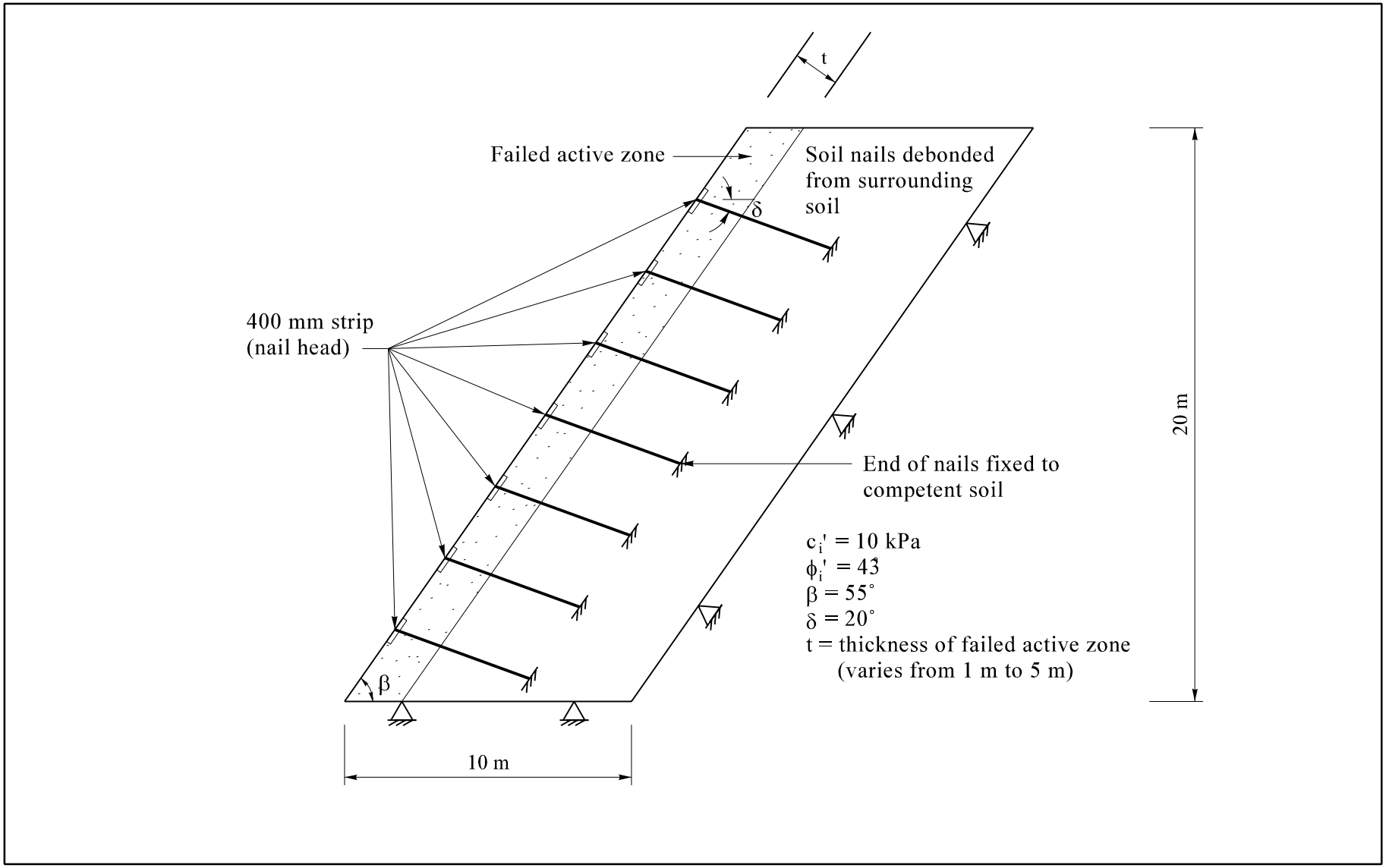

Figure 36 - Details of Slope Model for Simulation of Failed Active Zone

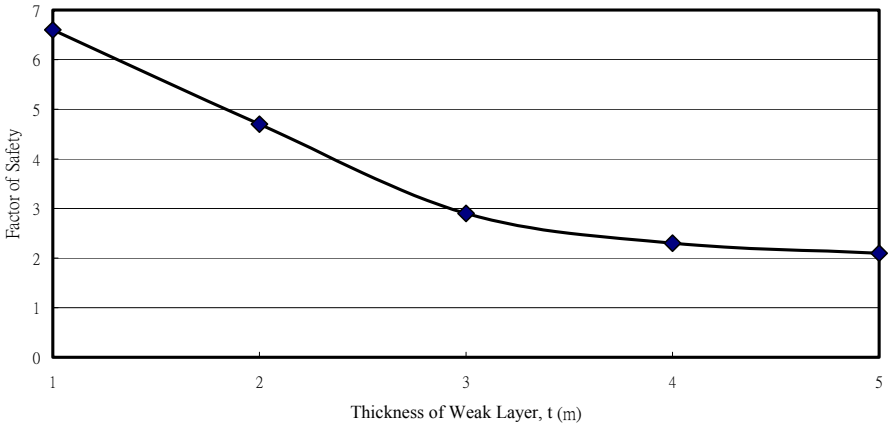

(a) Relationship between Factor of Safety and Thickness of Failed Active Zone

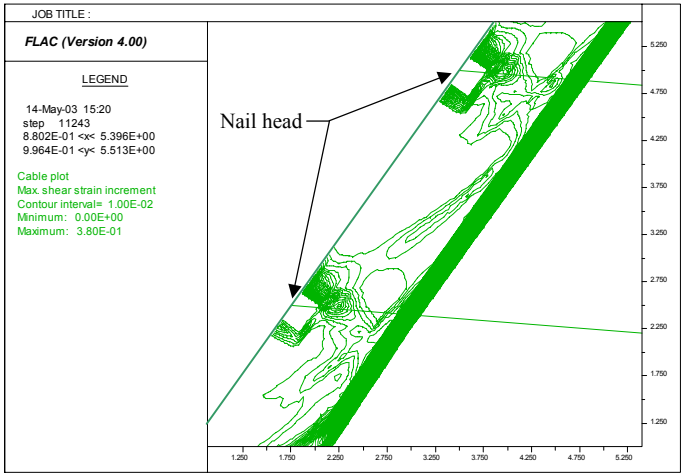

For t = 2 m

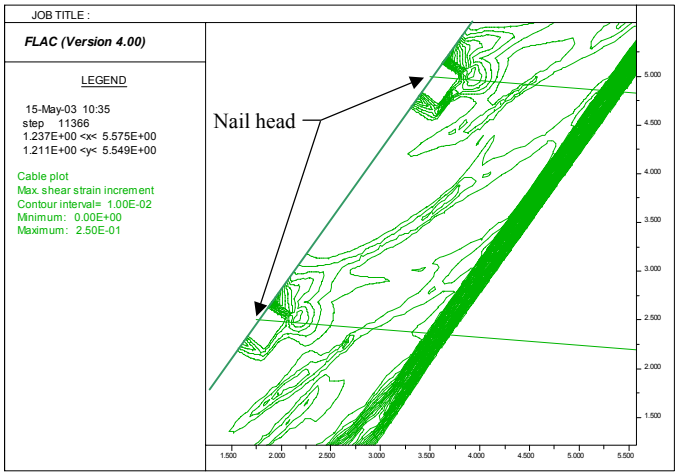

For t = 3 m

(b) Contour of Shear Strain

Figure 37 - Typical Results of Simulation of Failed Active Zone

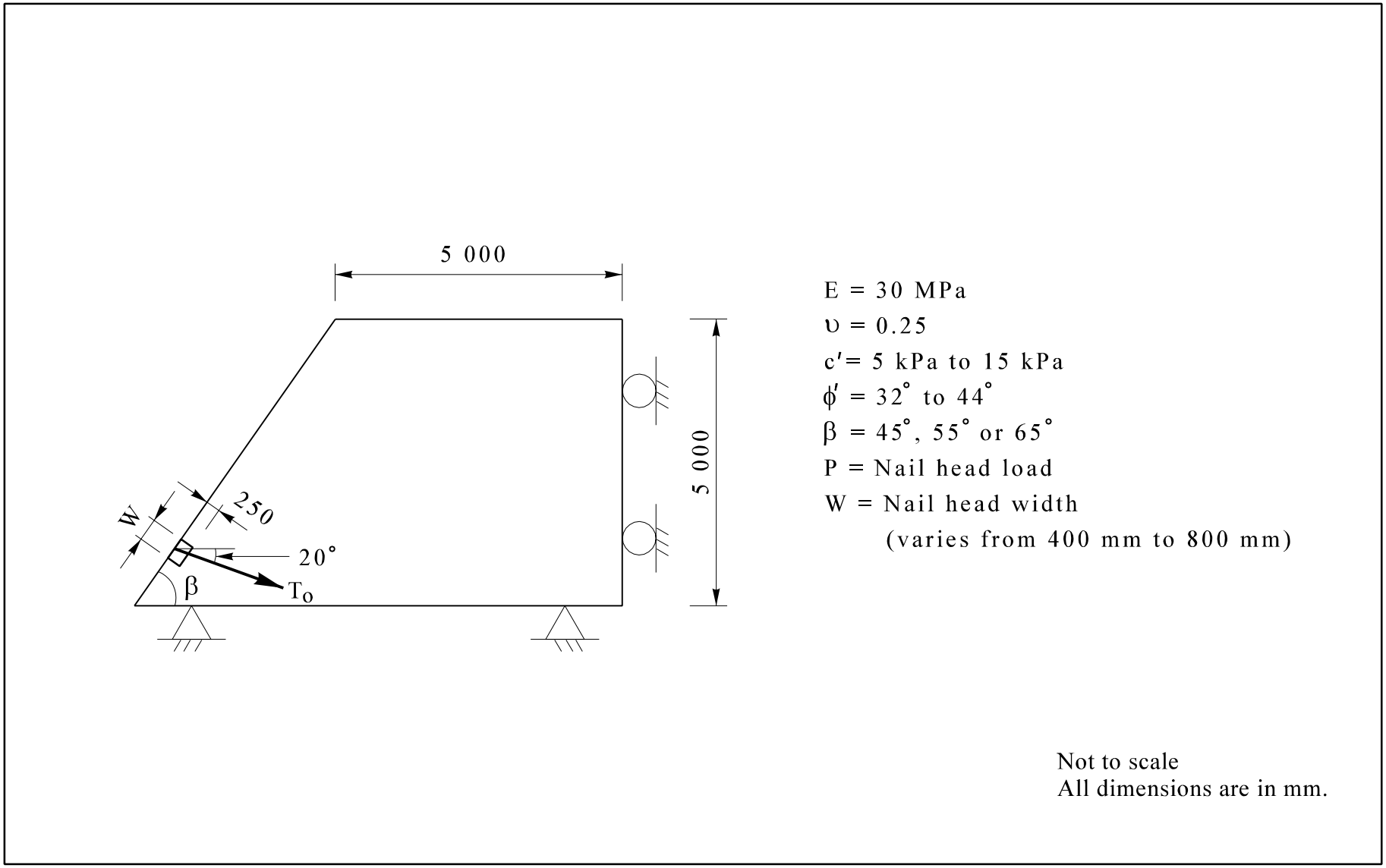

Figure 38 - Details of Slope Model for Bearing Failure Analysis

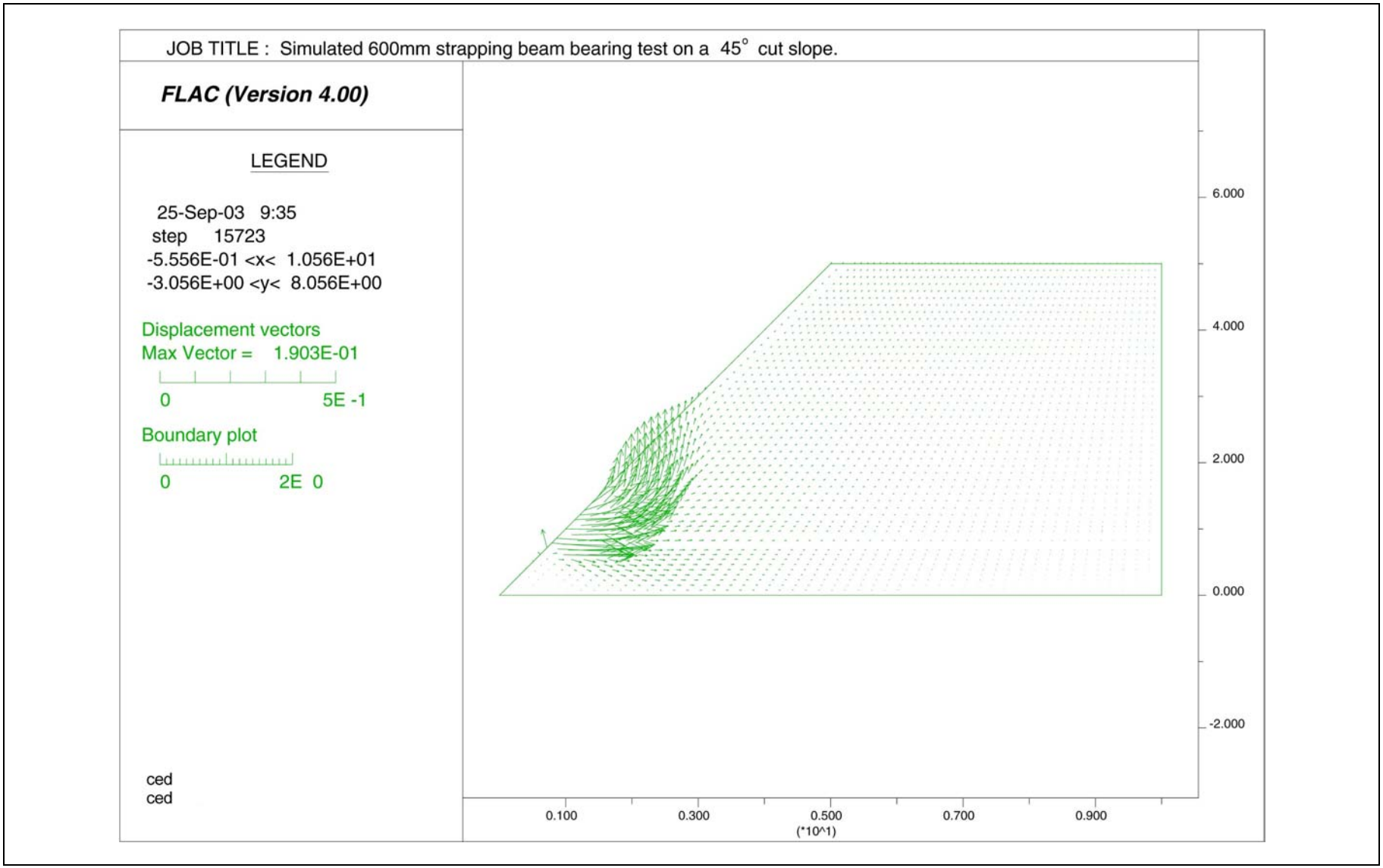

Figure 39 - Displacement Vectors at Bearing Capacity Failure for Nail Head of 600 mm by 600 mm

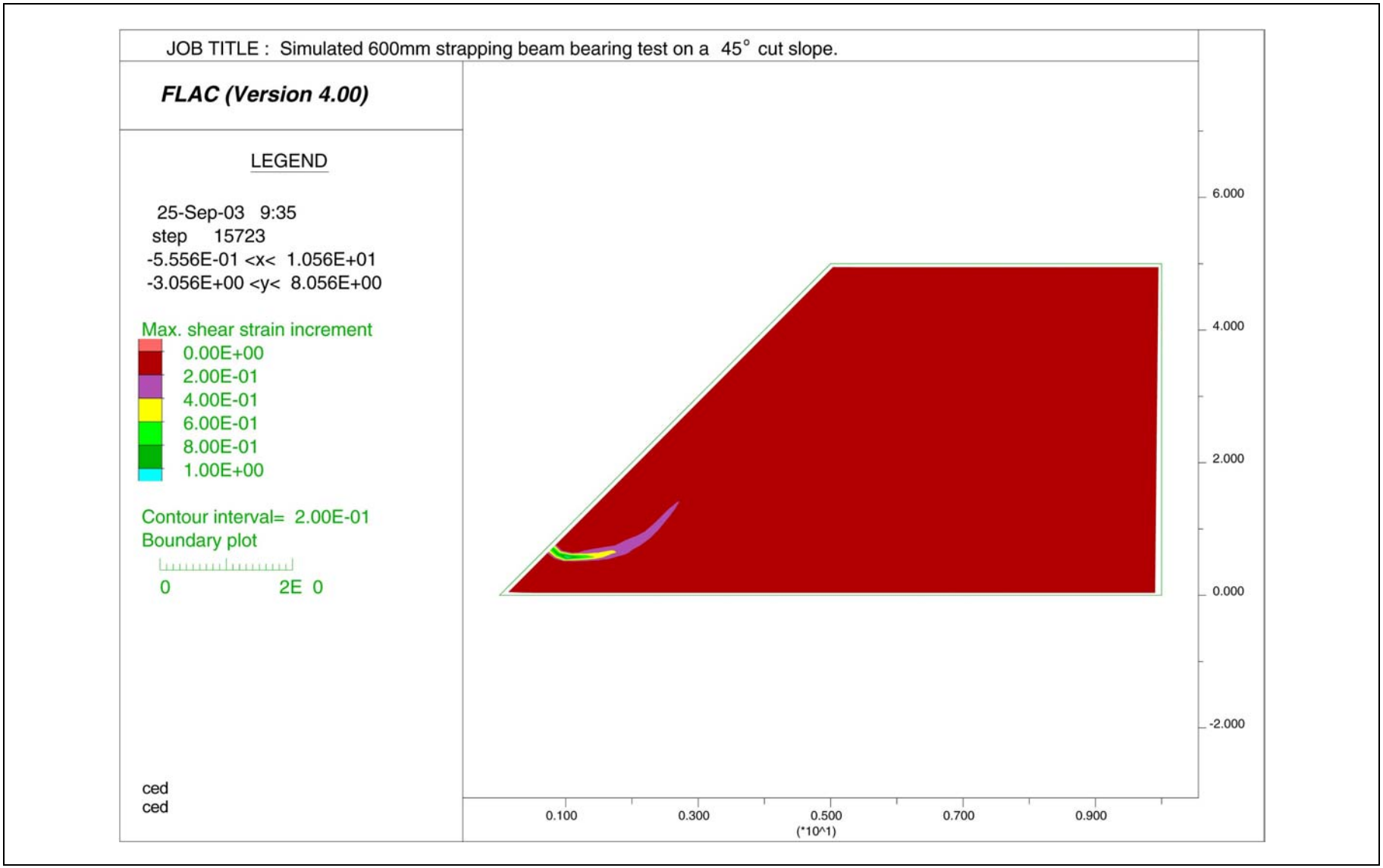

Figure 40 - Shear Strains at Bearing Capacity Failure for Nail Head of 600 mm by 600 mm

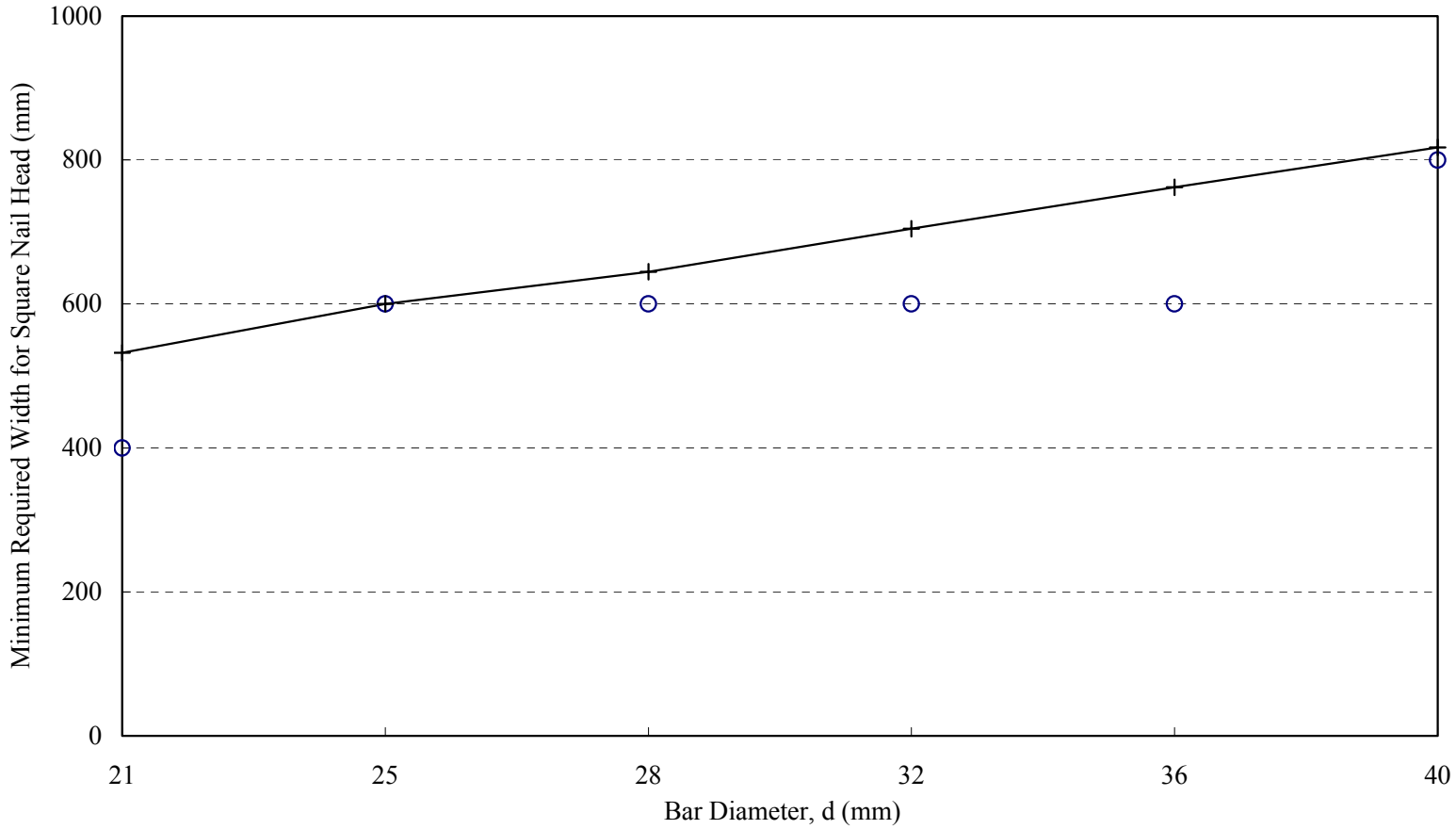

Legend:

○ FLAC analysis + HA68/94

Notes: (1) Nail head load = $230 \times \pi d^2/4$ (kN).
(2) Slope angle $\beta = 55°$, $c' = 5$ kPa and $\phi' = 38°$.

Figure 41 - Comparison of Nail Head Sizes Obtained from FLAC Analysis and HA 68/94

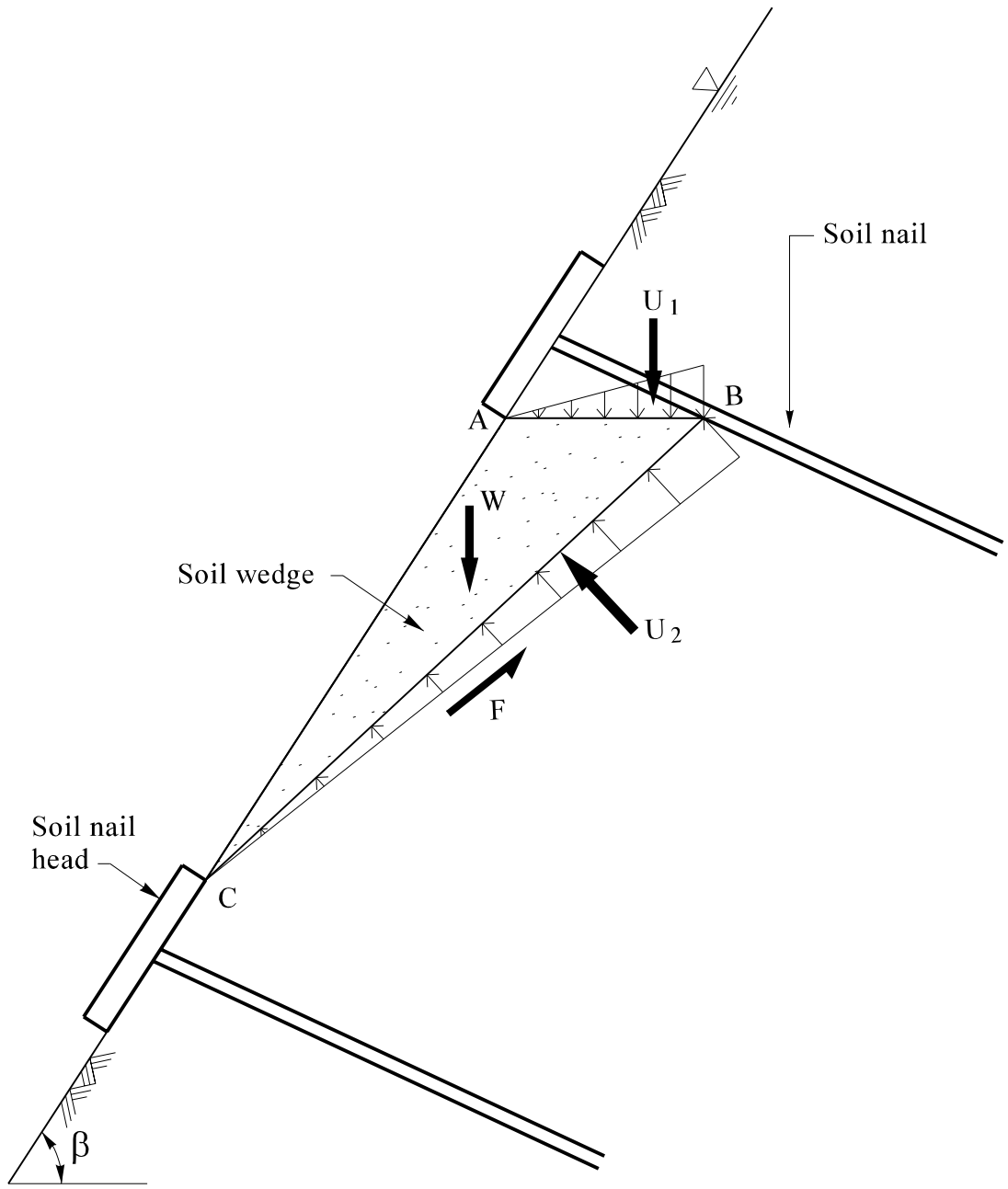

Legend:

F	Shearing resistance along plane BC		
U_1	Resultant water force on horizontal plane AB (determined by a flow net analysis)		
U_2	Resultant water force on plane BC		
W	Weight of soil wedge	▽	Groundwater surface

Note: Thickness of the soil wedge is the length of the horizontal plane AB.

Figure 42 - Generalized Loading on Soil Wedge

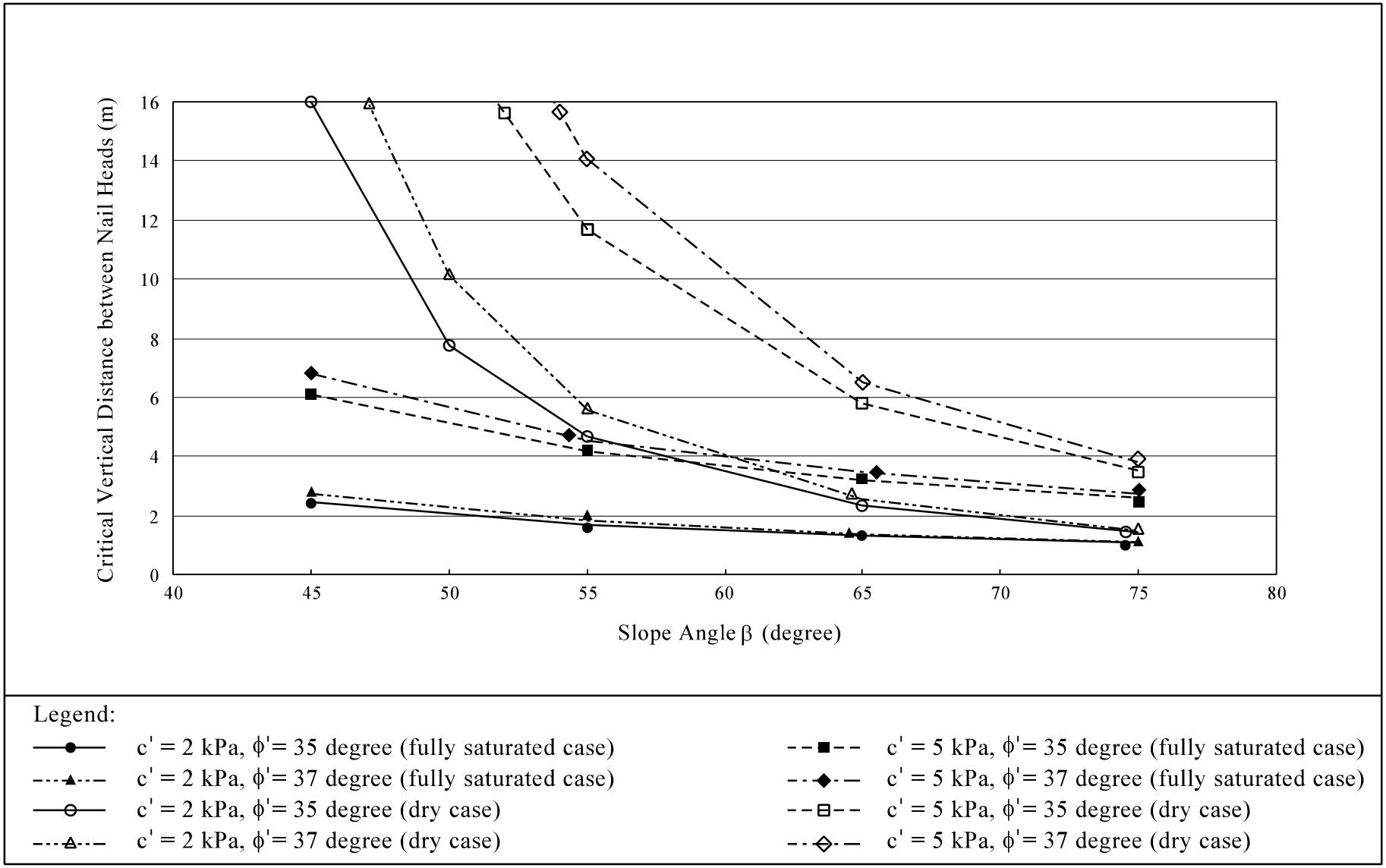

Figure 43 - Variation of Critical Vertical Distance with Slope Angles

Table of Contents
Table of Contents
Table of Contents
Table of Contents

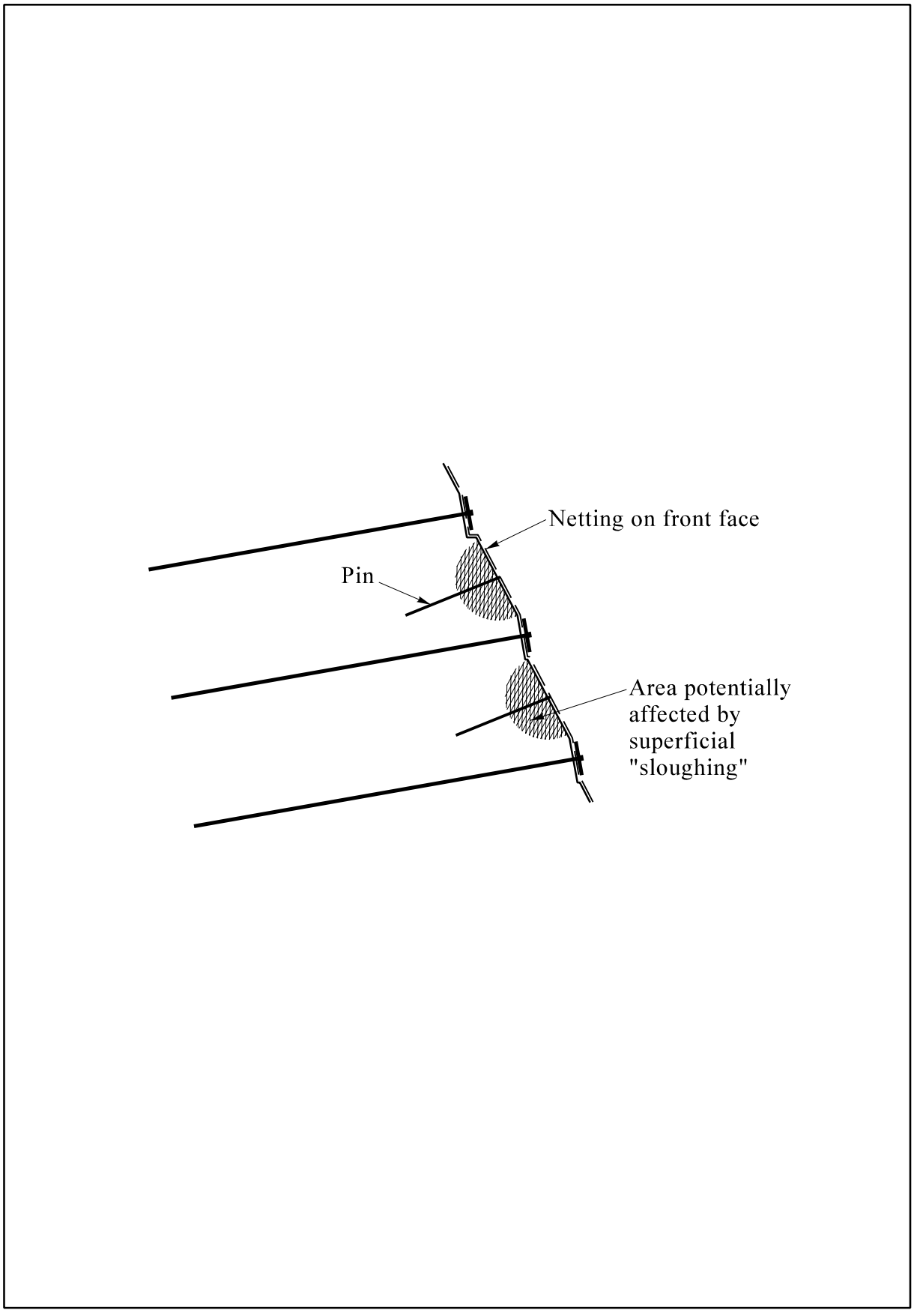

Figure 44 - Surface Protection between Nail Plates (after HA 68/94)

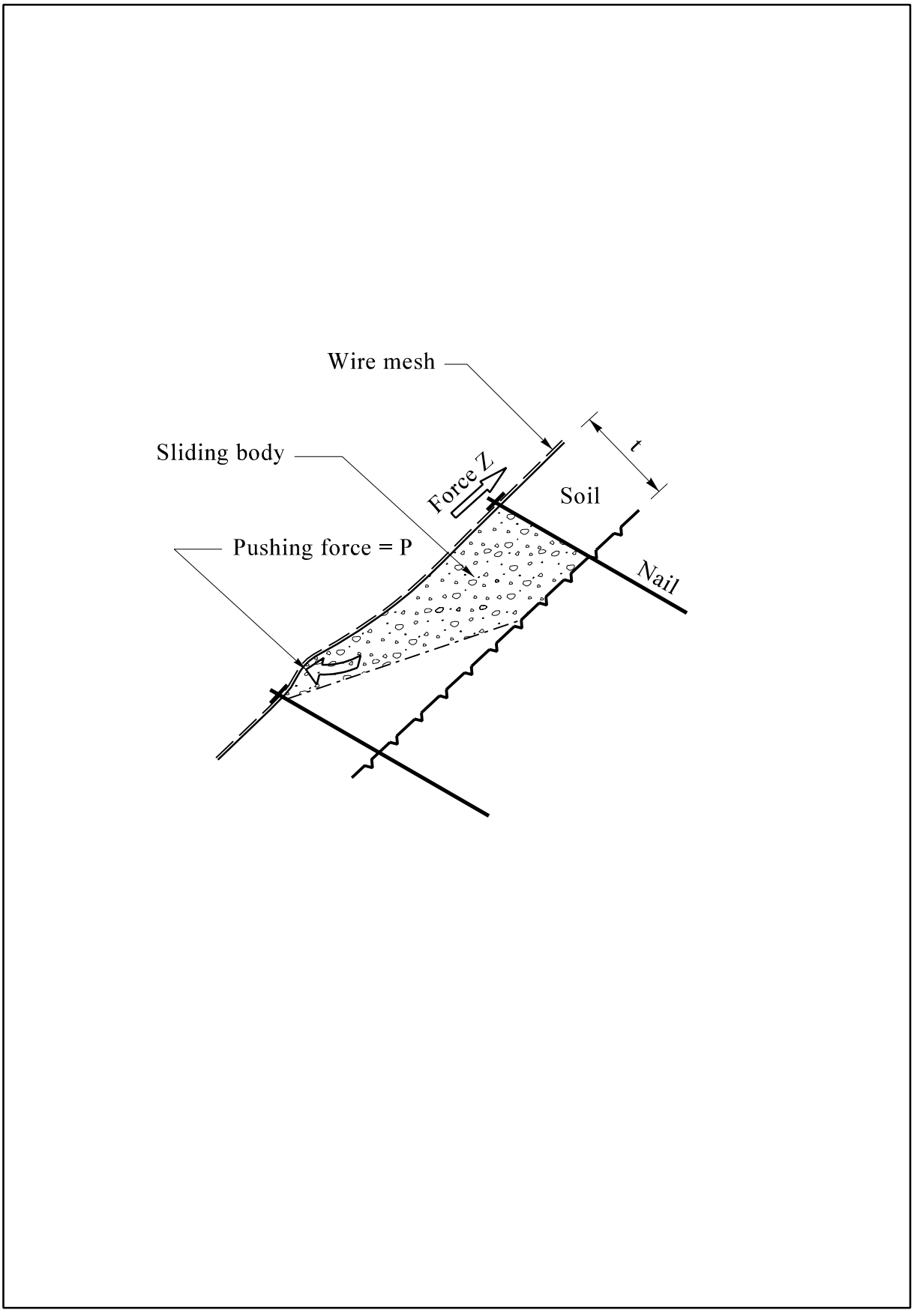

Figure 45- Pushing Force P and Tensile Force Z (after Rüegger et al, 2003)

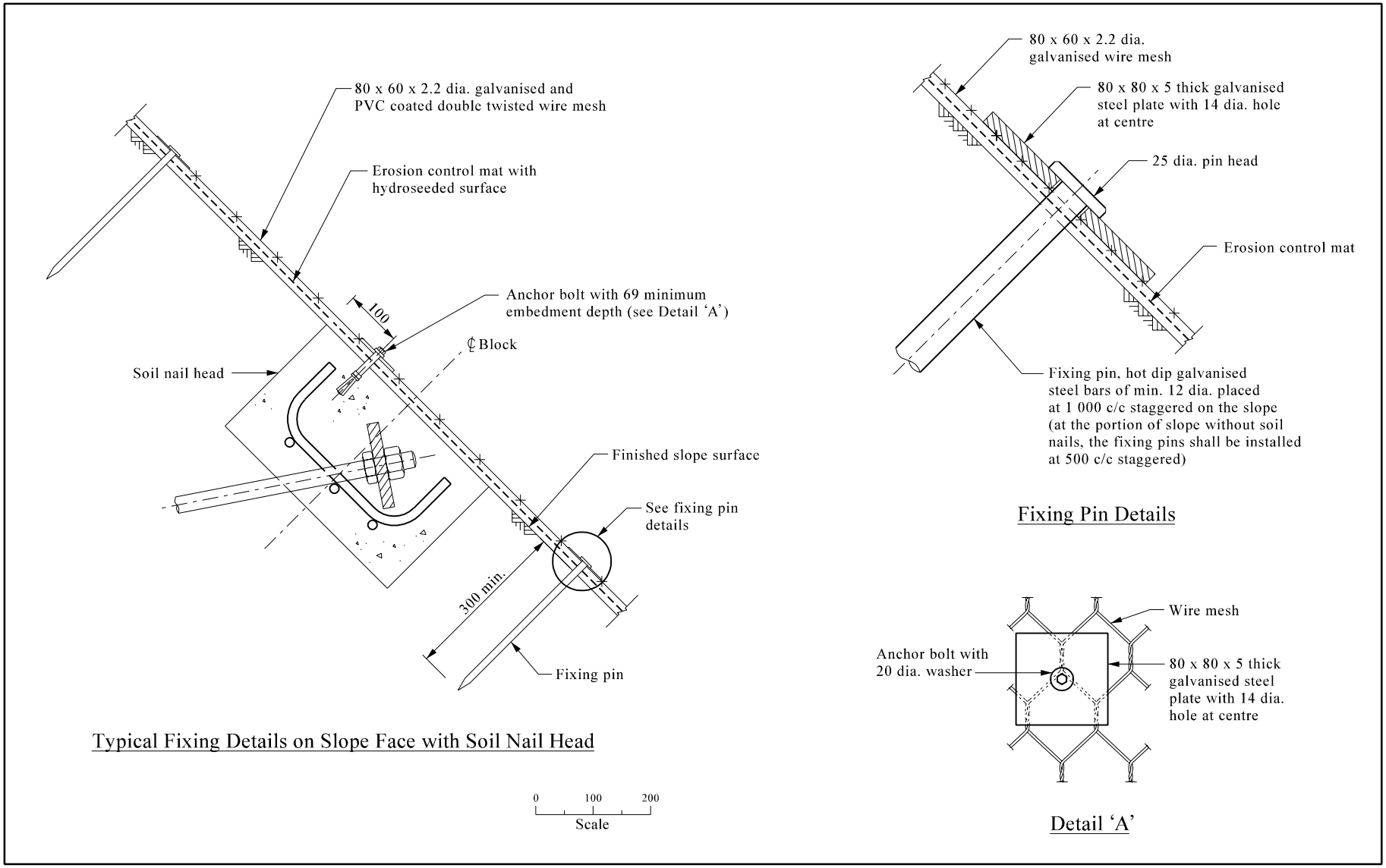

Figure 46 - Fixing Details for Erosion Control Mat and Wire Mesh with Soil Nails (Modified from CEDD Drawing No. C2511/2A)

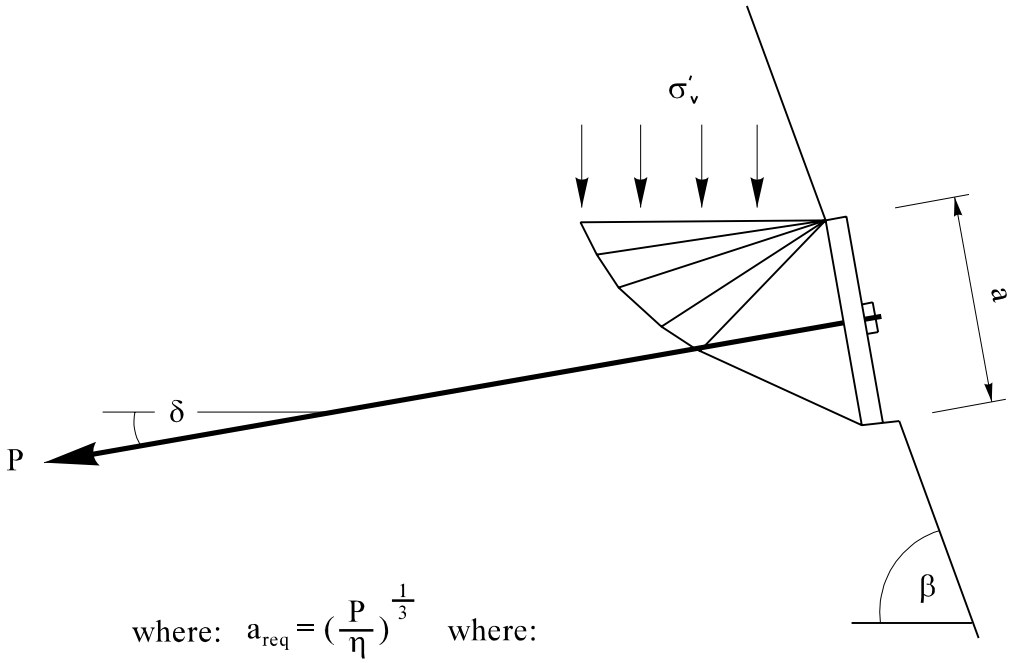

where: $a_{req} = \left(\frac{P}{\eta}\right)^{\frac{1}{3}}$ where:

$$\eta = \frac{\gamma (1 - r_u) \tan\beta \; e^{3\left(\frac{\pi}{4} - \frac{\phi'}{2} + \delta\right)\tan\phi'}}{2\cos\left(\frac{\pi}{4} + \frac{\phi'}{2}\right)(1 - \sin\phi')}$$

Legend:

P	Design load of soil nail
σ'_v	Effective vertical stress
γ	Unit weight of soil (kN/m^3)
β	Slope angle
r_u	Pore pressure parameter (= $u/\gamma h$)
u	Pore water pressure (kN/m^2)
h	Depth of overburden directly above point in question

Figure 47 - Lower-bound Nail Head Design Method (Adopted from Department of Transport (1994) with Modification)

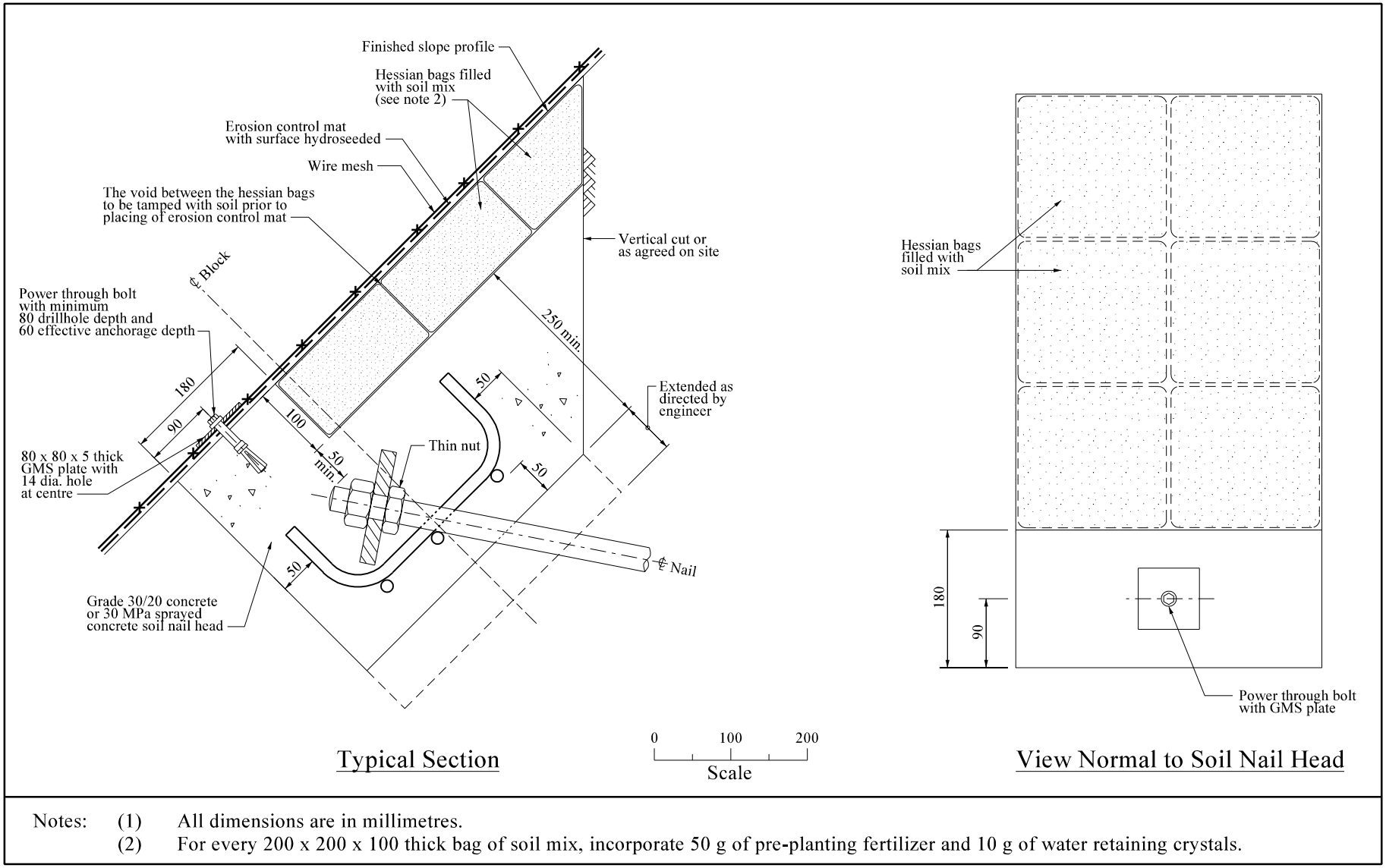

Notes: (1) All dimensions are in millimetres.
(2) For every 200 x 200 x 100 thick bag of soil mix, incorporate 50 g of pre-planting fertilizer and 10 g of water retaining crystals.

Figure 48 - Details of Recessed Soil Nail Head (Modified from CEDD Sketch No. R1067)

LIST OF PLATES

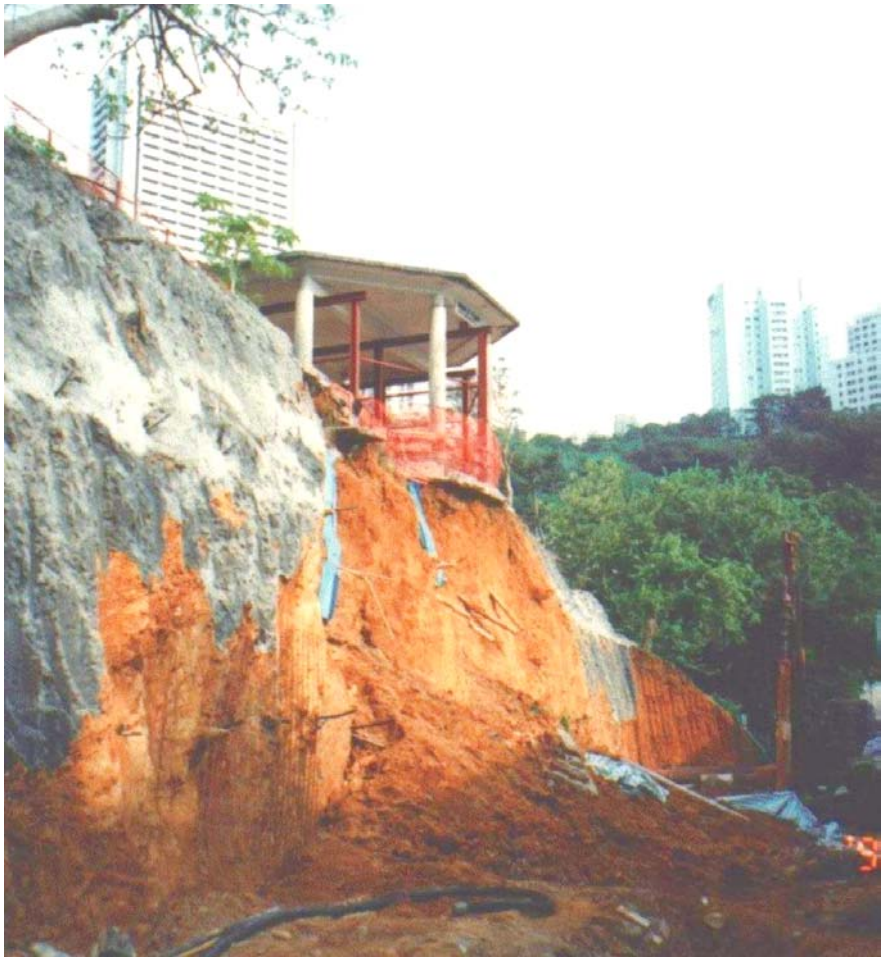

Plate 1 - Failure of Temporary Nailed Cut Slope by Sliding off Front of Soil Nails (Slope No. 11SW-A/C186)

Plate 2 - Failure of Temporary Nailed Cut Slope by Sliding off Front of Soil Nails (Slope No. 8SW-A/C8)

Plate 3 - Local Failure between Soil Nail Heads (Slope No. 6NE-B/C8)
(Extracted from Landslide Study Report LSR 1/2004, GEO (2004))

Plate 4 - Local Failure between Soil Nail Heads (Slope No. 6SE-D/C52)

Table of Contents
Table of Contents
Table of Contents

APPENDIX A

DERIVATIONS OF SOLUTION FOR DETERMINING NAIL HEAD SIZE GIVEN IN HA 68/94

Derivation of solution in HA 68/94 (Love, 2003):

The theoretical basis for the formula which appears on page E/3 of HA68/94 is as follows.

The nail plate stress, σ_n' (where $\sigma_n' = P/a^2$) may be related to the vertical effective stress, σ_v' acting above the fan zone, by the following relationship based on the method of stress characteristics:

$$\frac{\sigma_n'}{\sigma_v'} \approx \frac{(1 + \sin\phi)}{\cos^2\phi} e^{(2\theta)\tan\phi}$$

where θ is the angle (i.e. $\theta = \pi/4 - \phi/2 + \delta$).

The magnitude of σ_v' may by estimated as follows:

$$\sigma_v' \approx \gamma(1 - r_u)B \tan\beta$$

where B is the width of the top of the fan zone.

B may be related to the width of the nail plate, a, as follows using the equation for a log spiral:

$$B = \frac{a}{2\cos\left(\frac{\pi}{4} + \frac{\phi}{2}\right)} e^{\theta \tan\phi}$$

Putting all this together and simplifying yields the relevant formula.

Table of Contents
Table of Contents
Table of Contents

APPENDIX B

TYPICAL RESULTS OF FLAC ANALYSIS ON THE EFFECT OF NAIL HEADS

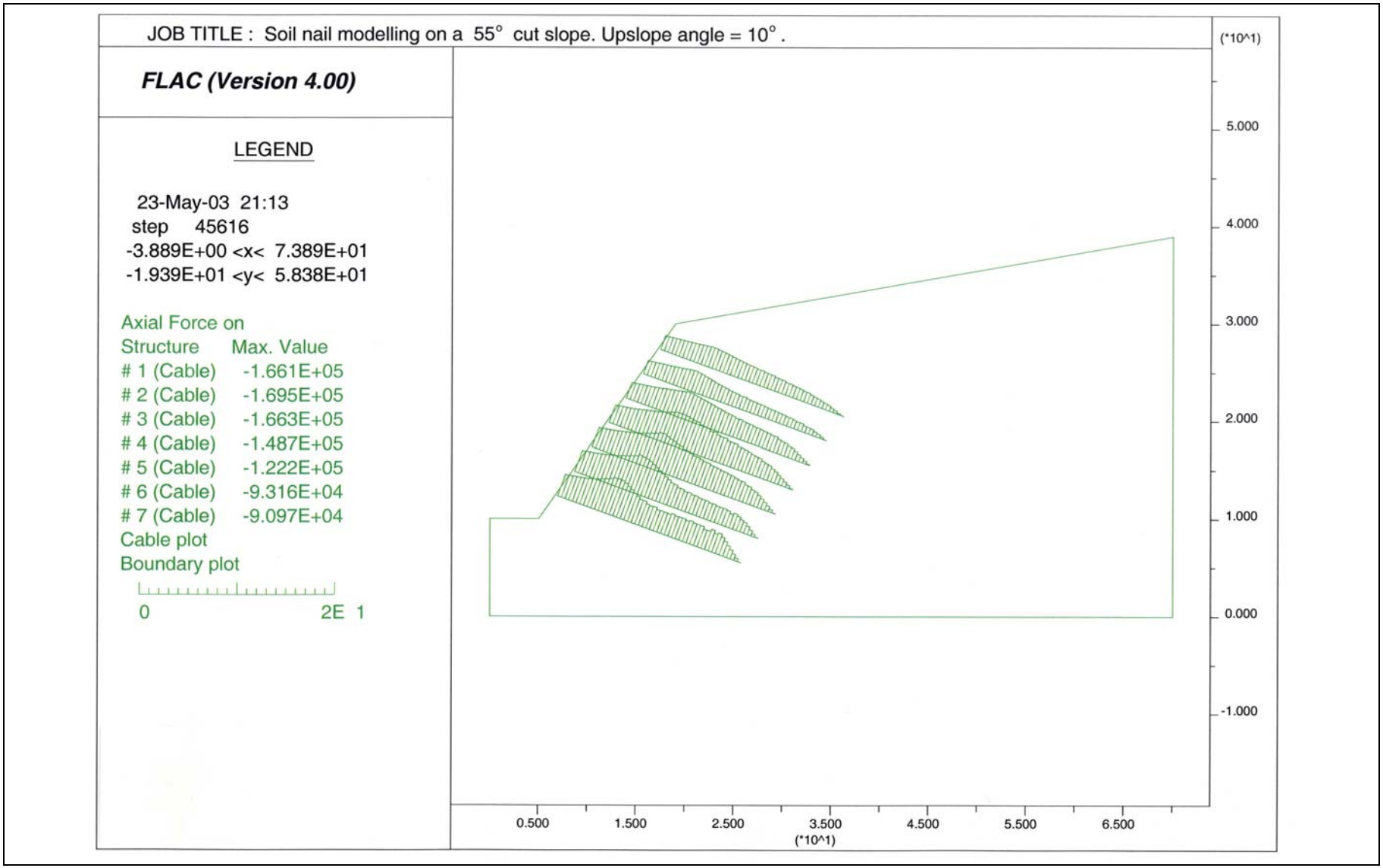

Figure B1 - Typical Result of Axial Force Distribution along Soil Nails

Table of Contents
Table of Contents
Table of Contents
Table of Contents
Table of Contents

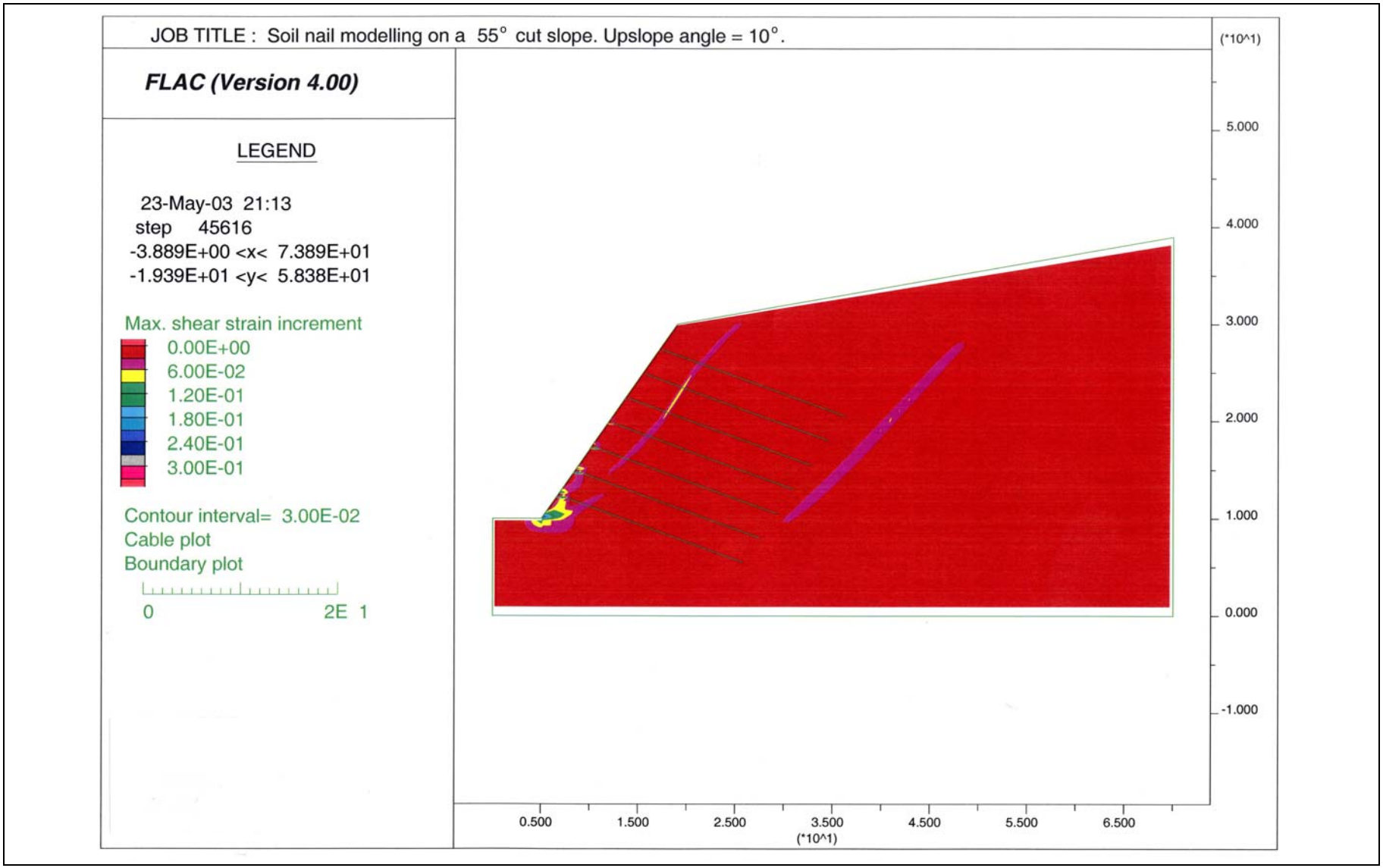

Figure B2 - Typical Result of Shear Strain Distribution

Table of Contents
Table of Contents
Table of Contents
Table of Contents
Table of Contents

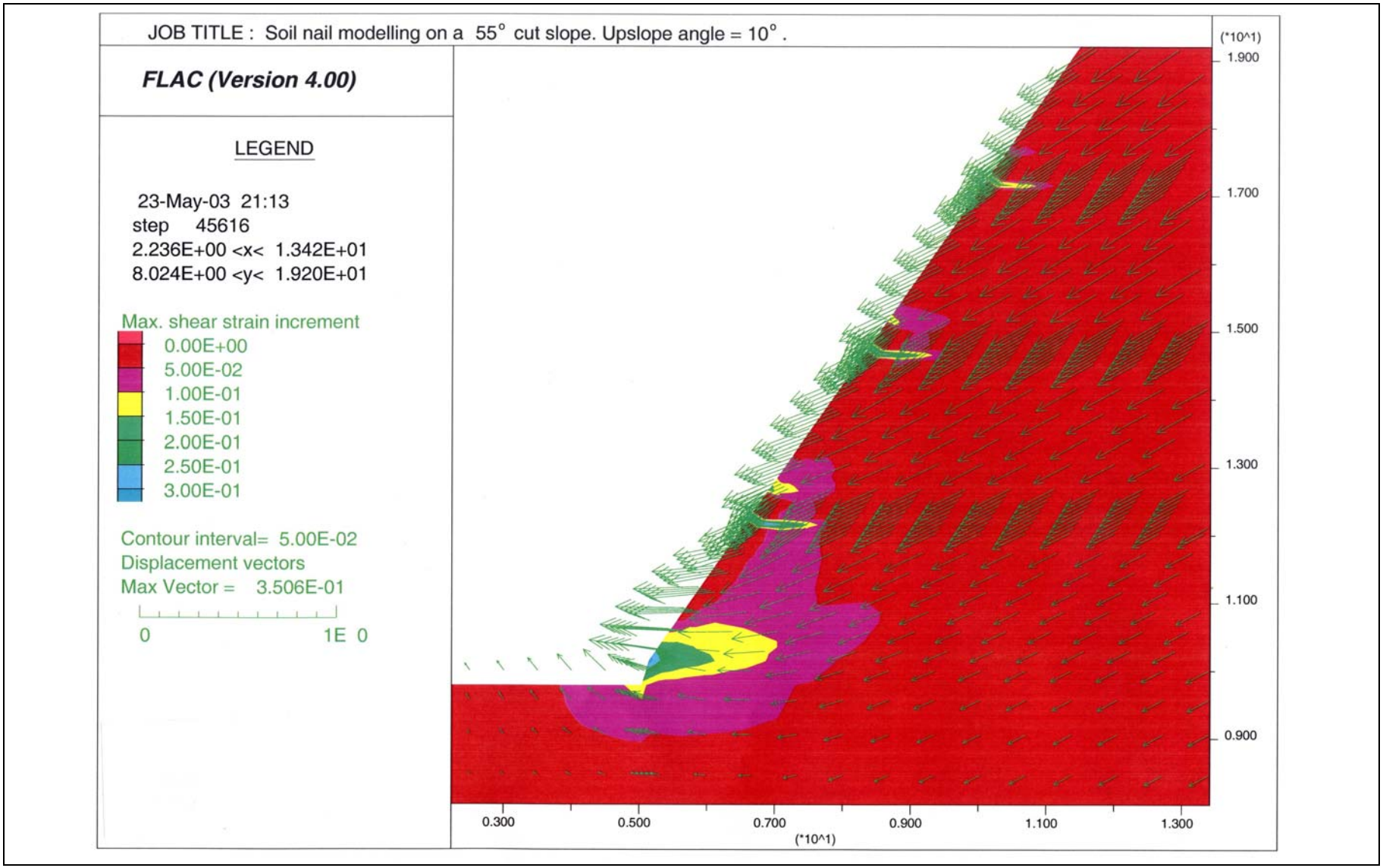

Figure B3 - Typical Result of Shear Strain and Displacement Vectors near the Slope Toe

Table of Contents
Table of Contents
Table of Contents

APPENDIX C

RESULTS OF STUDY OF BEARING FAILURE OF SOIL NAIL HEADS USING FLAC ANALYSIS

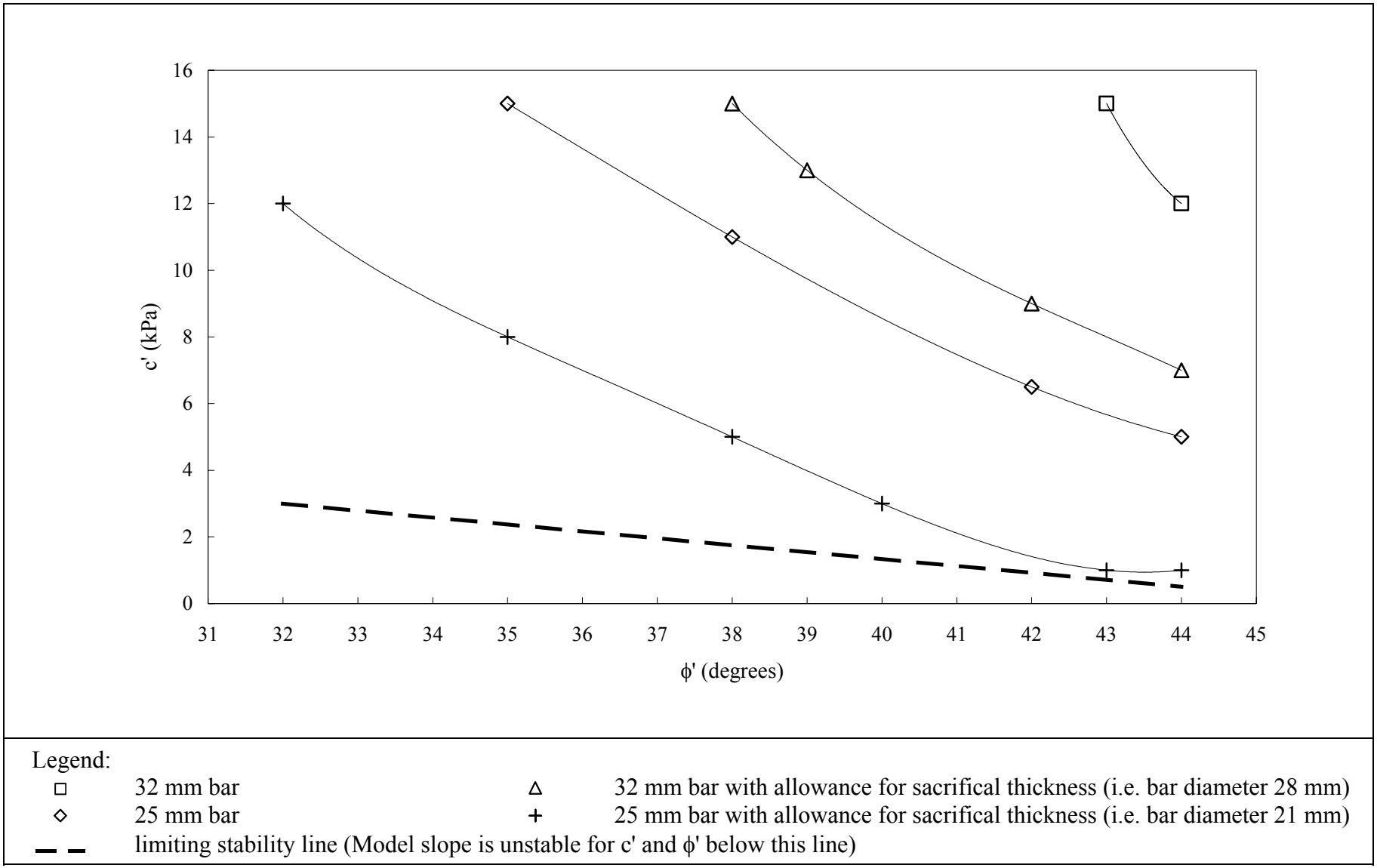

Figure C1 - Chart for 400 mm x 400 mm Nail Head and Slope Angle 45°

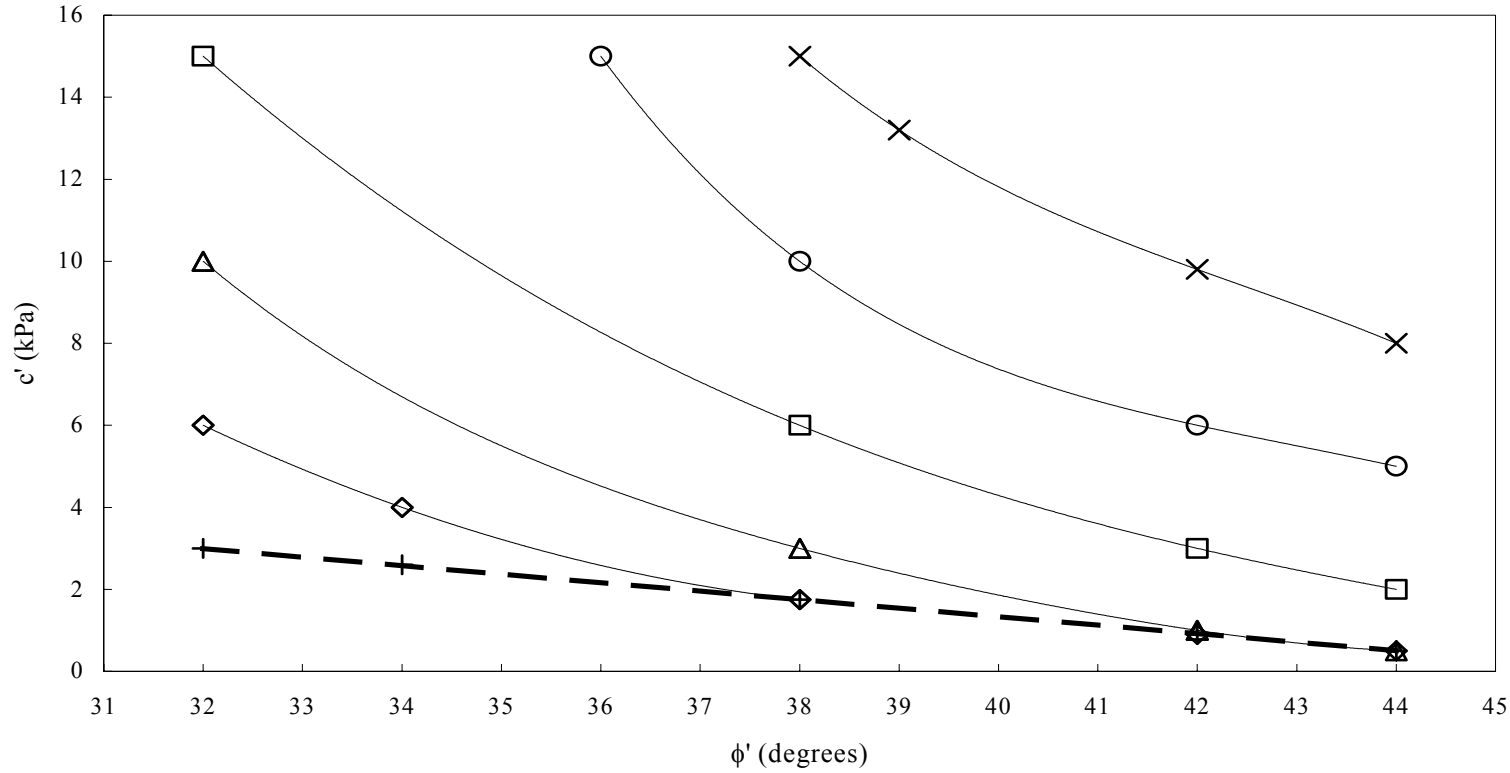

Legend:

×	40 mm bar	○	40 mm bar with allowance for sacrifical thickness (i.e. bar diameter 36 mm)
□	32 mm bar	△	32 mm bar with allowance for sacrifical thickness (i.e. bar diameter 28 mm)
◇	25 mm bar	+	25 mm bar with allowance for sacrifical thickness (i.e. bar diameter 21 mm)
— —	limiting stability line (Model slope is unstable for c' and ϕ' below this line)		

Figure C2 - Chart for 600 mm x 600 mm Nail Head and Slope Angle 45°

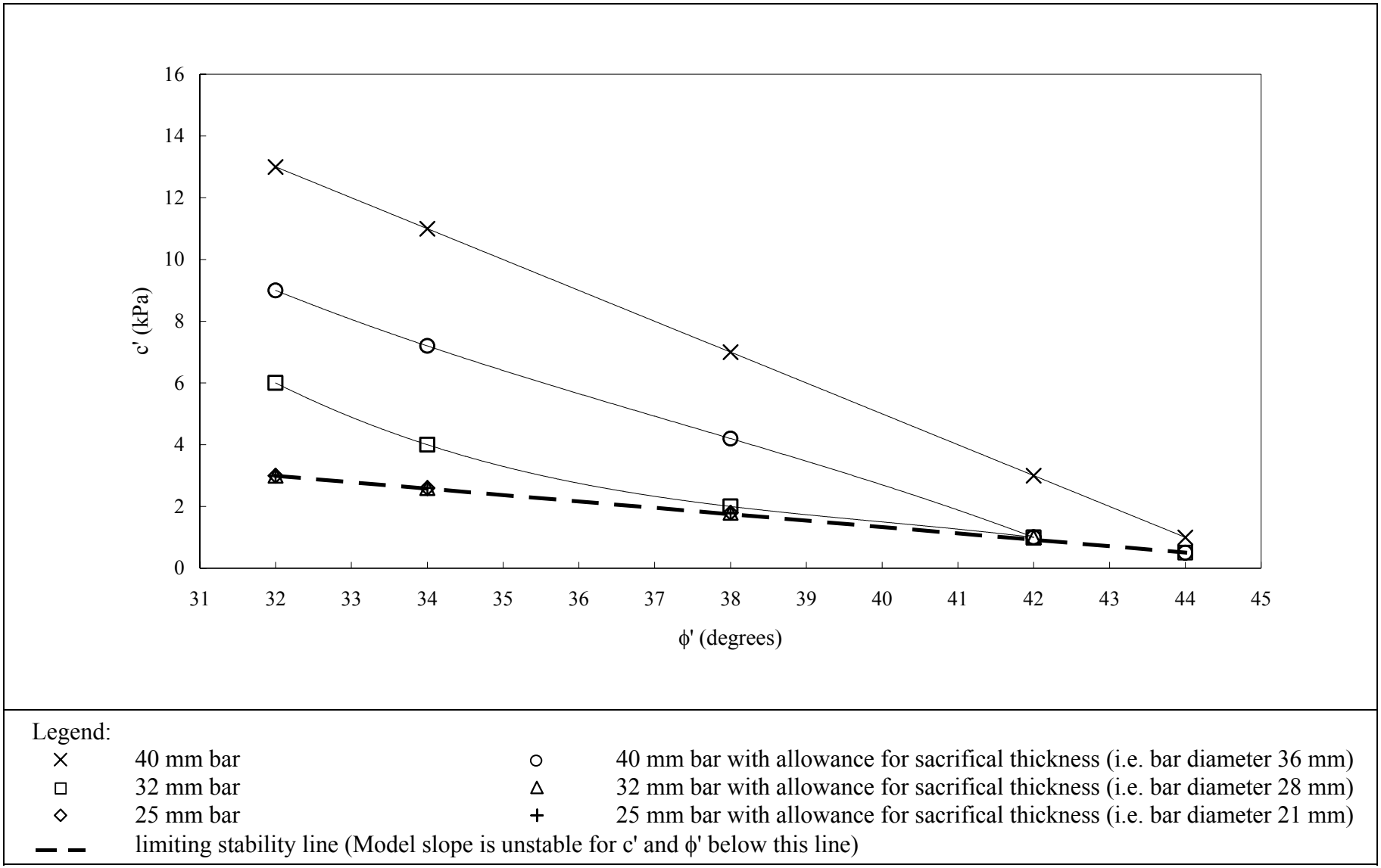

Figure C3 - Chart for 800 mm x 800 mm Nail Head and Slope Angle 45°

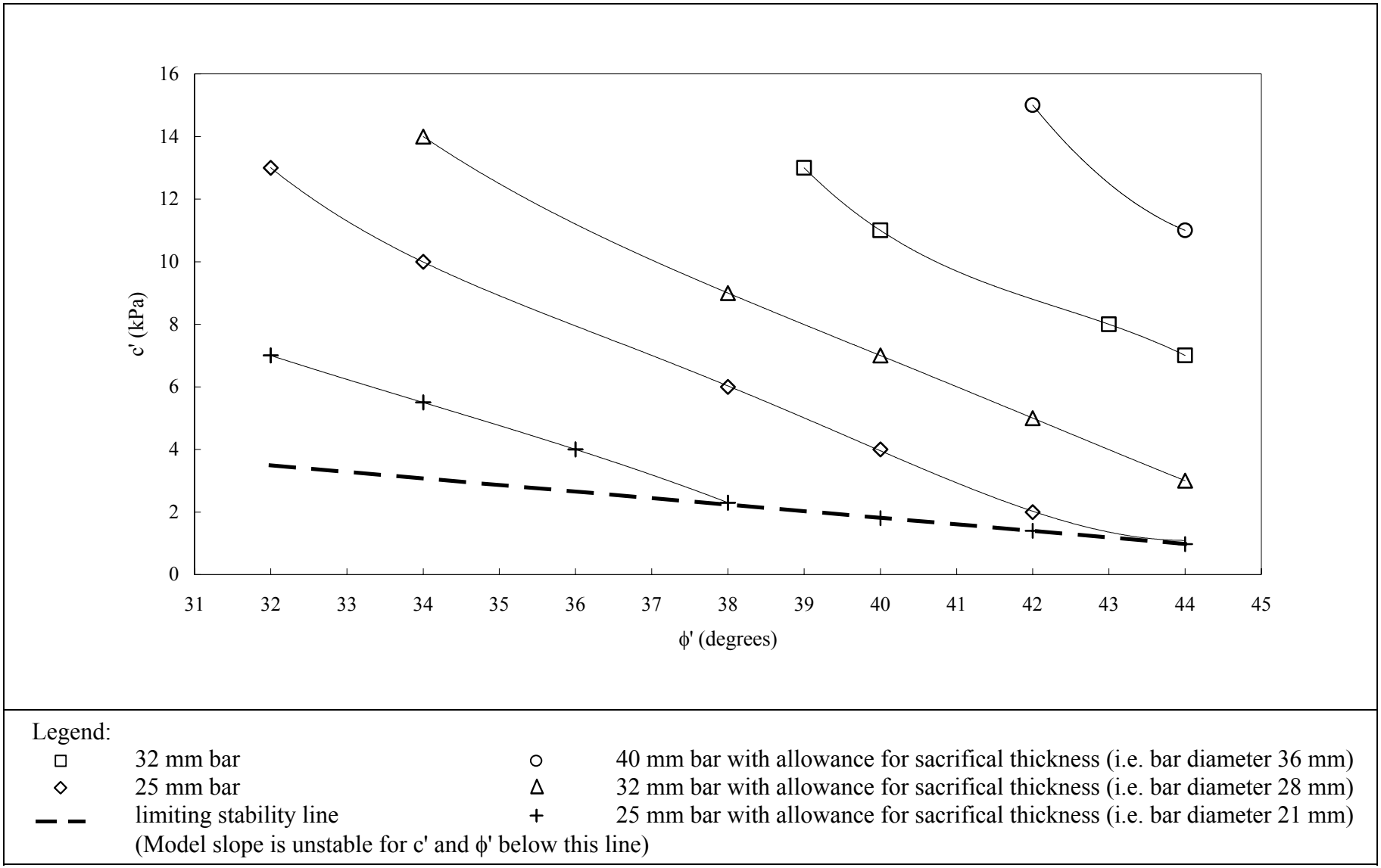

Figure C4 - Chart for 400 mm x 400 mm Nail Head and Slope Angle 55°

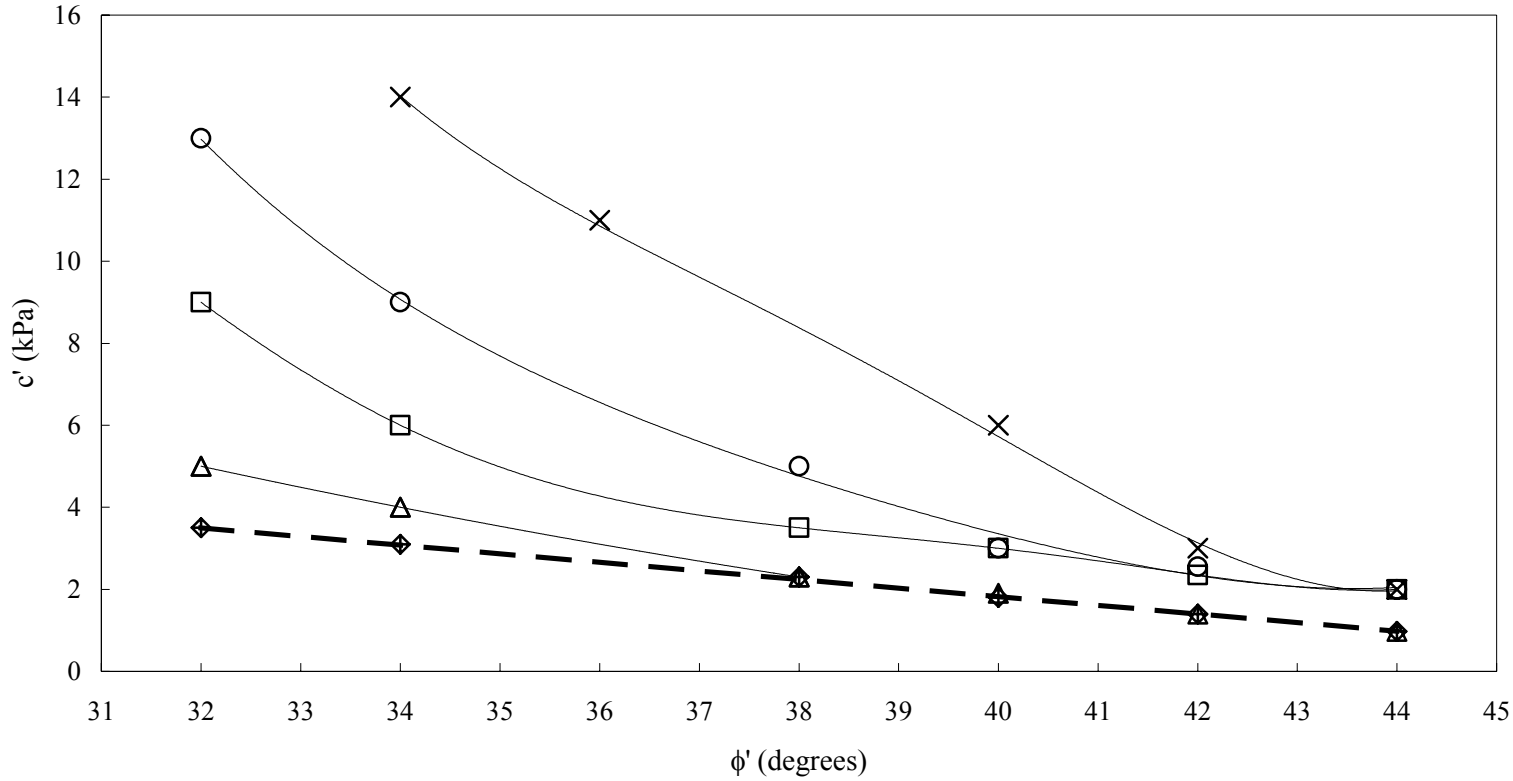

Legend:

×	40 mm bar	○	40 mm bar with allowance for sacrifical thickness (i.e. bar diameter 36 mm)
□	32 mm bar	△	32 mm bar with allowance for sacrifical thickness (i.e. bar diameter 28 mm)
◇	25 mm bar	+	25 mm bar with allowance for sacrifical thickness (i.e. bar diameter 21 mm)
— —	limiting stability line (Model slope is unstable for c' and ϕ' below this line)		

Figure C5 - Chart for 600 mm x 600 mm Nail Head and Slope Angle 55°

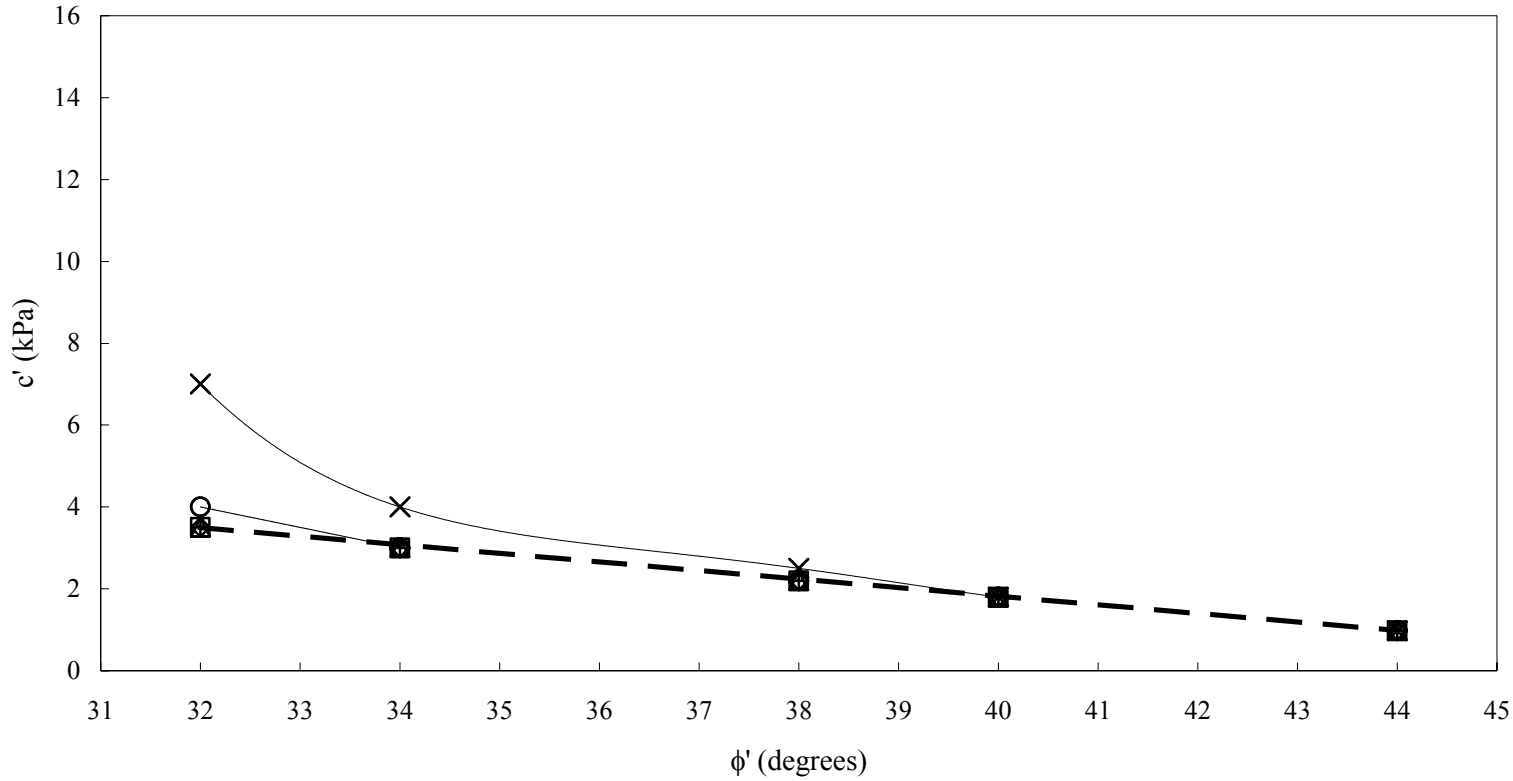

Legend:

×	40 mm soil nail bar	○	40 mm soil nail bar with allowance for sacrifical thickness (i.e. bar diameter 36 mm)
□	32 mm soil nail bar	△	32 mm soil nail bar with allowance for sacrifical thickness (i.e. bar diameter 28 mm)
◇	25 mm soil nail bar	+	25 mm soil nail bar with allowance for sacrifical thickness (i.e. bar diameter 21 mm)

— — limiting stability line (Model slope is unstable for c' and ϕ' below this line)

Figure C6 - Chart for 800 mm x 800 mm Nail Head and Slope Angle 55°

Table of Contents
Table of Contents
Table of Contents
Table of Contents
Table of Contents

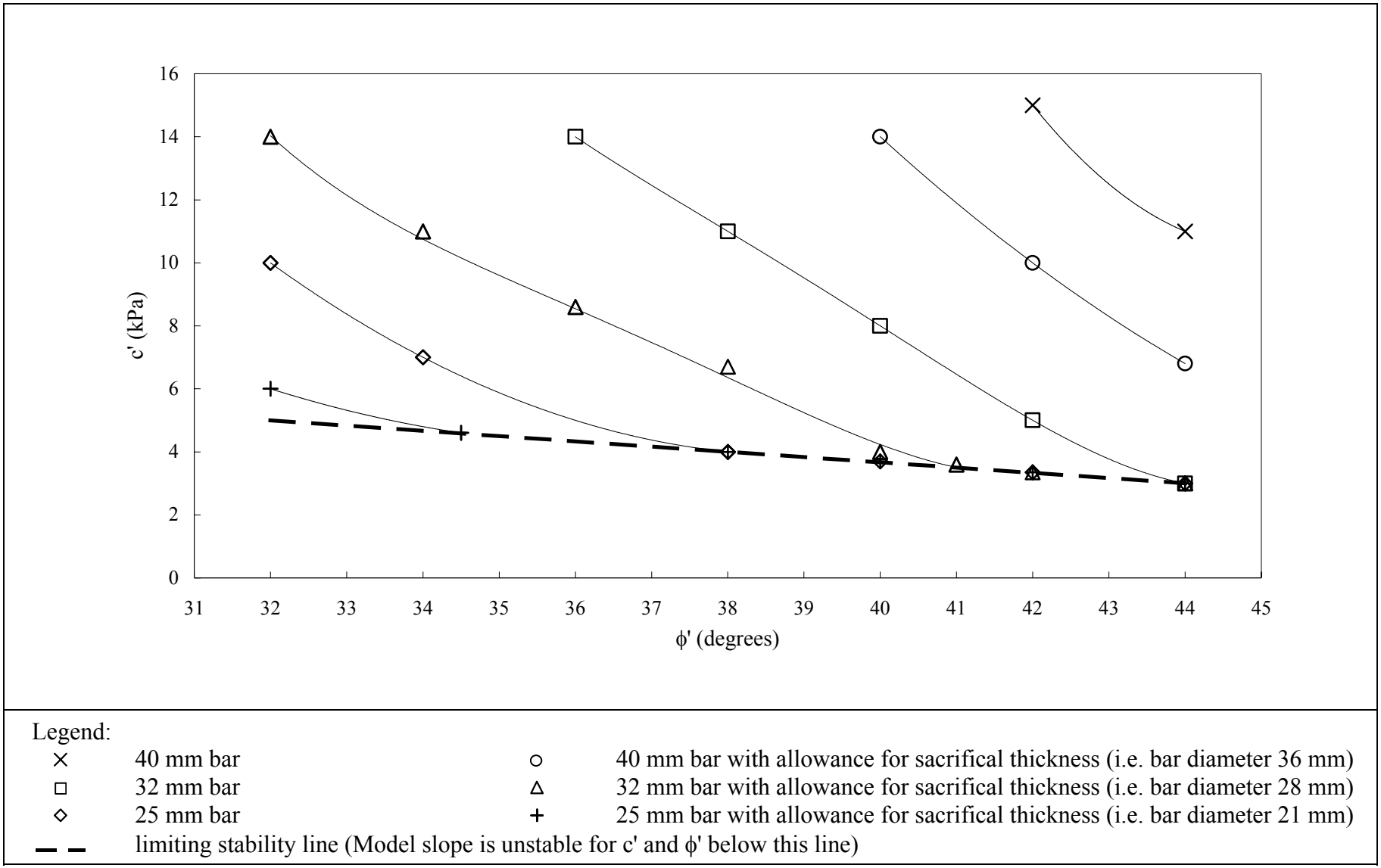

Figure C7 - Chart for 400 mm x 400 mm Nail Head and Slope Angle 65°

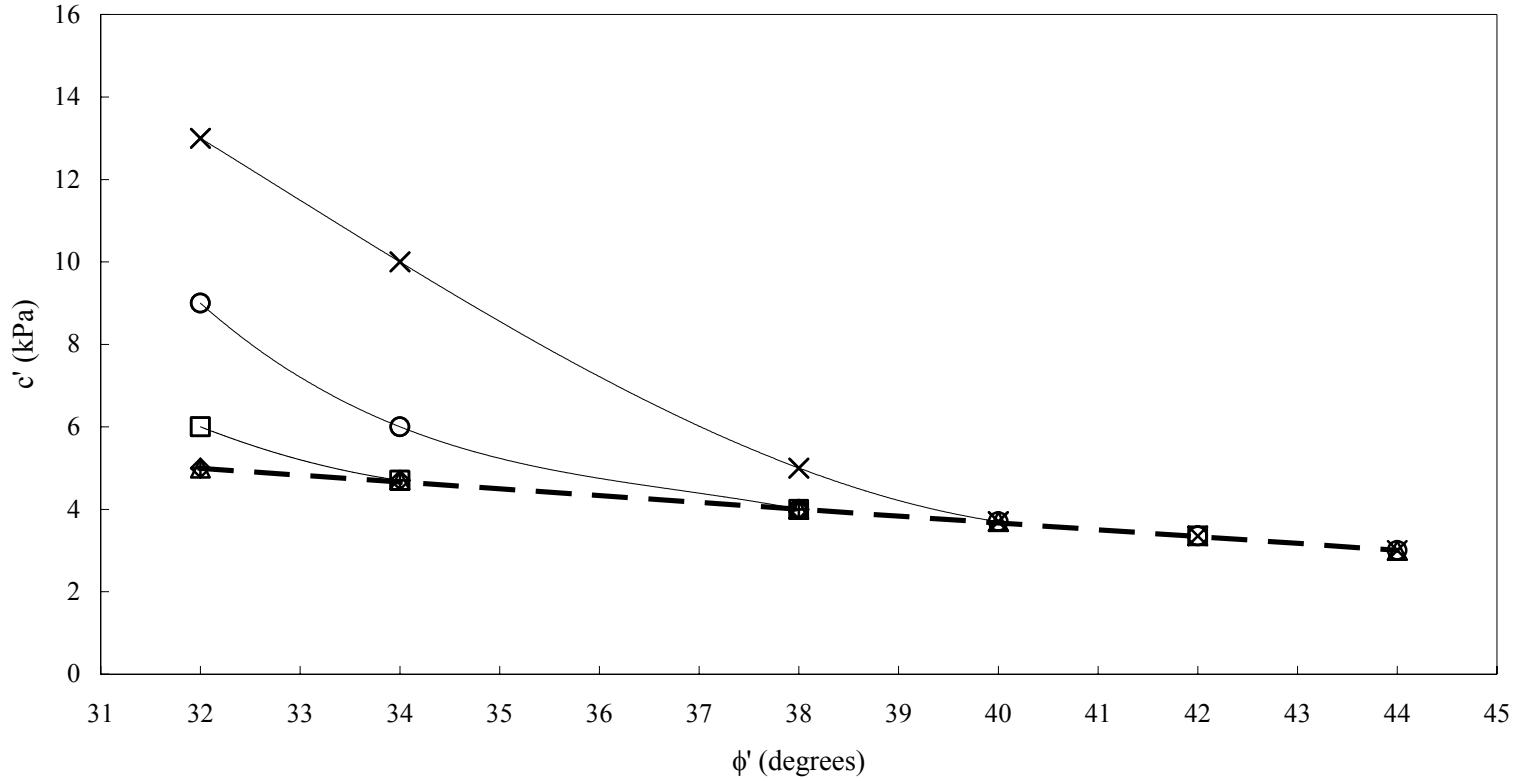

Legend:

×	40 mm bar	○	40 mm bar with allowance for sacrifical thickness (i.e. bar diameter 36 mm)
□	32 mm bar	△	32 mm bar with allowance for sacrifical thickness (i.e. bar diameter 28 mm)
◇	25 mm bar	+	25 mm bar with allowance for sacrifical thickness (i.e. bar diameter 21 mm)
— —	limiting stability line (Model slope is unstable for c' and ϕ' below this line)		

Figure C8 - Chart for 600 mm x 600 mm Nail Head and Slope Angle 65°

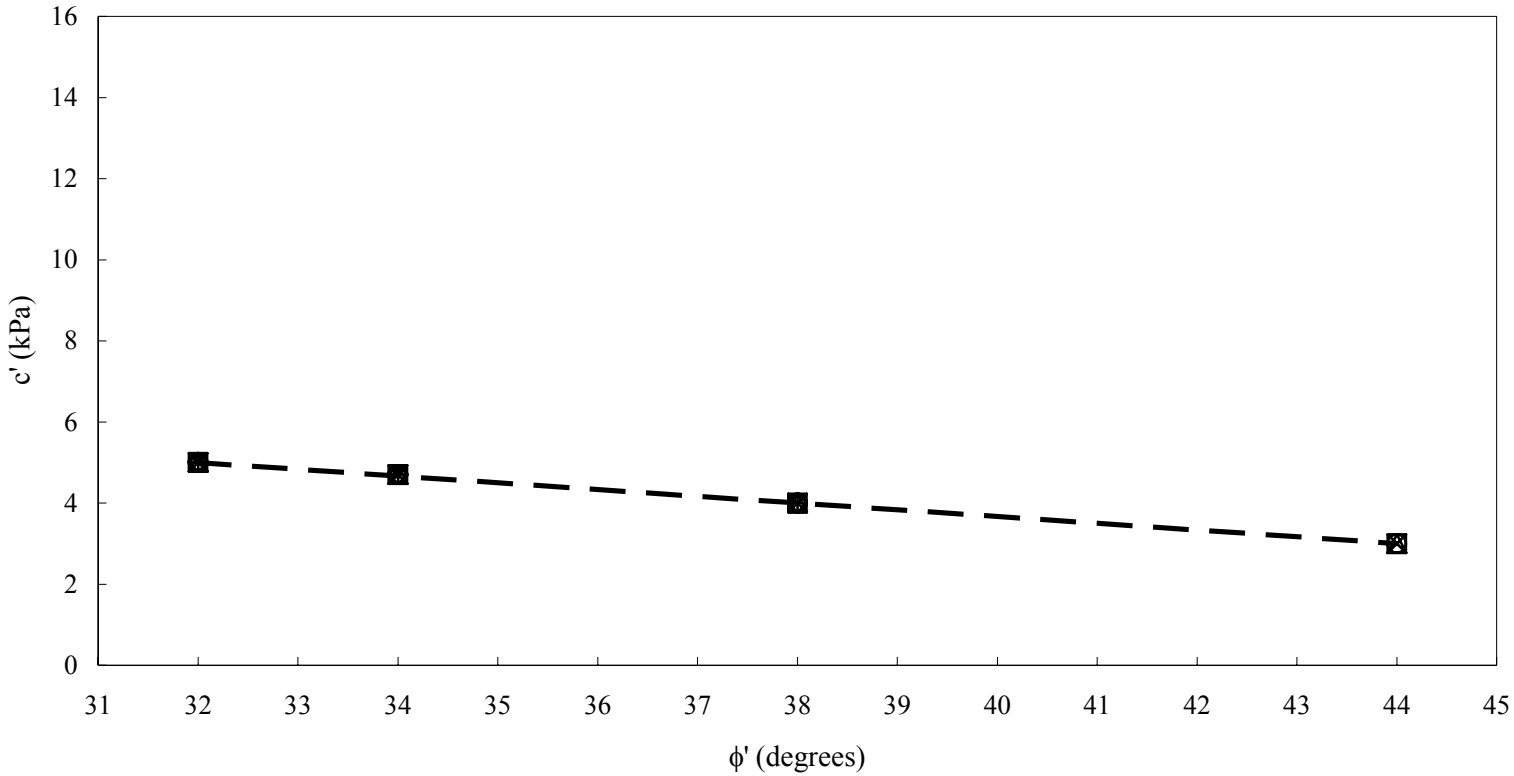

Legend:

×	40 mm bar	○	40 mm bar with allowance for sacrifical thickness (i.e. bar diameter 36 mm)
□	32 mm bar	△	32 mm bar with allowance for sacrifical thickness (i.e. bar diameter 28 mm)
◇	25 mm bar	+	25 mm bar with allowance for sacrifical thickness (i.e. bar diameter 21 mm)
— —	limiting stability line (Model slope is unstable for c' and ϕ' below this line)		

Figure C9 - Chart for 800 mm x 800 mm Nail Head and Slope Angle 65°

GEO PUBLICATIONS AND ORDERING INFORMATION
土力工程處刊物及訂購資料

A selected list of major GEO publications is given in the next page. An up-to-date full list of GEO publications can be found at the CEDD Website http://www.cedd.gov.hk on the Internet under "Publications". Abstracts for the documents can also be found at the same website. Technical Guidance Notes are published on the CEDD Website from time to time to provide updates to GEO publications prior to their next revision.

部份土力工程處的主要刊物目錄刊載於下頁。而詳盡及最新的土力工程處刊物目錄，則登載於土木工程拓展署的互聯網網頁 http://www.cedd.gov.hk 的"刊物"版面之內。刊物的摘要及更新刊物內容的工程技術指引，亦可在這個網址找到。

Copies of GEO publications (except maps and other publications which are free of charge) can be purchased either by:

writing to
Publications Sales Section,
Information Services Department,
Room 402, 4th Floor, Murray Building,
Garden Road, Central, Hong Kong.
Fax: (852) 2598 7482

or
- Calling the Publications Sales Section of Information Services Department (ISD) at (852) 2537 1910
- Visiting the online Government Bookstore at http://bookstore.esdlife.com
- Downloading the order form from the ISD website at http://www.isd.gov.hk and submit the order online or by fax to (852) 2523 7195
- Placing order with ISD by e-mail at puborder@isd.gov.hk

讀者可採用以下方法購買土力工程處刊物(地質圖及免費刊物除外):

書面訂購
香港中環花園道
美利大廈4樓402室
政府新聞處
刊物銷售組
傳真: (852) 2598 7482

或
- 致電政府新聞處刊物銷售小組訂購 (電話：(852) 2537 1910)
- 進入網上「政府書店」選購，網址爲 http://bookstore.esdlife.com
- 透過政府新聞處的網站 (http://www.isd.gov.hk) 於網上遞交訂購表格，或將表格傳真至刊物銷售小組 (傳真：(852) 2523 7195)
- 以電郵方式訂購 (電郵地址：puborder@isd.gov.hk)

1:100 000, 1:20 000 and 1:5 000 maps can be purchased from:

Map Publications Centre/HK,
Survey & Mapping Office, Lands Department,
23th Floor, North Point Government Offices,
333 Java Road, North Point, Hong Kong.
Tel: 2231 3187
Fax: (852) 2116 0774

讀者可於下列地點購買1:100 000，1:20 000及1:5 000地質圖：

香港北角渣華道333號
北角政府合署23樓
地政總署測繪處
電話: 2231 3187
傳真: (852) 2116 0774

Requests for copies of Geological Survey Sheet Reports, publications and maps which are free of charge should be sent to:

For Geological Survey Sheet Reports and maps which are free of charge:
Chief Geotechnical Engineer/Planning,
(Attn: Hong Kong Geological Survey Section)
Geotechnical Engineering Office,
Civil Engineering and Development Department,
Civil Engineering and Development Building,
101 Princess Margaret Road,
Homantin, Kowloon, Hong Kong.
Tel: (852) 2762 5380
Fax: (852) 2714 0247
E-mail: jsewell@cedd.gov.hk

For other publications which are free of charge:
Chief Geotechnical Engineer/Standards and Testing,
Geotechnical Engineering Office,
Civil Engineering and Development Department,
Civil Engineering and Development Building,
101 Princess Margaret Road,
Homantin, Kowloon, Hong Kong.
Tel: (852) 2762 5345
Fax: (852) 2714 0275
E-mail: ykhui@cedd.gov.hk

如欲索取地質調查報告、其他免費刊物及地質圖，請致函：

地質調查報告及地質圖:
香港九龍何文田公主道101號
土木工程拓展署大樓
土木工程拓展署
土力工程處
規劃部總土力工程師
(請交:香港地質調查組)
電話: (852) 2762 5380
傳真: (852) 2714 0247
電子郵件: jsewell@cedd.gov.hk

其他免費刊物:
香港九龍何文田公主道101號
土木工程拓展署大樓
土木工程拓展署
土力工程處
標準及測試部總土力工程師
電話: (852) 2762 5345
傳真: (852) 2714 0275
電子郵件: ykhui@cedd.gov.hk

Table of Contents
Table of Contents
Table of Contents

MAJOR GEOTECHNICAL ENGINEERING OFFICE PUBLICATIONS
土力工程處之主要刊物

GEOTECHNICAL MANUALS

Geotechnical Manual for Slopes, 2nd Edition (1984), 300 p. (English Version), (Reprinted, 2000).

斜坡岩土工程手冊(1998)，308頁(1984年英文版的中文譯本)。

Highway Slope Manual (2000), 114 p.

GEOGUIDES

Geoguide 1	Guide to Retaining Wall Design, 2nd Edition (1993), 258 p. (Reprinted, 2000).
Geoguide 2	Guide to Site Investigation (1987), 359 p. (Reprinted, 2000).
Geoguide 3	Guide to Rock and Soil Descriptions (1988), 186 p. (Reprinted, 2000).
Geoguide 4	Guide to Cavern Engineering (1992), 148 p. (Reprinted, 1998).
Geoguide 5	Guide to Slope Maintenance, 3rd Edition (2003), 132 p. (English Version).
岩土指南第五冊	斜坡維修指南，第三版(2003)，120頁(中文版)。
Geoguide 6	Guide to Reinforced Fill Structure and Slope Design (2002), 236 p.

GEOSPECS

Geospec 1	Model Specification for Prestressed Ground Anchors, 2nd Edition (1989), 164 p. (Reprinted, 1997).
Geospec 2	Model Specification for Reinforced Fill Structures (1989), 135 p. (Reprinted, 1997).
Geospec 3	Model Specification for Soil Testing (2001), 340 p.

GEO PUBLICATIONS

GCO Publication No. 1/90	Review of Design Methods for Excavations (1990), 187 p. (Reprinted, 2002).
GEO Publication No. 1/93	Review of Granular and Geotextile Filters (1993), 141 p.
GEO Publication No. 1/96	Pile Design and Construction (1996), 348 p. (Reprinted, 2003).
GEO Publication No. 1/2000	Technical Guidelines on Landscape Treatment and Bio-engineering for Man-made Slopes and Retaining Walls (2000), 146 p.

GEOLOGICAL PUBLICATIONS

The Quaternary Geology of Hong Kong, by J.A. Fyfe, R. Shaw, S.D.G. Campbell, K.W. Lai & P.A. Kirk (2000), 210 p. plus 6 maps.

The Pre-Quaternary Geology of Hong Kong, by R.J. Sewell, S.D.G. Campbell, C.J.N. Fletcher, K.W. Lai & P.A. Kirk (2000), 181 p. plus 4 maps.

TECHNICAL GUIDANCE NOTES

TGN 1	Technical Guidance Documents